



THE HONG KONG  
POLYTECHNIC UNIVERSITY

香港理工大學

Pao Yue-kong Library

包玉剛圖書館

---

## Copyright Undertaking

This thesis is protected by copyright, with all rights reserved.

**By reading and using the thesis, the reader understands and agrees to the following terms:**

1. The reader will abide by the rules and legal ordinances governing copyright regarding the use of the thesis.
2. The reader will use the thesis for the purpose of research or private study only and not for distribution or further reproduction or any other purpose.
3. The reader agrees to indemnify and hold the University harmless from and against any loss, damage, cost, liability or expenses arising from copyright infringement or unauthorized usage.

### IMPORTANT

If you have reasons to believe that any materials in this thesis are deemed not suitable to be distributed in this form, or a copyright owner having difficulty with the material being included in our database, please contact [lbsys@polyu.edu.hk](mailto:lbsys@polyu.edu.hk) providing details. The Library will look into your claim and consider taking remedial action upon receipt of the written requests.

IMMERSED FINITE ELEMENT METHODS FOR THE  
MULTI-LAYER POROUS WALL MODEL

HUILI ZHANG

Ph.D

The Hong Kong Polytechnic University

2017







THE HONG KONG POLYTECHNIC UNIVERSITY  
DEPARTMENT OF APPLIED MATHEMATICS

IMMERSED FINITE ELEMENT METHODS FOR  
THE MULTI-LAYER POROUS WALL MODEL

HUILI ZHANG

A THESIS SUBMITTED IN PARTIAL FULFILMENT OF THE REQUIREMENTS  
FOR THE DEGREE OF DOCTOR OF PHILOSOPHY

MAY 2017



# Certificate of Originality

I hereby declare that this thesis is my own work and that, to the best of my knowledge and belief, it reproduces no material previously published or written, nor material that has been accepted for the award of any other degree or diploma, except where due acknowledgement has been made in the text.

\_\_\_\_\_ (Signed)

\_\_\_\_\_ ZHANG Huili \_\_\_\_\_ (Name of student)





Dedicate to my parents.



# Abstract

The dissertation is concerned with the multi-layer porous wall model which is proposed to simulate the drug transfer mechanism in the arterial wall when treated with cardiovascular diseases. It is an interface problem with two types of interface points: the imperfect contact interface point at the first layer and the rough coefficient interface points at other layers. We firstly consider the linear and quadratic immersed finite element (IFE) methods to solve the steady-state problem. Then, we investigate fundamental properties of these IFE spaces. Through interpolation error analysis, we prove that these IFE spaces have optimal approximation capabilities. In addition, we get the optimal convergence rate by using both linear and quadratic IFE methods to solve the multi-layer porous wall model.

Furthermore, we analyze the long time stability and the asymptotic behavior of the IFE method for the multi-layer porous wall model for the drug-eluting stents (DES). With the help of the IFE methods for the spatial discretization, and the implicit Euler scheme for the temporal discretization, respectively, we deduce the global stability of fully discrete solution. Then, we investigate the asymptotic behavior of the discrete scheme which reveals that the multi-layer porous wall model converges to the corresponding elliptic equation if the body force approaches to a steady-state.

In addition, we use these IFE spaces to solve the unsteady problem. We prove that the backward Euler scheme has the optimal convergence rate in both the  $L^2$  and  $H^1$  norms. We also do some numerical experiments to verify the theoretical results.

In the last part, some conclusions and future work plans are given.

# Acknowledgements

I would like to take this opportunity to express my sincere gratitude to all the teachers, friends and family who helped and supported me along these years.

First and foremost, I want to express my deep gratitude to my supervisor, Prof. Lin Yanping, for his enlightening guidance, invaluable discussions and insightful ideas throughout the years. Not only his integrity and enthusiasm inspire me become better in research fields, but his precepts and examples will well profit me through my whole life. My every progress during these years could not be achieved without his guidance, consideration, patience, trust, encouragement and assistance.

Furthermore, I am thankful to Prof. Qiao Zhonghua for his kind encouragement and necessary assistance. I am grateful for his valuable advises and insightful comments on my research. I would also like to thank Prof. Zhao Xingqiu, Prof. Cui Jintao, and Prof. Li buyang for their patient and help during my study period in Polyu. I want to extend my sincere thanks to Prof. Wang Kun, Prof. Zhang xu, and Prof. He xiaoming, for their help in my research studies. Thanks are also given to my best friends, Dr. Peng Qiujin, Dr. Song Caiqin, Dr. Zhang Chuanjing, for their listening my depression and sharing their happiness. I am also thankful to all my schoolfellow and friends for their kindness and help.

Finally, I would like to express my special thanks to my parents for their love, encouragement and support. Their constant support provides inspiration for me to pursue in the academic road.



# Contents

<b>Certificate of Originality</b>	<b>iii</b>
<b>Abstract</b>	<b>vii</b>
<b>Acknowledgements</b>	<b>ix</b>
<b>List of Figures</b>	<b>xiii</b>
<b>List of Tables</b>	<b>xv</b>
<b>1 Introduction</b>	<b>1</b>
1.1 Multi-layer Porous Wall Model for the Drug-eluting Stents . . . . .	1
1.2 Survey of Previous Work for IFE Methods . . . . .	7
1.2.1 IFE Methods for One Dimensional Elliptic Interface Problems	7
1.2.2 IFE Methods for Two Dimensional Elliptic Interface Problems	10
1.2.3 IFE Methods for Other Interface Problems . . . . .	13
1.3 Outline of the Dissertation . . . . .	14
<b>2 Linear IFE Method</b>	<b>17</b>
2.1 Setting and Weak Solution . . . . .	17
2.2 Local Linear IFE Space for the First Interface . . . . .	21
2.3 Local Linear IFE Space for Other Interfaces . . . . .	27
2.4 Convergence of the Linear IFE Space . . . . .	32
2.5 Numerical Experiments . . . . .	35



<b>3</b>	<b>Quadratic IFE Method</b>	<b>39</b>
3.1	Local Quadratic IFE Space for the First Interface . . . . .	41
3.2	Local Quadratic IFE Space for Other Interfaces . . . . .	47
3.3	Convergence of quadratic IFE space . . . . .	52
3.4	Numerical Experiments . . . . .	53
<b>4</b>	<b>Long Time Stability and Asymptotic Analysis</b>	<b>59</b>
4.1	Long Time Stability . . . . .	61
4.2	Asymptotic Analysis . . . . .	65
4.2.1	Asymptotic Analysis on the $L^2$ Norm . . . . .	65
4.2.2	Asymptotic Analysis on the $H^1$ Norm . . . . .	69
4.3	Numerical Experiments . . . . .	73
<b>5</b>	<b>IFE Methods for the Time Dependent Multi-layer Porous Wall Model</b>	<b>81</b>
5.1	Error Estimation for Semi-discrete Scheme . . . . .	83
5.2	Error Estimation for Fully Discrete Scheme . . . . .	87
5.3	Numerical Experiments . . . . .	95
<b>6</b>	<b>Conclusions and Future Work</b>	<b>99</b>
6.1	Conclusions . . . . .	99
6.2	Future Work . . . . .	100
	<b>Bibliography</b>	<b>103</b>

# List of Figures

1.1	A drug-eluting stent implanted in a stenotic artery [46]. (Credit: US National Heart Lung and Blood institute) . . . . .	4
1.2	The cross-section of the drug-eluting stent implanted in a artery. . . . .	4
1.3	A sketch of the layered wall. ST indicates the metallic stent strut bearing the polymeric coating $([\alpha_{-1}, \alpha_0])$ , while the continuous wall layers are defined by $[\alpha_{i-1}, \alpha_i]$ , $i = 1, 2, \dots, n$ . This illustration is based on [51]. . . . .	4
1.4	A typical triangular interface element . . . . .	12
1.5	A typical rectangular interface element. . . . .	12
4.1	Errors $\ u_h^n - \bar{u}_h\ _0^2$ (left), and $\ u_h^n - \bar{u}_h\ _1^2$ (right) using the linear IFE method ( $h = 1/40$ ). . . . .	76
4.2	The values of $u_h^n(x)$ when iterate 50 times (left), and 100 times (right) using the linear IFE method by comparison with the exact solution of the steady problem ( $h = 1/40$ ). . . . .	76
4.3	Errors $\ u_h^n - \bar{u}_h\ _0$ (left), and $\ u_h^n - \bar{u}_h\ _1$ (right) using the quadratic IFE method ( $h = 1/40$ ). . . . .	76
4.4	The values of $u_h^n(x)$ when iterate 50 times (left), and 100 times (right) using the quadratic IFE method by comparison with the exact solution of the steady problem ( $h = 1/40$ ). . . . .	77
4.5	Linear IFE method (left) and Quadratic IFE method (right) ( $h = 1/40$ ). . . . .	77
4.6	The errors of $\ln(\ u_h^n - \bar{u}_h\ _0)$ and $\ln(\ u_h^n - \bar{u}_h\ _1)$ using linear (left) and Quadratic (right) IFE method ( $h = 1/40$ ). . . . .	77
4.7	Linear IFE method (left) and Quadratic IFE method (right) ( $h = 1/40$ ). . . . .	78
4.8	Linear IFE method (left) and Quadratic IFE method (right) ( $h = 1/40$ ). . . . .	78

4.9	Linear IFE method (left) and Quadratic IFE method (right) ( $h = 1/40$ ).	78
4.10	The errors of $\ln(\ u_h^n - \bar{u}_h\ _0)$ and $\ln(\ u_h^n - \bar{u}_h\ _1)$ using linear (left) and Quadratic (right) IFE method ( $h = 1/40$ ).	80
5.1	1D linear (left) and quadratic (right) IFE local basis function.	82
6.1	Controlled release polymeric device	101

# List of Tables

2.1	Errors and convergence rates of the linear IFE method when $n = 3$ with large values for $\beta_j, j = 1, 2, 3$ .	36
2.2	Errors and convergence rates the linear IFE method with $n = 6$ and large values for $\beta_j, j = 1, 2, 3$ .	37
2.3	Errors and convergence rates of the linear IFE method when $n = 3$ with small values for $\beta_j, j = 1, 2, 3$ .	37
2.4	Errors and convergence rates of the linear IFE method when $n = 6$ with small values for $\beta_j, j = 1, 2, 3$ .	38
3.1	Errors and convergence rates of the quadratic IFE method when $n = 3$ with large values for $\beta_j, j = 1, 2, 3$ .	55
3.2	Errors and convergence rates of the quadratic IFE method when $n = 6$ with large values for $\beta_j, j = 1, 2, 3$ .	56
3.3	Errors and convergence rates of the quadratic IFE method when $n = 3$ with small values for $\beta_j, j = 1, 2, 3$ .	56
3.4	Errors and convergence rates of the quadratic IFE method when $n = 6$ (right) with small values for $\beta_j, j = 1, 2, 3$ .	57
5.1	Errors and convergence rates of the linear IFE methods when $n = 6$ with small values for $\beta_j (j = 1, 2, 3)$ .	96
5.2	Errors and convergence rates of the quadratic IFE methods when $n = 6$ with small values for $\beta_j (j = 1, 2, 3)$ .	96
5.3	Errors and convergence rates of the linear IFE methods when $n = 6$ with large values for $\beta_j (j = 1, 2, 3)$ .	97
5.4	Errors and convergence rates of the quadratic IFE methods when $n = 6$ with large values for $\beta_j (j = 1, 2, 3)$ .	97



# Chapter 1

## Introduction

In this chapter, we start with the introduction to the multi-layer porous wall model for the drug-eluting stents (DES). It is one of the most complete models to simulate the drug release mechanism from the coating of the stents to the arterial wall when treat with the cardiovascular diseases. Next, we provide a brief survey of numerical methods for the interface problems and a short review of the recently developed immersed finite element (IFE) methods.

### 1.1 Multi-layer Porous Wall Model for the Drug-eluting Stents

It is known that coronary heart disease is one of the main cause of death in developed countries [49] and accounts for 18% of all deaths in the United States annually according to report from the American Heart Association [58]. The blockage or occlusion of one or more of the arteries which supply blood to the heart muscle is the characteristic of the coronary heart disease. The reason is atherosclerosis, a complex progressive inflammatory disease [34], which leads to the buildup of fatty plaque material near the inner surface of the arterial wall [45]. This leads to episodes of chest pain if left it untreated. Ultimately, the atherosclerotic plaque is vulnerable to rupture, leading to the formation of a blood clot which blocks the artery, causing a

heart attack.

Until relatively recent years, bypass surgery was required to treat with this kind of heart disease. Afterwards, the bypass surgery has been replaced by inserting a small metallic mesh devices, called a stent, into the occluded artery to maintain blood flow acting as a supporting scaffold. However, when a stent is implanted into an artery, the endothelium is severely damaged. The consequent inflammatory response, excessive proliferation and migration of smooth muscle cells lead to the development of in-stent restenosis, a reocclusion of the artery, which is a significant limitation of the bare metal stents [47]. Then, the introduction of DES significantly reduced the occurrence of in-stent restenosis by releasing a drug to inhibit smooth muscle cell proliferation, see Figure 1.1. In part of A, we see the deflated balloon catheter inserted into the narrowed coronary artery. In part of B, the balloon is inflated, compressing the plaque and restoring the size of the artery. Finally, part C shows the widened artery. Such a drug, released in a controlled manner through a permeable membrane, is aimed at preventing a possible restenosis by virtue of its anti-proliferative action against smooth muscle cells. The DES which have revolutionized the treatment of coronary heart disease consists of a tubular wire mesh coated with a thin layer of biocompatible polymeric gel containing a therapeutic drug. Although a number of animal experiments are recommended for preclinical safety and efficacy evaluation of these devices [56], incomplete understanding of the factors governing drug release and distribution following stenting currently limits the optimization of such drug release profiles.

In order to understand the drug release mechanism from the coating of the stents to the arteries, and enhance control of the rate of drug delivery, we focus on the multi-layer porous wall model for the DES, which is proposed to simulate the drug transfer in the arterial wall when treat with the cardiovascular diseases in this dissertation. Mathematical models and numerical simulations play an important role in

understanding the mass transfer mechanism. In the last years, a number of mathematical models [29, 46, 48, 50, 52, 57, 64] are proposed to simulate the drug transfer process in this kind of mass release from DES through the arterial wall. Most of these studies disregarded the complex multi-layered structure of the wall and considered a homogeneous porous material with averaged properties for simplicity. As is well known that the arterial wall is a porous heterogeneous structure, consisting of a sequence of adjacent layers with different structural and chemical properties [25], such as, the three distinct layers model (the intima, the media, and the adventitia) is introduced in [60], a four layers (endothelium, intima, internal elastic lamina and media) model is proposed in [24, 61], and so on. Each layer is treated as a macroscopically homogeneous medium with its own diffusive property and continuity of mass flux between any two adjacent layers is imposed. It is believed that a better modeling of the wall structure brings us a more effective description of the drug release from a DES. One of these complete wall models is the multi-layer wall model that takes into account the heterogeneous properties of the different layers constituting the arterial wall. Although the complex geometry of the stents would require the use of three-dimensional (3D) models, nevertheless most of the mass dynamics mainly occurs along the direction normal to the stents coating (see Figure 1.2) and the easier handling of the geometry allows a systematic analysis on a wide range of parameters which leads to the explicit of the governing equations. G. Pontrelli and F. Monte proposed a simplified 1D multi-layer porous wall model in [51], see the illustration in Figure. 1.3, which is a large version of the part surrounded by the blue lines in Figure 1.2. Let us briefly review this model firstly. Without loss of generality, let us consider a set of intervals  $[\alpha_{i-1}, \alpha_i]$ ,  $i = 0, 1, 2, \dots, n$  having thickness  $l_i = \alpha_i - \alpha_{i-1}$  modeling the coating and the arterial wall, see Figure. 1.3. Therefore, considered the complex multi-layer structure of the wall, the multi-layer porous wall model is



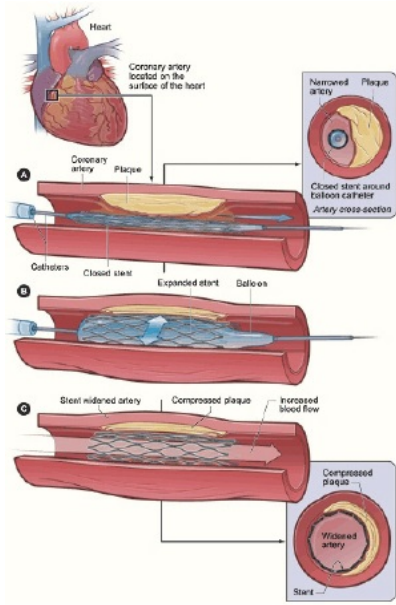


Figure 1.1: A drug-eluting stent implanted in a stenotic artery [46]. (Credit: US National Heart Lung and Blood institute)

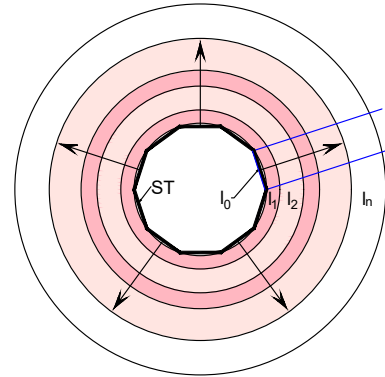


Figure 1.2: The cross-section of the drug-eluting stent implanted in a artery.

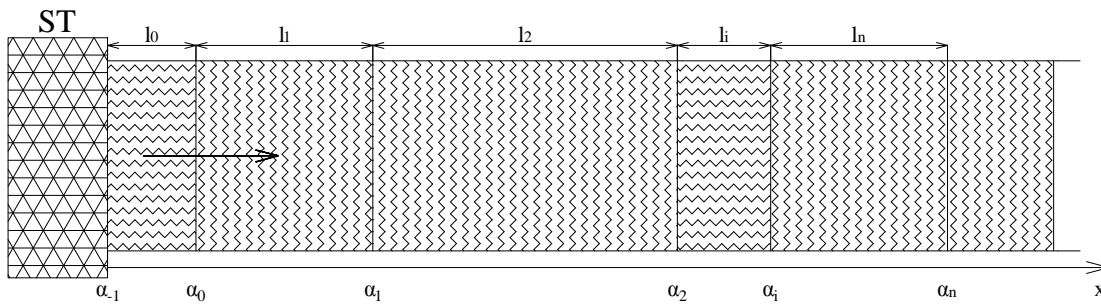


Figure 1.3: A sketch of the layered wall. ST indicates the metallic stent strut bearing the polymeric coating ( $[\alpha_{-1}, \alpha_0]$ ), while the continuous wall layers are defined by  $[\alpha_{i-1}, \alpha_i]$ ,  $i = 1, 2, \dots, n$ . This illustration is based on [51].

governed by the following interface initial-boundary value problem [51]:

$$\left\{ \begin{array}{ll} \frac{\partial u}{\partial t} + \frac{\partial}{\partial x} \left( -D \frac{\partial u}{\partial x} + 2\delta u \right) + \beta u = f, & x \in (\alpha_{-1}, \alpha_n), t > 0, \\ -D_0 \frac{\partial u}{\partial x} = 0, & x = \alpha_{-1}, t > 0, \\ u(x, 0) = u_0, & x \in (\alpha_{-1}, \alpha_0), \\ u(x, 0) = 0, & x \in (\alpha_{i-1}, \alpha_i), i = 1, 2, \dots, n, \\ u(\alpha_n, t) = 0, & t > 0, \end{array} \right. \quad (1.1)$$

where,  $D(x)$ ,  $\delta(x)$ ,  $\beta(x)$  and  $f(x, t)$  are functions on  $(\alpha_{-1}, \alpha_n)$  such that

$$\left\{ \begin{array}{ll} D(x) = D_i, & \text{when } x \in (\alpha_{i-1}, \alpha_i), 0 \leq i \leq n, t > 0, \\ \delta(x) = \delta_i, & \text{when } x \in (\alpha_{i-1}, \alpha_i), 0 \leq i \leq n, \delta_0 = 0, t > 0, \\ \beta(x) = \beta_i, & \text{when } x \in (\alpha_{i-1}, \alpha_i), 0 \leq i \leq n, \beta_0 = 0, t > 0, \\ f(x, t) = f_i(x, t), & \text{when } x \in (\alpha_{i-1}, \alpha_i), 0 \leq i \leq n, t > 0, \end{array} \right. \quad (1.2)$$

with  $D_i$  the drug diffusivity.  $\delta_i$  and  $\beta_i$  denote for a constant characteristic convection parameter and drug reaction coefficient in  $[\alpha_{i-1}, \alpha_i]$ ,  $i = 1, 2, \dots, n$ , respectively. We also assume that  $D_i > 0$  for  $0 \leq i \leq n$  and  $\delta_i, \beta_i > 0$  for  $1 \leq i \leq n$ . At the initial time ( $t = 0$ ), the drug is contained only in the coating and it is distributed with maximum concentration  $u_0$  and, subsequently, released into the arterial wall. Here, and throughout this paper, a mass volume-averaged concentration  $u(x, t)$  is considered. We know that the metallic strut is impermeable to the drug, so there is no mass flux passes through the boundary surface at  $x = \alpha_{-1}$ . Therefore, a zero-flux condition is normally imposed and the initial drug concentration is taken to be uniform. In the outmost  $n$ -th layer, the absorbing conditions is more realistic, since the vasa vasorum of the adventitia are continually replenished with fresh blood and sweep away any residual drug [48].

In addition, to prolong the drug release time, a permeable membrane (called topcoat) of permeability  $p$  is located at the first interface ( $x = \alpha_0$ ) between the coating and the arterial wall. Thus, the mass flux passed through it continuously while the drug concentration might have a possible jump. In this case, the mass transfer through the topcoat can be described by the following equation:

$$\begin{cases} [u]_{\alpha_0} = \lambda D_0 u'(\alpha_0^-), \\ -D_0 u'(\alpha_0^-) = -D_1 u'(\alpha_0^+) + 2\delta_1 u(\alpha_0^+), \end{cases} \quad (1.3)$$

where,  $\lambda = 1/p$ , and  $u(\alpha_0^\pm) = \lim_{x \rightarrow \alpha_0^\pm} u(x)$ ,  $[u]_{\alpha_0} = u(\alpha_0^+) - u(\alpha_0^-)$ . Throughout this dissertation, we will use  $u'$ ,  $u''$  to denote the the partial derivatives of  $u$  with respect to the space variable  $x$ . Besides,  $u_t$ ,  $u_{tt}$  shall be used to denote the partial derivatives of  $u$  with respect to the time variable  $t$ . To close this mass transfer system, the jump conditions requiring the continuity of flux and concentration are assigned at each interface point  $x = \alpha_i$  ( $i = 1, 2, \dots, n-1$ ):

$$\begin{cases} u(\alpha_i^-) = u(\alpha_i^+), \\ -D_i u'(\alpha_i^-) + 2\delta_i u(\alpha_i^-) = -D_{i+1} u'(\alpha_i^+) + 2\delta_{i+1} u(\alpha_i^+). \end{cases} \quad (1.4)$$

For the system (1.1)-(1.4), if the body force  $f(x, t)$  converges to a steady-state force  $\bar{f}(x)$  as  $t \rightarrow \infty$  in  $L^2$  norm, that is  $\lim_{t \rightarrow \infty} \|f(x, t) - \bar{f}(x)\|_0 = 0$ , we get the corresponding steady-state equations:

$$(-D\bar{u}'(x) + 2\delta\bar{u}(x))' + \beta\bar{u}(x) = \bar{f}(x), \quad x \in [\alpha_{-1}, \alpha_n], \quad (1.5)$$

$$D_0 \bar{u}'(\alpha_{-1}) = 0, \quad (1.6)$$

$$\bar{u}(\alpha_n) = 0, \quad (1.7)$$

with jump conditions (1.3) and (1.4).

## 1.2 Survey of Previous Work for IFE Methods

An popular method of solving interface problems with rough coefficients is to use the IFE method. IFE methods have been developed for over decades since the first article [30] was published. In IFE methods, we can use a mesh independent of the interface, such as the Cartesian mesh, and allow the interface to go through the interior of the elements. Therefore, the mesh in an IFE method consists of interface elements whose interior are cut through by the interface and the rest called non-interface elements. The basic idea of IFE method is to construct special basis functions according to the jump conditions on interface elements while using standard basis functions in the non-interface elements. There have been many publications about IFE methods solving the elliptic interface problems [2, 3, 14, 17, 18, 23, 28, 30, 32, 35, 36, 44, 63], elasticity interface problems [15, 42, 44], biharmonic interface problems [37], Stokes interface problems [1], moving interface problems [20, 38, 39], and so on.

### 1.2.1 IFE Methods for One Dimensional Elliptic Interface Problems

In 1998, Li firstly introduced a linear IFE method for one dimensional two-point boundary value problem with one interface in [30]:

$$\begin{cases} -(\beta(x)u')' + q(x)u(x) = f(x), & 0 < x < 1, \\ u(0) = 0, u(1) = 0, \end{cases} \quad (1.8)$$

with  $\beta(x) > 0$  is a piecewise continuous function and has a finite jump at the interface point  $0 < \alpha < 1$ . The natural jump conditions hold as follows:

$$[u]_{\alpha} = 0, [\beta u']_{\alpha} = 0,$$

here,  $[u]_\alpha$  is a jump of function  $u$  at the interface point  $\alpha$ , and

$$\beta(x) = \begin{cases} \beta^-(x), & 0 < x \leq \alpha, \\ \beta^+(x), & \alpha \leq x < 1. \end{cases}$$

In a uniform partition  $0 = x_1 < x_2 < \dots < x_n = 1$  of the interval  $[0, 1]$  with the mesh size  $h = x_i - x_{i-1}$ , assume that there exists an index  $j$  such that the interface point  $\alpha \in [x_j, x_{j+1}]$ . Then, we call  $[x_j, x_{j+1}]$  and  $[x_i, x_{i+1}]$ ,  $i \neq j$ , the interface element and non-interface element, respectively. By denoting  $\rho = \frac{\beta^-}{\beta^+}$  and  $D = h - \frac{\beta^+ - \beta^-}{\beta^+}(x_{j+1} - \alpha)$ , the two piecewise linear local basis functions on the interface element  $[x_j, x_{j+1}]$  were constructed as follows:

$$\phi_j = \begin{cases} 0, & 0 < x < x_{j-1}, \\ \frac{x - x_{j-1}}{x_j - x_{j-1}}, & x_{j-1} \leq x < x_j \\ 1 + \frac{x_j - x}{D}, & x_j \leq x < \alpha, \\ \frac{\rho(x_{j+1} - x)}{D}, & \alpha \leq x < x_{j+1}, \\ 0, & x_{j+1} \leq x < 1, \end{cases}$$

$$\phi_{j+1} = \begin{cases} 0, & 0 < x < x_j, \\ \frac{x - x_j}{D}, & x_j \leq x < \alpha, \\ 1 + \frac{\rho(x - x_{j+1})}{D}, & \alpha \leq x < x_{j+1}, \\ \frac{x - x_{j+2}}{x_{j+1} - x_{j+2}}, & x_{j+1} \leq x < x_{j+2}, \\ 0, & x_{j+2} \leq x < 1. \end{cases}$$

For the non-interface element  $[x_1, x_{i+1}]$ , the linear basis functions were defined as follows:

$$\phi_i = \begin{cases} 0, & 0 < x < x_{i-1}, \\ \frac{x - x_{i-1}}{x_i - x_{i-1}}, & x_{i-1} \leq x < x_i, \\ \frac{x - x_{i+1}}{x_i - x_{i+1}}, & x_i \leq x < x_{i+1}, \\ 0, & x_{i+1} \leq x < 1, \end{cases}$$

$$\phi_{i+1} = \begin{cases} 0, & 0 < x < x_i, \\ \frac{x - x_i}{x_{i+1} - x_i}, & x_i \leq x < x_{i+1}, \\ \frac{x - x_{i+2}}{x_{i+1} - x_{i+2}}, & x_{i+1} \leq x < x_{i+2}, \\ 0, & x_{i+2} \leq x < 1. \end{cases}$$

Then, for the uniform partition defined before, the local linear IFE space  $\mathcal{S}_h(T)$  was defined as follows:

$$\mathcal{S}_h(T) = \begin{cases} \text{span}\{\phi_i, \phi_{i+1}\}, & \text{if } T = [x_i, x_{i+1}], i \neq j, \\ \text{span}\{\phi_j, \phi_{j+1}\}, & \text{if } T = [x_j, x_{j+1}]. \end{cases}$$

These local finite element spaces are used to form the global finite element space. IFE spaces formed by higher degree polynomials have been constructed. In particular, several types of quadratic IFE basis functions were introduced in [8, 36]. The approximation capability of corresponding IFE spaces was analyzed. The arbitrary degree IFE spaces were form in [2]. In [4, 10], the authors solve the variable coefficients elliptic problem and Penns bioheat transfer equation with nonhomogenous flux jump condition. By using the computed solution from the IFE method, an inexpensive and effective flux recovery technique is employed to approximate the flux over the whole domain. The optimal convergence for the IFE approximation and

its flux is carried out. The construction of the finite element space falls into the general framework of Babuška and J.E. Osborn [6, 7] from which we can deduce the construction above.

These one dimensional IFE basis functions introduced above are continuous. A Galerkin scheme using any of these IFE spaces is a conforming finite element method. Approximation properties of these IFE spaces and error estimates of the related IFE solutions have been proved to be optimal in both  $L^2$  and  $H^1$  norms [3]. Let

$$H^p(\Omega) = \{u \in C(\Omega) : u|_{\Omega^\pm} \in H^{p+1}(\Omega^\pm), \text{ and } [\beta u^{(j)}]_\alpha = 0, j = 1, 2, \dots, p\}.$$

Then, we recall the results in the following theorems [63].

**Theorem 1.1.** *There exists a constant  $C$  independent of the location of the interface point  $\alpha$ , such that for all  $u \in H^p(\Omega)$ ,*

$$\|I_p u - u\|_0 + h \|I_p u - u\|_1 \leq C \frac{4^p}{(p-1)!} h^{p+1} |u|_{p+1}.$$

Here,  $I_p u$  is the  $p$ -th degree IFE interpolation of  $u$ .

**Theorem 1.2.** *There exists a constant  $C$  independent of the location of the interface point  $\alpha$ , such that*

$$\|u_h - u\|_0 + h \|u_h - u\|_1 \leq C \frac{4^p}{(p-1)!} h^{p+1} |u|_{p+1}.$$

Here,  $u_h$  is the  $p$ -th degree IFE solution for the one dimensional elliptic interface problems, and  $u \in H^p(\Omega)$  is the solution of the interface problem defined by (1.8).

## 1.2.2 IFE Methods for Two Dimensional Elliptic Interface Problems

IFE methods for two dimensional elliptic interface problems have been extensively studied in the past decade, see [10, 11, 13, 14, 17–19, 28, 31, 32, 35, 55, 59], and the

references therein. Firstly, we will briefly recall the IFE methods for two dimensional elliptic interface problems. For a Cartesian triangle partition  $\mathcal{T}_h$  of the domain  $\Omega = \Omega^- \cup \Omega^+ \cup \Gamma$  ( $\Gamma$  denotes the interface), there are two types of the element: interface elements and non-interface elements. For an interface element  $T$ ,  $T \cap \Omega^s \neq \emptyset$ ,  $s = -, +$ , we define the basis function on the triangular element  $T$  as follows:

$$\phi_i(x, y) = \begin{cases} \phi_i^-(x, y) = a^-x + b^-y + c^-, & x \in T^-, \\ \phi_i^+(x, y) = a^+x + b^+y + c^+, & x \in T^+, \\ \phi_i^-(D) = \phi_i^+(D), \phi_i^-(E) = \phi_i^+(E), \\ \int_{\overline{DE}} \beta^- \frac{\partial \phi_i^-}{\partial \mathbf{n}_{DE}} ds = \int_{\overline{DE}} \beta^+ \frac{\partial \phi_i^+}{\partial \mathbf{n}_{DE}} ds, \\ \phi_i(A_j) = \delta_{ij}, \quad i, j = 1, 2, 3, \end{cases}$$

here,  $D = (x_D, y_D)$ ,  $E = (x_E, y_E)$  are the two interface points where the interface intersected the edge of the element  $T$ , and  $\mathbf{n}_{DE}$  is the unit normal vector of the straight line  $\overline{DE}$ , see Figure 1.4. The coefficients  $a^-, b^-, c^-, a^+, b^+, c^+$  can be uniquely determined by the above 6 conditions. For the rectangle partition (see Figure 1.5), we define the bilinear basis functions as follows:

$$\phi_i(x, y) = \begin{cases} \phi_i^-(x, y) = a^- + b^-x + c^-y + d^-xy, & x \in T^-, \\ \phi_i^+(x, y) = a^+ + b^+x + c^+y + d^+xy, & x \in T^+, \\ \phi_i^-(D) = \phi_i^+(D), \phi_i^-(E) = \phi_i^+(E), \phi_i^-\left(\frac{D+E}{2}\right) = \phi_i^+\left(\frac{D+E}{2}\right), \\ \int_{\overline{DE}} \beta^- \frac{\partial \phi_i^-}{\partial \mathbf{n}_{DE}} ds = \int_{\overline{DE}} \beta^+ \frac{\partial \phi_i^+}{\partial \mathbf{n}_{DE}} ds, \\ \phi_i(A_j) = \delta_{ij}, \quad i, j = 1, 2, 3, 4. \end{cases}$$

Also, these 8 conditions can determined the bilinear functions uniquely. Another IFE methods for two dimensional elliptic interface problems is the nonconforming IFE



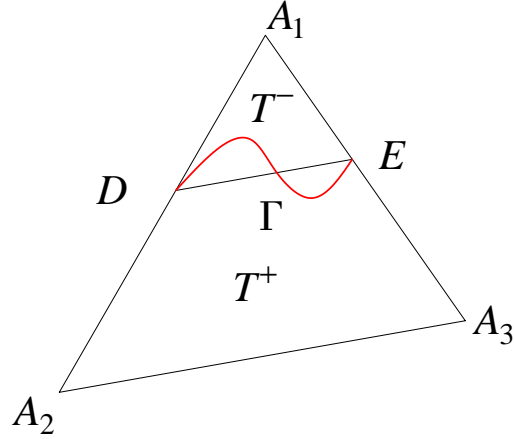


Figure 1.4: A typical triangular interface element

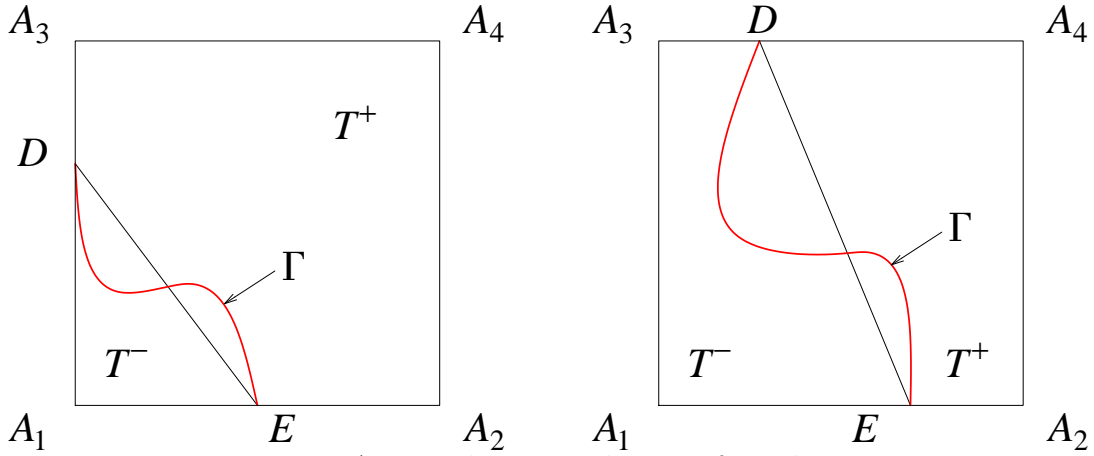


Figure 1.5: A typical rectangular interface element.

methods, which are firstly constructed in [63] using the mid-point value and integral value degrees of freedom, respectively. Those IFE functions are derived from the well-known nonconforming rotated  $Q_1$  finite element [54]. General speaking, there are two types of IFE methods for two dimensional elliptic interface problems: the conforming IFE methods and nonconforming IFE methods. In [32], both conforming and nonconforming linear IFE methods have been developed on triangle meshes for the two dimensional elliptic interface problems. For other recent results concerning numerical methods for the IFE methods, we refer for instance to [23, 35], et al.

### 1.2.3 IFE Methods for Other Interface Problems

IFE methods have been extended to other types of interface problems involving a system of PDEs, time dependent PDEs, and higher order PDEs.

In [33], the authors used the nonconforming linear IFE method based on the triangular Cartesian mesh to solve the planar elasticity interface problem, and derived that  $O(h)$  convergence in  $L^\infty$  norm. In [13, 15], the authors presented a conforming linear IFE method and the optimal convergence rate in  $L^\infty$  norm was derived for the elasticity problem. The nonconforming bilinear IFE method was developed for the elasticity problem and studied the error behaviors for both the linear and bilinear IFE methods in  $L^2$  and  $H^1$  norms in [44]. In [5], the authors proposed a backward Euler scheme using IFE methods to solve a semi-linear parabolic problem with interface and get the corresponding error estimate. In [41], by the help of the Laplace transform, the authors proposed a IFE methods to solving the parabolic interface problem. An immersed Eulerian-Lagrangian localized adjoint method was developed for transient advection-diffusion problem with interface. In [44], the authors indicated that the bilinear IFE functions are guaranteed to be applicable to a larger class of elasticity interface problems than linear IFE functions. In [42], the authors proposed a nonconforming IFE method for solving planar elasticity interface problems with structured (or Cartesian) meshes even if the material interface has a nontrivial geometry and observed the optimal approximation capability. In addition, the IFE functions developed in [42] are applicable to arbitrary configurations of elasticity materials and interface locations and the displacement Galerkin method based on this IFE space is robust (locking-free).

In [9], the authors modified the stiffness matrix of the IFE method to develop an IFE method for an interface problem with periodic structure on an infinite domain. In [40], with the enhanced stability due to the added penalty, the authors use the

IFE methods contain extra stabilization terms introduced only at interface edges for penalizing the discontinuity in IFE functions to solve the elliptic interface problem. In [43] the author combined the IFE methods and discontinuous Galerkin (DG) to derive a priori error estimates for a class of interior penalty DG methods for a classic second-order elliptic interface problem and got the optimal convergence rate in the energy norm.

IFE methods have been used also for other time dependent problems with moving interfaces, such as in [20], the authors developed several fully discrete IFE schemes for solving the parabolic equation with moving interfaces. In [39], the authors used the IFE methods together with the method of lines (MoL) to solve the parabolic interface problems. The IFE-MoL schemes were extended to handle the nonhomogeneous flux jump conditions with moving interface problems in [38], see [3, 8, 12, 20, 23, 35, 37, 39] for more details.

### 1.3 Outline of the Dissertation

In this dissertation, we focus on the IFE methods for the multi-layer porous wall model. The rest of this dissertation is organized as follows.

In Chapter 2, we construct the linear IFE method to solve the steady-state problem on an uniform partition. The approximation capabilities will be analyzed via the error estimations of the interpolation. Not only can the linear IFE methods be proven to have the optimal convergence rate in both  $L^2$  and  $H^1$  norms, but also numerical results indicate that their convergence rates do not deteriorate when the mesh becomes finer.

In Chapter 3, we solve the elliptic interface problem using the quadratic IFE method on an Cartesian mesh. Error estimation for this quadratic method will be carried out. Finally, we develop numerical schemes based on the quadratic IFE

method to demonstrate features of this quadratic IFE methods.

In Chapter 4, we analyze the long time stability and the asymptotic behavior of the model. With the help of the IFE methods for the spatial discretization, and the implicit Euler scheme for the temporal discretization, respectively, we deduce the global stability of fully discrete solution. Then, we investigate the asymptotic behavior of the discrete scheme which reveals that the multi-layer porous wall model converges to the corresponding elliptic equation if  $f(x; t)$  approaches to a steady-state  $\bar{f}(x)$  as  $t \rightarrow \infty$ . Finally, some numerical experiments are given to verify the theoretical predictions.

In Chapter 5, typical semi-discrete and fully discrete schemes are presented and analyzed. Optimal convergence for the both semi-discrete and fully discrete scheme is proved. Finally, some numerical experiments are provided to confirm our theoretical results.

In Chapter 6, we give some conclusions for this dissertation and discuss the future research plan.



# Chapter 2

## Linear IFE Method

It is clearly that the steady-state problem (1.3)-(1.7) is an interface problem with two types of interface points: the imperfect contact interface point at  $\alpha_0$  and the rough coefficient interface points at  $\alpha_j, 1 \leq j \leq n-1$ . A popular method of solving interface problems with rough coefficients is to use the IFE method. The basic idea of IFE method is to construct special basis functions according to the jump conditions on interface elements while using standard basis functions in the non-interface elements. In this chapter, we develop linear IFE method for the steady-state problem of the multi-layer porous wall model. The steady-state model has its own importance and the IFE spaces developed are also applicable to the dynamic multi-layer porous wall model.

### 2.1 Setting and Weak Solution

In this section, we study the existence and uniqueness of the weak solution for the interface problem described by (1.3)-(1.7). We still use  $u$  in stead of  $\bar{u}$  to denote the concentration in the steady-state problem in the rest of this chapter if there is no danger of causing confusion. We start from the following space for the weak problem:

$$H_\alpha^k(\alpha_{-1}, \alpha_n) = \{v \in L^2(\alpha_{-1}, \alpha_n) \mid v|_{\Omega^\pm} \in H^k(\Omega^\pm), v(\alpha_n) = 0\}, \quad (2.1)$$

where  $k \geq 1$  is an integer and  $\Omega^- = (\alpha_{-1}, \alpha_0)$ ,  $\Omega^+ = (\alpha_0, \alpha_n)$ . On the space  $H_\alpha^k(\alpha_{-1}, \alpha_n)$ , we define the following norm:

$$\|u\|_{k,(\alpha_{-1},\alpha_n)} = \sqrt{\|u\|_{k,\Omega^-}^2 + \|u\|_{k,\Omega^+}^2}. \quad (2.2)$$

In addition, we use  $\|\cdot\|_{0,\Omega}$  to denote the  $L^2$  norm throughout this dissertation. Sometimes, the subscript of the domain  $\Omega$  will be omitted if there is no danger of causing confusion. Multiplying (1.5) by the test function  $v \in H_\alpha^1(\Omega)$ , integrating on the domain  $\Omega$ , and using integration by parts yields

$$\begin{aligned} & \int_{\alpha_{-1}}^{\alpha_n} (-Du' + 2\delta u)'v + \beta uv \, dx \\ &= \int_{\alpha_{-1}}^{\alpha_0} -Du''v \, dx + \int_{\alpha_0}^{\alpha_n} (-Du' + 2\delta u)'v + \beta uv \, dx \\ &= -Du'v|_{\alpha_{-1}}^{\alpha_0} + \int_{\alpha_{-1}}^{\alpha_0} Du'v' \, dx + (-Du'v + 2\delta uv)|_{\alpha_0}^{\alpha_n} + \int_{\alpha_0}^{\alpha_n} (Du' - 2\delta u)v' + \beta uv \, dx. \end{aligned}$$

Using the jump conditions and boundary conditions in (1.3)-(1.7), we have

$$\begin{aligned} & \int_{\alpha_{-1}}^{\alpha_n} (-Du' + 2\delta u)'v + \beta uv \, dx \\ &= \frac{[v]_{\alpha_0}[u]_{\alpha_0}}{\lambda} + \int_{\alpha_{-1}}^{\alpha_n} (v'(x)(Du'(x) - 2\delta u(x)) + \beta v(x)u(x)) \, dx. \end{aligned}$$

Now it is natural to write the following weak problem for the interface problem described by (1.3)-(1.7): find  $u \in H_\alpha^1(\Omega)$  such that

$$a(u, v) = (f, v), \quad \forall v \in H_\alpha^1(\Omega), \quad (2.3)$$

where the bilinear form  $a(u, v)$  is defined as

$$\begin{aligned} a(u, v) &= \frac{[v]_{\alpha_0}[u]_{\alpha_0}}{\lambda} \\ &+ \int_{\alpha_{-1}}^{\alpha_n} (v'(x)(Du'(x) - 2\delta u(x)) + \beta v(x)u(x)) \, dx, \quad \forall u, v \in H_\alpha^1(\Omega). \end{aligned} \quad (2.4)$$

We now consider a bilinear form related with  $a(u, v)$ :

$$a_0(u, v) = \frac{[v]_{\alpha_0}[u]_{\alpha_0}}{\lambda} + \int_{\alpha_{-1}}^{\alpha_n} (Dv'(x)u'(x) + \beta v(x)u(x)) dx, \forall u, v \in H_\alpha^1(\Omega). \quad (2.5)$$

It is obvious that  $a_0(u, v)$  is a symmetric semi-positive-definite bilinear form on  $H_\alpha^1(\Omega)$ . Now, let  $u \in H_\alpha^1(\Omega)$  be such that  $a_0(u, u) = 0$ . Then

$$\frac{([u]_{\alpha_0})^2}{\lambda} + \int_{\alpha_{-1}}^{\alpha_n} (D(u'(x))^2 + \beta(u(x))^2) dx = a_0(u, u) = 0, \quad (2.6)$$

which, because of the positiveness of  $D$  and  $\beta$  described in (1.2), leads to  $\|u\|_{1,(\Omega^+)} = 0$ . This further implies  $u(\alpha_0^+) = 0$ . Then, by (2.6), we have

$$\frac{(u(\alpha_0^-))^2}{\lambda} + \int_{\alpha_{-1}}^{\alpha_0} D_0(u'(x))^2 dx = 0. \quad (2.7)$$

Thus,  $u(\alpha_0^-) = 0$  and  $u'(x) = 0, \forall x \in \Omega^-$ . Therefore,  $u = 0$  on  $\Omega^-$  and we have  $u = 0$  on  $\Omega$ . All of these show that  $a_0(u, v)$  is a symmetric positive-definite bilinear form on  $H_\alpha^1(\Omega)$ ; hence, we can use it to define a norm as follows:

$$\|u\|_{a_0} = \left( \frac{([u]_{\alpha_0})^2}{\lambda} + \int_{\alpha_{-1}}^{\alpha_n} (D(u'(x))^2 + \beta(u(x))^2) dx \right)^{1/2}, \forall u \in H_\alpha^1(\Omega).$$

**Lemma 2.1.** *There exist positive constants  $C_i(D, \beta, \lambda), i = 1, 2$  such that*

$$C_1 \|u\|_{1,(\alpha_{-1}, \alpha_n)} \leq \|u\|_{a_0} \leq C_2 \|u\|_{1,(\alpha_{-1}, \alpha_n)}, \forall u \in H_\alpha^1(\Omega). \quad (2.8)$$

*Proof.* The existence of  $C_2(D, \lambda, \beta)$  for (2.8) follows from the definition of  $\|\cdot\|_{a_0}$  and the Sobolev imbedding theorem; hence, we prove the first inequality by showing the continuity of identity mapping:

$$I : (H_\alpha^1(\Omega), \|\cdot\|_{a_0}) \rightarrow (H_\alpha^1(\alpha_{-1}, \alpha_n), \|\cdot\|_{1,\Omega}),$$



here, the spaces  $(H_\alpha^1(\Omega), \|\cdot\|_{a_0})$  and  $(H_\alpha^1(\Omega), \|\cdot\|_{1,\Omega})$ , denote the linear space  $H_\alpha^1(\Omega)$  as normed spaces with norm  $\|\cdot\|_{a_0}$  and norm  $\|\cdot\|_{1,\Omega}$ , respectively. Let  $u \in H_\alpha^1(\Omega)$  and let  $\{u_m\}_{i=1}^\infty \subseteq H_\alpha^1(\Omega)$  be a sequence such that  $\lim_{m \rightarrow \infty} \|u_m - u\|_{a_0} = 0$ . Then, by

$$\min_{1 \leq i \leq n} \{D_i, \beta_i\} \|u_m - u\|_{1,\Omega^+}^2 \leq \|u_m - u\|_{a_0}^2,$$

we have  $\lim_{m \rightarrow \infty} \|u_m - u\|_{1,\Omega^+} = 0$ . This further implies that  $\lim_{m \rightarrow \infty} |u_m(\alpha_0^+) - u(\alpha_0^+)| = 0$ . Then, from

$$\begin{aligned} & |u_m(\alpha_0^-) - u(\alpha_0^-)| \\ & \leq |u_m(\alpha_0^+) - u(\alpha_0^+)| + \lambda^{1/2} \frac{|(u_m(\alpha_0^+) - u(\alpha_0^+)) - (u_m(\alpha_0^-) - u(\alpha_0^-))|}{\lambda^{1/2}} \\ & \leq |u_m(\alpha_0^+) - u(\alpha_0^+)| + \lambda^{1/2} \|u_m - u\|_{a_0}, \end{aligned}$$

we have  $\lim_{m \rightarrow \infty} |u_m(\alpha_0^-) - u(\alpha_0^-)| = 0$ . In addition, from

$$D_0 \|u'_m - u'\|_{0,\Omega^-}^2 \leq \|u_m - u\|_{a_0},$$

we know that  $\lim_{m \rightarrow \infty} \|u'_m - u'\|_{0,\Omega^-} = 0$ . Finally, by

$$u_m(x) - u(x) = u_m(\alpha_0^-) - u(\alpha_0^-) - \int_x^{\alpha_0} (u'_m(s) - u'(s)) ds,$$

we conclude that  $\lim_{m \rightarrow \infty} \|u_m - u\|_{0,\Omega^-} = 0$ . Therefore,  $\lim_{m \rightarrow \infty} \|u_m - u\|_{1,\Omega^-} = 0$  which, together with  $\lim_{m \rightarrow \infty} \|u_m - u\|_{1,\Omega^+} = 0$ , leads to  $\lim_{m \rightarrow \infty} \|u_m - u\|_{1,\Omega} = 0$ , and the continuity of the identity mapping  $I$  is proven.  $\square$

**Theorem 2.1.** *The bilinear form  $a(u, v)$  defined by (2.4) is continuous and coercive under the assumption that  $(C_1(D, \lambda, \beta))^2 > 2 \max_{1 \leq i \leq n} \delta_i$ . Thus, the weak problem (4.2)*

*admits a unique solution  $u \in H_\alpha^1(\Omega)$  for every  $f \in L^2(\Omega)$ .*

*Proof.* Again, the continuity of  $a(u, v)$  follows directly from its definition and the Sobolev imbedding theorem. Then, by Lemma 2.1, we have

$$\begin{aligned}
a(u, u) &= a_0(u, u) - 2 \int_{\alpha_{-1}}^{\alpha_n} \delta u'(x) u(x) dx = \|u\|_{a_0}^2 - 2 \int_{\alpha_{-1}}^{\alpha_n} \delta u'(x) u(x) dx \\
&\geq (C_1(D, \lambda, \beta))^2 \|u\|_{1, \Omega}^2 - 2 \max_{1 \leq i \leq n} \delta_i \|u\|_{1, \Omega}^2 \\
&= ((C_1(D, \lambda, \beta))^2 - 2 \max_{1 \leq i \leq n} \delta_i) \|u\|_{1, \Omega}^2,
\end{aligned}$$

from which the coercivity follows because of the assumption that  $(C_1(D, \lambda, \beta))^2 > 2 \max_{1 \leq i \leq n} \delta_i$ . Finally, the existence and uniqueness of the weak solution to (4.2) follows from the Lax-Milgram theorem.  $\square$

## 2.2 Local Linear IFE Space for the First Interface

In this section, we develop a linear IFE space on the first interface element and carry out its approximation property. We start from the construction of a linear IFE space for the interface problem. Form a uniform partition  $\mathcal{T}_h$  for the solution domain  $[\alpha_{-1}, \alpha_n]$  as follows:

$$\begin{aligned}
\alpha_{-1} &= x_0 < x_1 < x_2 < \dots < x_i < x_{i+1} < \dots < x_{N-1} < x_N = \alpha_n, \\
h_i &= x_i - x_{i-1} = h, \quad i = 1, 2, \dots, N, \\
\mathcal{T}_h &= \{[x_i, x_{i+1}], \quad i = 0, 1, 2, \dots, N-1\}.
\end{aligned} \tag{2.9}$$

As usual, we call  $\mathcal{N}_h = \{x_i\}_{i=0}^N$  the set of nodes. For each element  $T \in \mathcal{T}_h$ , we call it an interface element if  $T \cap \{\alpha_i\}_{i=0}^{n-1} \neq \emptyset$ ; otherwise, we name it a non-interface element. Without loss of generality, we assume that each interface element contains only one interface point. Throughout this dissertation,  $\mathcal{T}_h^{int}$  denotes the collection of interface elements, and  $\mathcal{T}_h^{non} = \mathcal{T}_h / \mathcal{T}_h^{int}$  denotes the collection of non-interface elements. On each non-interface element  $T = [x_i, x_{i+1}] \in \mathcal{T}_h^{non}$ , we let  $\phi_i(x)$ ,  $\phi_{i+1}(x)$  be the two

linear Lagrange shape functions associated with nodes  $x_i$  and  $x_{i+1}$ , respectively, i.e.,

$$\phi_j(x_k) = \delta_{j,k}, \quad k, j = i, i + 1.$$

Then, we have

$$\phi_i(x) = \frac{x - x_{i+1}}{x_i - x_{i+1}}, \quad \phi_{i+1}(x) = \frac{x - x_i}{x_{i+1} - x_i}.$$

Following the general framework of finite element method, on each non-interface element  $T = [x_i, x_{i+1}]$ , the local linear IFE space is the standard linear finite element space, i.e.,

$$S_h(T) = \text{span}\{\phi_i(x), \phi_{i+1}(x)\}, \quad T = [x_i, x_{i+1}], \quad T \cap \{\alpha_i\}_{i=0}^{n-1} = \emptyset,$$

Our main effort is to develop local linear IFE spaces on all the interface elements. Then, all the local IFE spaces are put together to form a conforming IFE space for solving the interface problem. For the construction of the local linear IFE space on an interface element  $T = [x_i, x_{i+1}]$  containing the  $j$ -th interface point  $\alpha_j$  for  $j \in \{0, 1, 2, \dots, n-1\}$ , we will use the following linear polynomials:

$$\begin{aligned} \check{L}_{i,\alpha_j}(x) &= \frac{\alpha_j - x}{\alpha_j - x_i}, & \check{L}_{\alpha_j,i}(x) &= \frac{x - x_i}{\alpha_j - x_i}, \\ \check{L}_{\alpha_j,i+1}(x) &= \frac{x_{i+1} - x}{x_{i+1} - \alpha_j}, & \check{L}_{i+1,\alpha_j}(x) &= \frac{x - \alpha_j}{x_{i+1} - \alpha_j}. \end{aligned} \tag{2.10}$$

Firstly, let us consider the local linear IFE space on the interface element  $T = [x_i, x_{i+1}]$  such that  $\alpha_0 \in T$ . We note that the interface jump conditions across  $\alpha_0$  are different from those at other interface points. Let

$$\begin{aligned} \psi_i^0(x) &= \begin{cases} \check{L}_{i,\alpha_0}(x) + a_i \check{L}_{\alpha_0,i}(x), & x \in [x_i, \alpha_0], \\ d_i \check{L}_{\alpha_0,i+1}(x), & x \in [\alpha_0, x_{i+1}], \end{cases} \\ \psi_{i+1}^0(x) &= \begin{cases} a_{i+1} \check{L}_{\alpha_0,i}(x), & x \in [x_i, \alpha_0], \\ d_{i+1} \check{L}_{\alpha_0,i+1}(x) + \check{L}_{i+1,\alpha_0}(x), & x \in [\alpha_0, x_{i+1}]. \end{cases} \end{aligned} \tag{2.11}$$

Then  $\psi_i^0(x)$  and  $\psi_{i+1}^0(x)$  are piecewise linear polynomials such that  $\psi_k^0(x_j) = \delta_{kj}$ ,  $j, k = i, i + 1$ . The coefficients in these piecewise linear functions can be further determined by the interface jump conditions across  $\alpha_0$  which is stated in the following theorem.

**Theorem 2.2.** *Coefficients of  $\psi_i^0(x)$  and  $\psi_{i+1}^0(x)$  defined in (2.11) are uniquely determined by interface jump conditions in (1.3) across  $\alpha_0$  such that the coefficients  $a_i, a_{i+1}, d_i, d_{i+1}$  of  $\psi_i^0(x)$  and  $\psi_{i+1}^0(x)$  are as follows:*

$$\begin{aligned}
a_i &= \frac{1}{\Delta}(-D_0\check{L}'_{i,\alpha_0} - 2\lambda D_0\delta_1\check{L}'_{i,\alpha_0} + D_0D_1\lambda\check{L}'_{i,\alpha_0}\check{L}'_{\alpha_0,i+1}), \\
d_i &= \frac{-1}{\Delta}D_0\check{L}'_{i,\alpha_0}, \\
a_{i+1} &= \frac{1}{\Delta}(D_1\check{L}'_{i+1,\alpha_0}), \\
d_{i+1} &= \frac{1}{\Delta}(D_1\check{L}'_{i+1,\alpha_0} + D_0D_1\lambda\check{L}'_{\alpha_0,i}\check{L}'_{i+1,\alpha_0}),
\end{aligned} \tag{2.12}$$

here,  $\Delta = 2\delta_1 + D_0\check{L}'_{\alpha_0,i} - D_1\check{L}'_{\alpha_0,i+1} + 2\delta_1\lambda D_0\check{L}'_{\alpha_0,i} - \lambda D_0D_1\check{L}'_{\alpha_0,i}\check{L}'_{\alpha_0,i+1}$ .

*Proof.* Applying the jump conditions (1.3) across  $\alpha_0$  to  $\psi_i^0(x)$  and  $\psi_{i+1}^0(x)$ , by direct calculations, we can see that  $a_i, d_i$  satisfy

$$\begin{cases} d_i - a_i = \lambda D_0(\check{L}'_{i,\alpha_0} + a_i\check{L}'_{\alpha_0,i}), \\ d_i - a_i = \lambda D_1d_i\check{L}'_{\alpha_0,i+1} - 2\lambda\delta_1d_i, \end{cases}$$

while  $a_{i+1}, d_{i+1}$  satisfy

$$\begin{cases} d_{i+1} - a_{i+1} = \lambda D_0a_{i+1}\check{L}'_{\alpha_0,i}, \\ d_{i+1} - a_{i+1} = \lambda D_1(d_{i+1}\check{L}'_{\alpha_0,i+1} + \check{L}'_{i+1,\alpha_0}) - 2\lambda\delta_1d_{i+1}. \end{cases}$$

It is easy to see that they are two linear systems about  $a_i, d_i, a_{i+1}, d_{i+1}$ , and the determinant of their coefficient matrices both are  $\Delta$ . In addition, by direct calculation,

we get

$$\Delta = 2\delta_1 + \frac{D_0}{\alpha_0 - x_i} + \frac{D_1}{x_{i+1} - \alpha_0} + \frac{2\delta_1\lambda D_0}{\alpha_0 - x_i} + \frac{\lambda D_0 D_1}{(\alpha_0 - x_i)(x_{i+1} - \alpha_0)}.$$

Since each term on the right hand side is positive, we can easily verify that  $\Delta > 0$ . Hence each of these two systems has a unique solution, and  $a_i, a_{i+1}, d_i, d_{i+1}$  are uniquely determined. In addition, they can be expressed as (2.12).  $\square$

Theorem 2.2 indicates that  $\psi_i^0(x)$  and  $\psi_{i+1}^0(x)$  are well defined IFE shape functions on the interface element  $T = [x_i, x_{i+1}]$  containing the first interface points  $\alpha_0$ , and we can then use them to form a local linear IFE space

$$S_h(T) = \text{span}\{\psi_i^0, \psi_{i+1}^0\},$$

where the superscript in  $\psi_i^0$  and  $\psi_{i+1}^0$  emphasizes that this local linear IFE space is for the element  $T = [x_i, x_{i+1}]$  containing the first interface points  $\alpha_0$ .

For the approximation capability, we consider the IFE interpolation in  $S_h(T)$ . For every  $u \in L^2(T)$  such that  $u|_{[x_i, \alpha_0]} \in C^0[x_i, \alpha_0]$  and  $u|_{[\alpha_0, x_{i+1}]} \in C^0[\alpha_0, x_{i+1}]$ , its linear IFE interpolation is

$$\check{I}_h^0 u(x) := u(x_i)\psi_i^0(x) + u(x_{i+1})\psi_{i+1}^0(x). \quad (2.13)$$

Then, by Theorem 2.2, we can write the IFE interpolation as follows

$$\check{I}_h^0 u(x) = \begin{cases} u(x_i)\check{L}_{i,\alpha_0}(x) + u_I^- \check{L}_{\alpha_0,i}(x), & x \in [x_i, \alpha_0], \\ u_I^+ \check{L}_{\alpha_0,i+1}(x) + u(x_{i+1})\check{L}_{i+1,\alpha_0}(x), & x \in (\alpha_0, x_{i+1}], \end{cases} \quad (2.14)$$

where  $u_I^-$  and  $u_I^+$  have the following expression:

$$\begin{aligned} u_I^- &= \frac{1}{\Delta}(-D_0 u(x_i)\check{L}'_{i,\alpha_0} + D_1 u(x_{i+1})\check{L}'_{i+1,\alpha_0} - 2\lambda u(x_i)D_0\check{L}'_{i,\alpha_0}\delta_1 \\ &\quad + D_0 D_1 \lambda u(x_i)\check{L}'_{i,\alpha_0}\check{L}'_{\alpha_0,i+1}), \\ u_I^+ &= \frac{1}{\Delta}(D_0 u(x_i)\check{L}'_{i,\alpha_0} + D_1 u(x_{i+1})\check{L}'_{i+1,\alpha_0} + D_0 D_1 \lambda u(x_{i+1})\check{L}'_{\alpha_0,i}\check{L}'_{i+1,\alpha_0}), \end{aligned}$$

here  $\Delta$  is same to that one used in Theorem 2.2. On the other hand, we can also form a standard linear finite element interpolation of  $u$  on  $T = [x_i, x_{i+1}]$  as follows

$$\tilde{I}_h^0 u(x) := \begin{cases} u(x_i)\check{L}_{i,\alpha_0}(x) + u(\alpha_0^-)\check{L}_{\alpha_0,i}(x), & x \in [x_i, \alpha_0], \\ u(\alpha_0^+)\check{L}_{\alpha_0,i+1}(x) + u(x_{i+1})\check{L}_{i+1,\alpha_0}(x), & x \in [\alpha_0, x_{i+1}]. \end{cases} \quad (2.15)$$

Then, we have the following standard error estimates for linear finite element interpolation:

$$\begin{aligned} \|u - \tilde{I}_h^0\|_{0,(x_i,\alpha_0)} + h\|u - \tilde{I}_h^0\|_{1,(x_i,\alpha_0)} &\leq Ch^2\|u\|_{2,(x_i,\alpha_0)}, \\ \|u - \tilde{I}_h^0\|_{0,(\alpha_0,x_{i+1})} + h\|u - \tilde{I}_h^0\|_{1,(\alpha_0,x_{i+1})} &\leq Ch^2\|u\|_{2,(\alpha_0,x_{i+1})}, \end{aligned} \quad (2.16)$$

provided further that  $u|_{(x_i,\alpha_0)} \in H^2(x_i, \alpha_0)$  and  $u|_{(\alpha_0,x_{i+1})} \in H^2(\alpha_0, x_{i+1})$ .

We can then estimate the error in  $\tilde{I}_h^0 u$  by the splitting  $u - \tilde{I}_h^0 u = u - \tilde{I}_h^0 u + \tilde{I}_h^0 u - \tilde{I}_h^0 u$ .

**Theorem 2.3.** *Let  $T = [x_i, x_{i+1}]$  be an interface element containing the first interface point  $\alpha_0$ . Then, for every  $u \in L^2(T)$  such that  $u|_{(x_i,\alpha_0)} \in H^2(x_i, \alpha_0)$  and  $u|_{(\alpha_0,x_{i+1})} \in H^2(\alpha_0, x_{i+1})$ , we have*

$$\|u - \tilde{I}_h^0 u\|_{0,(x_i,x_{i+1})} + h\|u - \tilde{I}_h^0 u\|_{1,(x_i,x_{i+1})} \leq Ch^2\|u\|_{2,(x_i,x_{i+1})}, \quad (2.17)$$

where  $C$  is a constant independent of  $\alpha_0 \in [x_i, x_{i+1}]$ .

*Proof.* By (2.14) and (2.15), we have

$$\tilde{I}_h^0 u - \tilde{I}_h^0 u = \begin{cases} (u(\alpha^-) - u_I^-)\check{L}_{\alpha_0,i}(x), & x \in [x_i, \alpha_0], \\ (u(\alpha^+) - u_I^+)\check{L}_{\alpha_0,i+1}(x), & x \in [\alpha_0, x_{i+1}]. \end{cases} \quad (2.18)$$

By simple calculations and the jump conditions, we have

$$\begin{aligned} |u(\alpha^+) - u_I^+| &= \frac{1}{\Delta} | -D_0(\tilde{I}_h^0 u - u)'(\alpha_0^-) + D_1(\tilde{I}_h^0 u - u)'(\alpha_0^+) \\ &\quad + D_0 D_1 \lambda \check{L}'_{\alpha_0,i}(\tilde{I}_h^0 u - u)'(\alpha_0^+) | \\ &\leq \frac{1}{\Delta} (|J_1| + |J_2| + |J_3|), \end{aligned} \quad (2.19)$$

where

$$J_1 = D_0 e'(\alpha_0^-), \quad J_2 = D_1 e'(\alpha_0^+), \quad J_3 = D_0 D_1 \lambda \check{L}'_{\alpha_0, i} e'(\alpha_0^+),$$

with  $e(x) = \tilde{I}_h^0 u(x) - u(x)$ . Because  $e(x_i) = e(\alpha_0^-) = e(\alpha_0^+) = e(x_{i+1}) = 0$ , we have

$$|e'(\alpha_0^-)| \leq (\alpha_0 - x_i)^{1/2} \|u\|_{2, (x_i, \alpha_0)}, \quad |e'(\alpha_0^+)| \leq (x_{i+1} - \alpha_0)^{1/2} \|u\|_{2, (x_i, \alpha_0)}.$$

Then, following the standard procedure, we obtain

$$\begin{aligned} |J_1| &\leq D_0 (\alpha_0 - x_i)^{\frac{1}{2}} \|u\|_{2, (x_i, \alpha_0)}, \\ |J_2| &\leq D_1 (x_{i+1} - \alpha_0)^{\frac{1}{2}} \|u\|_{2, (\alpha_0, x_{i+1})}, \\ |J_3| &\leq D_0 D_1 (\alpha_0 - x_i)^{-1} (x_{i+1} - \alpha_0)^{\frac{1}{2}} \|u\|_{2, (\alpha_0, x_{i+1})}. \end{aligned}$$

In addition, the following estimate for  $\Delta$  holds:

$$\frac{1}{\Delta} \leq C \min\{(\alpha_0 - x_i), (x_{i+1} - \alpha_0), (\alpha_0 - x_i)(x_{i+1} - \alpha_0)\}.$$

We can easily get that

$$\begin{aligned} \frac{|J_1|}{\Delta} &\leq C (\alpha_0 - x_i)^{\frac{3}{2}} \|u\|_{2, (x_i, \alpha_0)} \leq Ch^{\frac{3}{2}} \|u\|_{2, (x_i, \alpha_0)}, \\ \frac{|J_2|}{\Delta} &\leq C (x_{i+1} - \alpha_0)^{\frac{3}{2}} \|u\|_{2, (\alpha_0, x_{i+1})} \leq Ch^{\frac{3}{2}} \|u\|_{2, (\alpha_0, x_{i+1})}, \\ \frac{|J_3|}{\Delta} &\leq C (x_{i+1} - \alpha_0)^{\frac{3}{2}} \|u\|_{2, (\alpha_0, x_{i+1})} \leq Ch^{\frac{3}{2}} \|u\|_{2, (\alpha_0, x_{i+1})}. \end{aligned}$$

Then, by applying these estimates to (2.19) and using the norm defined in (2.2), we obtain

$$|u_I^+ - u(\alpha^+)| \leq Ch^{\frac{3}{2}} (\|u\|_{2, (x_i, \alpha_0)} + \|u\|_{2, (\alpha_0, x_{i+1})}) \leq Ch^{\frac{3}{2}} \|u\|_{2, (x_i, x_{i+1})}.$$

Hence, by (2.18) and the fact that

$$\|\check{L}_{\alpha_0, i+1}(x)\|_{0, (\alpha_0, x_{i+1})} + h \|\check{L}_{\alpha_0, i+1}(x)\|_{1, (\alpha_0, x_{i+1})} \leq Ch^{1/2},$$

we have

$$\|\tilde{I}_h^0 u - \check{I}_h^0 u\|_{0,(\alpha_0, x_{i+1})} + h\|\tilde{I}_h^0 u - \check{I}_h^0 u\|_{1,(\alpha_0, x_{i+1})} \leq Ch^2\|u\|_{2,(x_i, x_{i+1})}. \quad (2.20)$$

Since  $\|u - \check{I}_h^0 u\|_{k,(\alpha_0, x_{i+1})} \leq \|u - \tilde{I}_h^0 u\|_{k,(\alpha_0, x_{i+1})} + \|\tilde{I}_h^0 u - \check{I}_h^0 u\|_{k,(\alpha_0, x_{i+1})}$ ,  $k = 0, 1$ , by (2.16) and (2.20), we have the following estimate:

$$\|u - \check{I}_h^0 u\|_{0,(\alpha_0, x_{i+1})} + h\|u - \check{I}_h^0 u\|_{1,(\alpha_0, x_{i+1})} \leq Ch^2\|u\|_{2,(x_i, x_{i+1})}. \quad (2.21)$$

Similarly, we can show

$$\|u - \check{I}_h^0 u\|_{0,(x_i, \alpha_0)} + h\|(u - \check{I}_h^0 u)\|_{1,(x_i, \alpha_0)} \leq Ch^2\|u\|_{2,(x_i, x_{i+1})}. \quad (2.22)$$

Finally, estimates given in (2.17) follows from (2.21) together with (2.22).  $\square$

## 2.3 Local Linear IFE Space for Other Interfaces

We now consider the local linear IFE space on the interface element  $T = [x_i, x_{i+1}]$  such that  $\alpha_j \in T$  for an integer  $j \in \{1, 2, \dots, n-1\}$ . As before, we let

$$\begin{aligned} \psi_i^j(x) &= \begin{cases} \check{L}_{i, \alpha_j}(x) + b_i \check{L}_{\alpha_j, i}(x), & x \in [x_i, \alpha_j], \\ c_i \check{L}_{\alpha_j, i+1}(x), & x \in [\alpha_j, x_{i+1}], \end{cases} \\ \psi_{i+1}^j(x) &= \begin{cases} b_{i+1} \check{L}_{\alpha_j, i}(x), & x \in [x_i, \alpha_j], \\ c_{i+1} \check{L}_{\alpha_j, i+1}(x) + \check{L}_{i+1, \alpha_j}(x), & x \in [\alpha_j, x_{i+1}]. \end{cases} \end{aligned} \quad (2.23)$$

We note that the interface jump conditions at  $\alpha_j$ ,  $j \in \{1, 2, \dots, n-1\}$  are the same type and they can be used to determine coefficients in  $\psi_i^j(x)$  and  $\psi_{i+1}^j(x)$  as stated in the following theorem.

**Theorem 2.4.** *Assume that  $\delta_j \leq \delta_{j+1}$ , then coefficients of  $\psi_i^j(x)$  and  $\psi_{i+1}^j(x)$  defined by (2.23) are uniquely determined by interface jump conditions in (1.4) across  $\alpha_j$  such*



that the coefficients  $b_i, b_{i+1}, c_i, c_{i+1}$  of  $\psi_i^j(x)$  and  $\psi_{i+1}^j(x)$  are as follows:

$$\begin{aligned} b_i &= c_i = \frac{-1}{\Delta} D_j \check{L}'_{i,\alpha_j}, \\ b_{i+1} &= c_{i+1} = \frac{1}{\Delta} D_{j+1} \check{L}'_{i+1,\alpha_j}, \end{aligned} \tag{2.24}$$

here,  $\Delta = -D_{j+1} \check{L}'_{\alpha_j, i+1} + D_j \check{L}'_{\alpha_j, i} + 2\delta_{j+1} - 2\delta_j$ .

Before we go to the proof, we should mention here that the  $\Delta$  we used here has a new value different from the one in Theorem 2.2. This abuse will not cause any confusion, since each  $\Delta$  appear in its theorem only. Throughout this dissertation, there are several times of this kind of reuse about  $\Delta$ .

*Proof.* By applying the jump conditions in (1.4) across  $\alpha_j$  to  $\psi_i^j(x)$  and  $\psi_{i+1}^j(x)$ , we can see that coefficients  $b_i$  and  $c_i$  satisfy

$$\begin{cases} b_i = c_i, \\ D_j(\check{L}'_{i,\alpha_j} + b_i \check{L}'_{\alpha_j, i}) - 2\delta_j b_i = D_{j+1} c_i \check{L}'_{\alpha_j, i+1} - 2\delta_{j+1} c_i, \end{cases}$$

while  $b_{i+1}$  and  $c_{i+1}$  satisfy

$$\begin{cases} b_{i+1} = c_{i+1}, \\ D_j b_{i+1} \check{L}'_{\alpha_j, i} - 2\delta_j b_{i+1} = D_{j+1}(c_{i+1} \check{L}'_{\alpha_j, i+1} + \check{L}'_{i+1,\alpha_j}) - 2\delta_{j+1} c_{i+1}. \end{cases}$$

The determinant of coefficient matrices in these two linear systems is  $\Delta$ . Since  $\delta_{i+1} \geq \delta_i$ , it can be easy to shown that  $\Delta > 0$ . Hence each of these two systems must have a unique solution, respectively, and  $b_i, b_{i+1}, c_i, c_{i+1}$  are uniquely determined and they can expressed as in (2.24).  $\square$

**Remark 2.1.** *It seems to the authors that the assumption  $\delta_j \leq \delta_{j+1}$  is a reasonable assumption for practical applications. Recall that  $\delta_j$  is the convection parameter in*

the layer  $[\alpha_{j-1}, \alpha_j]$ . According to the model setup, a larger  $j$  means the layer  $[\alpha_{j-1}, \alpha_j]$  is closer to the blood flow in the artery; hence, it is reasonable to assume a larger convection there.

It is obvious that functions  $\psi_k^j(x)$ ,  $k = i, i + 1$  defined by (2.23) are such that  $\psi_k^j(x_l) = \delta_{k,l}$ ,  $k, l = i, i + 1$ . Again, these functions are linear IFE shape functions and they can be used to define a local linear IFE space:

$$S_h(T) = \text{span}\{\psi_i^j, \psi_{i+1}^j\},$$

where the superscript in  $\psi_i^j$  and  $\psi_{i+1}^j$  emphasizes that this local linear IFE space is for the  $T = [x_i, x_{i+1}]$  containing the  $j$ -th interface point  $\alpha_j$  for  $j \in \{1, 2, \dots, n-1\}$ .

For the approximation capability of  $S_h(T)$  with  $\alpha_j \in T$  for some  $j \in \{1, 2, \dots, n-1\}$ , we consider the error in the linear IFE interpolation in  $S_h(T)$ . For every  $u \in C^0(T) = C^0([x_i, x_{i+1}])$ , its linear IFE interpolation is

$$\check{I}_h^j u(x) := u(x_i)\psi_i^j(x) + u(x_{i+1})\psi_{i+1}^j(x). \quad (2.25)$$

By Theorem 2.4, the linear IFE interpolation on  $T = [x_i, x_{j+1}]$  can be written as

$$\check{I}_h^j u(x) = \begin{cases} u(x_i)\check{L}_{i,\alpha_j}(x) + u_{\alpha_j}^I \check{L}_{\alpha_j,i}(x), & x \in [x_i, \alpha_j], \\ u_{\alpha_j}^I \check{L}_{\alpha_j,i+1}(x) + u(x_{i+1})\check{L}_{i+1,\alpha_j}(x), & x \in [\alpha_j, x_{i+1}], \end{cases} \quad (2.26)$$

here,

$$u_{\alpha_j}^I = \frac{1}{\Delta} (-u(x_i)D_j \check{L}'_{i,\alpha_j} + u(x_{i+1})D_{j+1} \check{L}'_{i+1,\alpha_j}).$$

We can also form the standard linear Lagrange interpolation of  $u$  on  $T = [x_i, x_{i+1}]$  as follows:

$$\check{I}_h^j u(x) := \begin{cases} u(x_i)\check{L}_{i,\alpha_j}(x) + u(\alpha_j)\check{L}_{\alpha_j,i}(x), & x \in [x_i, \alpha_j], \\ u(\alpha_j)\check{L}_{\alpha_j,i+1}(x) + u(x_{i+1})\check{L}_{i+1,\alpha_j}(x), & x \in [\alpha_j, x_{i+1}]. \end{cases} \quad (2.27)$$

The standard finite element approximation theory provides the following error bounds for  $\tilde{I}_h^j u$ :

$$\begin{aligned} \|u - \tilde{I}_h^j u\|_{0,(x_i,\alpha_j)} + h\|u - \tilde{I}_h^j u\|_{1,(x_i,\alpha_j)} &\leq Ch^2\|u\|_{2,(x_i,\alpha_j)}, \\ \|u - \tilde{I}_h^j u\|_{0,(\alpha_j,x_{i+1})} + h\|u - \tilde{I}_h^j u\|_{1,(\alpha_j,x_{i+1})} &\leq Ch^2\|u\|_{2,(\alpha_j,x_{i+1})}. \end{aligned} \quad (2.28)$$

We now turn to the error estimation for  $u - \check{I}_h^j u$ .

**Theorem 2.5.** *Let  $T = [x_i, x_{i+1}]$  be an interface element containing the  $j$ -th interface point  $\alpha_j$ ,  $j = 1, 2, \dots, n-1$  and assume that  $\delta_j \leq \delta_{j+1}$ . Then, for every  $u \in C^0(T)$  such that  $u|_{(x_i,\alpha_j)} \in H^2(x_i, \alpha_j)$  and  $u|_{(\alpha_j,x_{i+1})} \in H^2(\alpha_j, x_{i+1})$ , we have*

$$\|u - \check{I}_h^j u\|_{0,(x_i,x_{i+1})} + h\|u - \check{I}_h^j u\|_{1,(x_i,x_{i+1})} \leq Ch^2\|u\|_{2,(x_i,x_{i+1})}, \quad (2.29)$$

where  $C$  is a constant independent of  $\alpha_j \in [x_i, x_{i+1}]$ .

*Proof.* Let us consider the estimation on the subelement  $[x_i, \alpha_j]$ . By the jump conditions, we have

$$\tilde{I}_h^j u(x) - \check{I}_h^j u(x) = (u(\alpha_j) - u_{\alpha_j}^I) \check{L}_{\alpha_j,i}(x) = \frac{x_i - x}{\Delta(x_{i+1} - \alpha_j)(\alpha_j - x_i)} (I + II + III), \quad (2.30)$$

here

$$\begin{aligned} I &= D_j \check{L}_{i,\alpha_j}(x_{i+1})(u(\alpha_j) - u(x_i)), \\ II &= D_{j+1}(u(x_{i+1}) - u(\alpha_j)), \\ III &= -2u(\alpha_j)(x_{i+1} - \alpha_j)(\delta_{j+1} - \delta_j). \end{aligned}$$

Clearly, we have

$$\int_{x_i}^{\alpha_j} \int_x^{\alpha_j} u''(y) dy dx = u'(\alpha_j^-)(\alpha_j - x_i) + (u(x_i) - u(\alpha_j^-)),$$

and

$$\int_{\alpha_j}^{x_{i+1}} \int_{\alpha_j}^x u''(y) dy dx = (u(x_{i+1}) - u(\alpha_j^+)) - u'(\alpha_j^+)(x_{i+1} - \alpha_j),$$

which means

$$\begin{aligned}
I + II &= -D_j \check{L}_{i,\alpha_j}(x_{i+1}) \int_{x_i}^{\alpha_j} \int_x^{\alpha_j} u''(y) dy dx + D_{j+1} \int_{\alpha_j}^{x_{i+1}} \int_{\alpha_j}^x u''(y) dy dx \\
&\quad + D_{j+1} u'(\alpha_j^+)(x_{i+1} - \alpha_j) - D_j(x_{i+1} - \alpha_j) u'(\alpha_j^-), \\
&= J_1 + J_2,
\end{aligned} \tag{2.31}$$

where

$$\begin{aligned}
J_1 &= -D_j \check{L}_{i,\alpha_j}(x_{i+1}) \int_{x_i}^{\alpha_j} \int_x^{\alpha_j} u''(y) dy dx + D_{j+1} \int_{\alpha_j}^{x_{i+1}} \int_{\alpha_j}^x u''(y) dy dx, \\
J_2 &= D_{j+1} u'(\alpha_j^+)(x_{i+1} - \alpha_j) - D_j(x_{i+1} - \alpha_j) u'(\alpha_j^-).
\end{aligned}$$

By the jump condition at  $\alpha_j$ , we have

$$\begin{aligned}
&J_2 + III \\
&= (D_{j+1} u'(\alpha_j^+) - 2\delta_{j+1} u(\alpha_j^+) - D_j u'(\alpha_j^-) + 2\delta_j u(\alpha_j^-))(x_{i+1} - \alpha_j) = 0.
\end{aligned} \tag{2.32}$$

Then, it remains to estimate  $J_1$ . Noted that

$$\begin{aligned}
|J_1| &\leq D_j |\check{L}_{i,\alpha_j}(x_{i+1})| \int_{x_i}^{\alpha_j} \int_{x_i}^{\alpha_j} |u''(y)| dy dx + D_{j+1} \int_{\alpha_j}^{x_{i+1}} \int_{\alpha_j}^{x_{j+1}} |u''(y)| dy dx \\
&\leq Ch^{3/2} \|u\|_{2,(x_i,x_{i+1})},
\end{aligned}$$

by using the assumption that  $\delta_{j+1} \geq \delta_j$ , we have

$$\Delta(x_{i+1} - \alpha_j)(\alpha_j - x_i) \geq D_j(x_{i+1} - \alpha_j) + D_{j+1}(\alpha_j - x_i) \geq \min\{D_j, D_{j+1}\}h.$$

Therefore,

$$\left| \frac{J_1}{\Delta(x_{i+1} - \alpha_j)(\alpha_j - x_i)} \right| \leq Ch^{1/2} \|u\|_{2,(x_i,x_{i+1})}. \tag{2.33}$$

Then, applying (2.31), (2.32), and (2.33) to (2.30), we obtain

$$\begin{aligned}
& \|\tilde{I}_h^j u - \check{I}_h^j u\|_{0,(x_i,\alpha_j)} \\
& \leq Ch^{1/2} \|x - x_i\|_{0,(x_i,\alpha_j)} \|u\|_{2,(x_i,x_{i+1})} \\
& \leq Ch^{1/2} \left( \int_{x_i}^{\alpha_j} |x - x_i|^2 dx \right)^{1/2} \|u\|_{2,(x_i,x_{i+1})} \leq Ch^2 \|u\|_{2,(x_i,x_{i+1})},
\end{aligned}$$

and  $\|\tilde{I}_h^j u - \check{I}_h^j u\|_{1,(x_i,\alpha_j)} \leq Ch \|u\|_{2,(x_i,x_{i+1})}$ . These two estimates lead to

$$\|\tilde{I}_h^j u - \check{I}_h^j u\|_{0,(x_i,\alpha_j)} + h \|\tilde{I}_h^j u - \check{I}_h^j u\|_{1,(x_i,\alpha_j)} \leq Ch^2 \|u\|_{2,(x_i,x_{i+1})}.$$

Applying the similar arguments to the subelement  $[\alpha_j, x_{i+1}]$ , we obtain

$$\|\tilde{I}_h^j u - \check{I}_h^j u\|_{0,(\alpha_j,x_{i+1})} + h \|\tilde{I}_h^j u - \check{I}_h^j u\|_{1,(\alpha_j,x_{i+1})} \leq Ch^2 \|u\|_{2,(x_i,x_{i+1})}.$$

Hence, we have

$$\|\tilde{I}_h^j u - \check{I}_h^j u\|_{0,(x_i,x_{i+1})} + h \|\tilde{I}_h^j u - \check{I}_h^j u\|_{1,(x_i,x_{i+1})} \leq Ch^2 \|u\|_{2,(x_i,x_{i+1})}.$$

Finally, using the triangle inequality and the classical approximation result (2.28),

we can derive the estimate in (2.29) as follows:

$$\begin{aligned}
& \|u - \check{I}_h^j u\|_{0,(x_i,x_{i+1})} + h \|u - \check{I}_h^j u\|_{1,(x_i,x_{i+1})} \\
& \leq \|u - \tilde{I}_h^j u\|_{0,(x_i,x_{i+1})} + h \|u - \tilde{I}_h^j u\|_{1,(x_i,x_{i+1})} \\
& \quad + \|\tilde{I}_h^j u - \check{I}_h^j u\|_{0,(x_i,x_{i+1})} + h \|\tilde{I}_h^j u - \check{I}_h^j u\|_{1,(x_i,x_{i+1})} \\
& \leq Ch^2 \|u\|_{2,(x_i,x_{i+1})}.
\end{aligned}$$

□

## 2.4 Convergence of the Linear IFE Space

Using the local linear IFE spaces on each element  $T \in \mathcal{T}_h$ , we can define a linear IFE space globally on whole solution domain  $(\alpha_{-1}, \alpha_n)$  as follows:

$$S_h(\alpha_{-1}, \alpha_n) = \{v \in L^2(\alpha_{-1}, \alpha_n) \mid v|_{\Omega^\pm} \in C^0(\Omega^\pm), v|_T \in S_h(T), \forall T \in \mathcal{T}_h\},$$

where, we recall that the local linear IFE space  $S_h(T)$  is defined by

$$S_h^{(1)}(T) = \begin{cases} \text{span}\{\phi_i, \phi_{i+1}\}, & T = [x_i, x_{i+1}], T \cap \{\alpha_i\}_{i=0}^{n-1} = \emptyset, \\ \text{span}\{\psi_i^j, \psi_{i+1}^j\}, & T = [x_i, x_{i+1}], \alpha_j \in T, j \in \{0, 1, 2, \dots, n-1\}. \end{cases}$$

For a function  $u \in H_\alpha^1(\alpha_{-1}, \alpha_n)$ , we define its linear IFE interpolation  $\check{I}_h u \in S_h(\alpha_{-1}, \alpha_n)$  piecewisely such that, for every element  $T = [x_i, x_{i+1}]$ ,

$$\check{I}_h u|_T = \begin{cases} u(x_i)\phi_i(x) + u(x_{i+1})\phi_{i+1}(x), & \text{when } T \cap \{\alpha_i\}_{i=0}^{n-1} = \emptyset, \\ u(x_i)\psi_i^j(x) + u(x_{i+1})\psi_{i+1}^j(x), & \text{when } \alpha_j \in T, j \in \{0, 1, 2, \dots, n-1\}. \end{cases}$$

Then, we derive an error bound for the linear IFE interpolation in the following theorem.

**Theorem 2.6.** *Assume that  $\delta_j \leq \delta_{j+1}$ ,  $j = 1, 2, \dots, n-1$ , then there exists a positive constant  $C$  independent of  $h$  and the position of  $\alpha_j$ ,  $j = 0, 1, \dots, n-1$  such that*

$$\|u - \check{I}_h u\|_{0,(\alpha_{-1}, \alpha_n)} + h\|u - \check{I}_h u\|_{1,(\alpha_{-1}, \alpha_n)} \leq Ch^2\|u\|_{2,(\alpha_{-1}, \alpha_n)}, \forall u \in H_\alpha^2(\alpha_{-1}, \alpha_n). \quad (2.34)$$

*Proof.* By the definition of  $\check{I}_h u$ , we have for  $k = 1, 2$ ,

$$\begin{aligned} \|u - \check{I}_h u\|_{k,(\alpha_{-1}, \alpha_n)} &= \sum_{T \in \mathcal{T}_h} \|u - \check{I}_h^j u\|_{k,T} \\ &= \sum_{T \in \mathcal{T}_h^{non}} \|u - \check{I}_h^j u\|_{k,T} + \sum_{T \in \mathcal{T}_h^{int}} \|u - \check{I}_h^j u\|_{k,T}, \\ &= \sum_{T \in \mathcal{T}_h^{non}} \|u - \tilde{I}_h u\|_{k,T} + \sum_{T \in \mathcal{T}_h^{int}} \|u - \check{I}_h^j u\|_{k,T}. \end{aligned}$$

Then, estimates for the standard linear finite element interpolation error  $\|u - \tilde{I}_h u\|_{k,T}$ ,  $T \in \mathcal{T}_h^{non}$  and the estimates for the linear IFE interpolation error  $\|u - \check{I}_h u\|_{k,T}$ ,  $T \in \mathcal{T}_h^{int}$  given in Theorems 2.3 and 2.5 imply that

$$\|u - \check{I}_h u\|_{k,(\alpha_{-1}, \alpha_n)} \leq Ch^{2-k}\|u\|_{2,(\alpha_{-1}, \alpha_n)}, \quad k = 0, 1,$$

which further leads to (2.34).  $\square$

We now discuss the linear IFE solution to the interface problem described by (1.3)-(1.7). Let

$$S_{h,0}(\alpha_{-1}, \alpha_n) = \{v | v \in S_h(\alpha_{-1}, \alpha_n), v|_{x=\alpha_n} = 0\},$$

and the linear IFE solution  $u_h \in S_{h,0}(\alpha_{-1}, \alpha_n)$  is then defined to be such that

$$a(u_h, v_h) = (f, v_h), \forall v_h \in S_{h,0}(\alpha_{-1}, \alpha_n). \quad (2.35)$$

The error bound for the linear IFE solution  $u_h$  is given in the following theorem.

**Theorem 2.7.** *Assume the condition required by Theorem 2.1 holds,  $\delta_j \leq \delta_{j+1}$ ,  $j = 1, 2, \dots, n-1$ , and that the solution  $u$  to the weak problem (4.2) is such that  $u \in H_\alpha^2(\alpha_{-1}, \alpha_n)$ . Then the linear IFE solution  $u_h$  defined by (2.35) satisfies the following estimate:*

$$\|u - u_h\|_{0,(\alpha_{-1}, \alpha_n)} + h\|u - u_h\|_{1,(\alpha_{-1}, \alpha_n)} \leq Ch^2\|u\|_{2,(\alpha_{-1}, \alpha_n)}. \quad (2.36)$$

*Proof.* It is easy to see that

$$a(u - u_h, v_h) = 0, \forall v_h \in V_h.$$

Hence, by using Theorem 2.1, we have

$$\begin{aligned} \|u - u_h\|_{1,(\alpha_{-1}, \alpha_n)}^2 &\leq Ca(u - u_h, u - u_h) = a(u - u_h, u - v_h) \\ &\leq C\|u - u_h\|_{1,(\alpha_{-1}, \alpha_n)}\|u - v_h\|_{1,(\alpha_{-1}, \alpha_n)}. \end{aligned}$$

The above inequality together with Theorem 2.6 imply

$$\begin{aligned} \|u - u_h\|_{1,(\alpha_{-1}, \alpha_n)} &\leq C \inf_{v \in S_{h,0}^{(1)}(\alpha_{-1}, \alpha_n)} \|u - v\|_{1,(\alpha_{-1}, \alpha_n)} \\ &\leq C\|u - \tilde{I}_h u\|_{1,(\alpha_{-1}, \alpha_n)} \leq Ch\|u\|_{2,(\alpha_{-1}, \alpha_n)}. \end{aligned}$$

Using the usual duality argument, we get

$$\|u - u_h\|_{0,(\alpha_{-1},\alpha_n)} \leq Ch^2 \|u\|_{2,(\alpha_{-1},\alpha_n)}.$$

Then, (2.36) is proven.  $\square$

## 2.5 Numerical Experiments

In this section we present numerical examples for demonstrating the convergence of the linear IFE methods. We let the simulation interval be  $[0, 1]$ , and assume there are three interface points:  $\alpha_0 = 1/9$ ,  $\alpha_1 = 1/3$  and  $\alpha_2 = 2/3$ . These interface points separate the interval into four sub-intervals  $[0, 1/9]$ ,  $[1/9, 1/3]$ ,  $[1/3, 2/3]$  and  $[2/3, 1]$ . We set the exact solution  $u$  for this problem to be

$$u(x) = \begin{cases} u_0(x), & x \in [0, 1/9], \\ u_1(x), & x \in [1/9, 1/3], \\ u_2(x), & x \in [1/3, 2/3], \\ u_3(x), & x \in [2/3, 1], \end{cases} \quad (2.37)$$

with

$$u_0(x) = \frac{1}{30}x^{n-1}, \quad u_1(x) = \frac{1}{3}x^n, \quad u_2(x) = x^{n+1}, \quad u_3(x) = 3(1-x)x^{n+1},$$

here,  $n$  is an integer. We also let

$$\begin{aligned} D_1 &= \frac{18(n-1)D_0}{10n}, & \delta_1 &= \frac{1}{2}(9nD_1 - 8.1(n-1)D_0), \\ D_2 &= \frac{6nD_1 - 2\delta_1}{3(n+1)}, & \delta_2 &= \frac{1}{2}(3(n+1)D_2 - 3nD_1 + 2\delta_1), \\ D_3 &= \frac{8\delta_2 - 3(n+1)D_2}{3(n+5)}, & \delta_3 &= \frac{1}{4}(3(n-1)D_3 - 3(n+1)D_2 + 4\delta_2), \\ \lambda &= \frac{1}{81(n-1)D_0}. \end{aligned}$$



Then we can verify that  $u(x)$  satisfies the jump conditions (1.3)-(1.4). The right hand side term  $f_i(x)$ ,  $i = 0, 1, 2, 3$ , is determined by (1.5). We now report numerical results generated by applying the IFE methods developed in Section 2.2-Section 2.4 to the interface problem described by (1.3)-(1.7) whose exact solution is  $u(x)$  defined in (3.44).

**Example 2.1.** *In this group of numerical experiments, we observe that the proposed IFE methods work well for large values of  $\beta_i$ ,  $i = 1, 2, 3$  emphasizing a stronger reaction. We have tested these IFE methods with  $D_0$  arbitrarily chosen between  $10^{-2}$  and  $2 \times 10^{-2}$  and  $\beta_1 \in (1, 2)$ ,  $\beta_2 \in (10^2, 2 \times 10^2)$ ,  $\beta_3 \in (10^4, 2 \times 10^4)$ .*

Table 2.1: Errors and convergence rates of the linear IFE method when  $n = 3$  with large values for  $\beta_j, j = 1, 2, 3$ .

N	$L^2$ norm	rate	$H^1$ norm	rate
10	4.3701e-03		2.2745e-01	
20	9.1751e-04	2.2519	1.1101e-01	1.0348
40	2.0358e-04	2.1721	5.4916e-02	1.0154
80	4.7784e-05	2.0910	2.7257e-02	1.0106
160	1.1416e-05	2.0655	1.3569e-02	1.0063
320	2.8087e-06	2.0231	6.7707e-03	1.0030
640	6.9626e-07	2.0122	3.3820e-03	1.0014
1280	1.7385e-07	2.0018	1.6906e-03	1.0004
2560	4.3403e-08	2.0019	8.4523e-04	1.0001

Tables 2.1 and 2.2 present typical numerical results for errors and the convergence rates for the linear IFE method when  $n = 3$  and  $n = 6$ , respectively. In related computations for these data, we used the following parameters:

$$D_0 = 0.010616229584014, \beta_0 = 0, \beta_1 = 1.72333131659,$$

$$\beta_2 = 140.10036408113, \beta_3 = 16730.88858585343.$$

Data in these tables clearly show that the linear and quadratic IFE methods converge optimally in both the  $L^2$  and  $H^1$  norm.

Table 2.2: Errors and convergence rates the linear IFE method with  $n = 6$  and large values for  $\beta_j, j = 1, 2, 3$ .

N	$L^2$ norm	rate	$H^1$ norm	rate
10	5.8815e-03		2.7493e-01	
20	1.3050e-03	2.1721	1.4092e-01	0.9642
40	2.8071e-04	2.2169	6.9235e-02	1.0253
80	6.3358e-05	2.1475	3.4282e-02	1.0140
160	1.4811e-05	2.0968	1.6990e-02	1.0128
320	3.5812e-06	2.0482	8.4612e-03	1.0058
640	8.8460e-07	2.0173	4.2231e-03	1.0026
1280	2.2033e-07	2.0054	2.1106e-03	1.0006
2560	5.5041e-08	2.0011	1.0552e-03	1.0002

**Example 2.2.** *We have observed that the IFE methods also work well for small values of  $\beta_i, i = 1, 2, 3$  which let the model described by the interface problem (1.3)-(1.7) emphasize the diffusion or convection more than the reaction. In this group of numerical experiments, we have tested the IFE methods for  $\beta_i, i = 1, 2, 3$  randomly chosen such that  $\beta_1 \in (0.01, 0.02), \beta_2 \in (0.001, 0.002), \beta_3 \in (0.0001, 0.0002)$ .*

Table 2.3: Errors and convergence rates of the linear IFE method when  $n = 3$  with small values for  $\beta_j, j = 1, 2, 3$ .

N	$L^2$ norm	rate	$H^1$ norm	rate
10	4.9674e-03		2.1563e-01	
20	1.2271e-03	2.0172	1.0790e-01	0.9989
40	3.0870e-04	1.9910	5.3986e-02	0.9990
80	7.6854e-05	2.0060	2.7025e-02	0.9983
160	1.9307e-05	1.9930	1.3516e-02	0.9997
320	4.8130e-06	2.0041	6.7603e-03	0.9994
640	1.2293e-06	1.9691	3.3804e-03	0.9999
1280	3.0329e-07	2.0191	1.6904e-03	0.9999
2560	7.5839e-08	1.9997	8.4520e-04	1.0000

Typical numerical results are presented in Tables Tables 2.3 and 2.4 which, again, clearly demonstrate the optimal convergence of the proposed linear IFE method. In

Table 2.4: Errors and convergence rates of the linear IFE method when  $n = 6$  with small values for  $\beta_j, j = 1, 2, 3$ .

N	$L^2$ norm	rate	$H^1$ norm	rate
10	6.4165e-03		2.6721e-01	
20	1.6163e-03	1.9891	1.3491e-01	0.9860
40	3.9695e-04	2.0257	6.7431e-02	1.0005
80	1.0065e-04	1.9796	3.3759e-02	0.9982
160	2.4837e-05	2.0188	1.6876e-02	1.0003
320	6.2946e-06	1.9803	8.4407e-03	0.9996
640	1.5535e-06	2.0186	4.2202e-03	1.0001
1280	3.9354e-07	1.9810	2.1102e-03	0.9999
2560	9.7113e-08	2.0188	1.0551e-03	1.0000

related computations for these data, we used the following parameters:

$$D_0 = 0.010616229584014, \beta_0 = 0, \beta_1 = 0.015482995717499,$$

$$\beta_2 = 0.001133907855848 \beta_3 = 0.000162651593614.$$

# Chapter 3

## Quadratic IFE Method

In this chapter, we develop a quadratic IFE method to solve the interface problem (1.3)-(1.7). Let  $\mathcal{T}_h$  be the partition of the solution domain  $(\alpha_{-1}, \alpha_0)$  defined in (2.9). As usual, on each element  $T = [x_i, x_{i+1}]$ , we introduce another node  $x_{i+1/2} = \frac{x_i + x_{i+1}}{2}$  and the standard local quadratic finite element shape functions associated with the three local nodes:  $x_i$ ,  $x_{i+1/2}$  and  $x_{i+1}$ . On each non-interface element  $T = [x_i, x_{i+1}]$ , the local quadratic IFE space is the standard quadratic finite element space:

$$S_h(T) = \text{span}\{L_i(x), L_{i+1/2}(x), L_{i+1}(x)\}, \text{ when } T \cap \{\alpha_i\}_{i=0}^{n-1} = \emptyset,$$

here,

$$L_i(x) = \frac{(x - x_{i+1/2})(x - x_{i+1})}{(x_i - x_{i+1/2})(x_i - x_{i+1})},$$
$$L_{i+1/2}(x) = \frac{(x - x_i)(x - x_{i+1})}{(x_{i+1/2} - x_i)(x_{i+1/2} - x_{i+1})},$$
$$L_{i+1}(x) = \frac{(x - x_i)(x - x_{i+1/2})}{(x_{i+1} - x_i)(x_{i+1} - x_{i+1/2})}.$$

We need to construct quadratic IFE shape functions on interface elements. Let  $T = [x_i, x_{i+1}]$  be an interface element containing  $\alpha_j$ ,  $j \in \{0, 1, 2, \dots, n-1\}$ . Without loss of generality, our discussions in this section mainly focus on the case:  $x_i < x_{i+1/2} < \alpha_j < x_{i+1}$  in which we will use the following quadratic polynomials as the

building blocks for the quadratic IFE shape functions:

$$\begin{aligned}
L_{i,\alpha_j}(x) &= \frac{(x - x_{i+1/2})(x - \alpha_j)}{(x_i - x_{i+1/2})(x_i - \alpha_j)}, & L_{i+1/2,\alpha_j}(x) &= \frac{(x - x_i)(x - \alpha_j)}{(x_{i+1/2} - x_i)(x_{i+1/2} - \alpha_j)}, \\
L_{\alpha_j,i}(x) &= \frac{(x - x_{i+1/2})(x - x_i)}{(\alpha_j - x_{i+1/2})(\alpha_j - x_i)}, & H_{i+1,\alpha_j}(x) &= \frac{(x - \alpha_j)^2}{(x_{i+1} - \alpha_j)^2}, \\
H_{\alpha_j,0} &= 2\frac{x - x_{i+1}}{\alpha_j - x_{i+1}} - \frac{(x - x_{i+1})^2}{(\alpha_j - x_{i+1})^2}, & H_{\alpha_j,1} &= \frac{(x - \alpha_j)(x - x_{i+1})}{(\alpha_j - x_{i+1})}.
\end{aligned} \tag{3.1}$$

All the ideas and results in this section can be readily extended to the other case:  $x_i < \alpha_j < x_{i+1/2} < x_{i+1}$  in which we will use three Hermite type basis functions in the subinterval  $[x_i, \alpha_j]$  and three Lagrange type basis functions in the subinterval  $[\alpha_j, x_{i+1}]$  in forms similar to (3.1) as building blocks for the corresponding quadratic IFE shape functions.

The quadratic polynomials in (3.1) have the following properties:

$$\begin{aligned}
L'_{i,\alpha_j}(\alpha_j) &= \frac{(\alpha_j - x_{i+1/2})}{(x_i - x_{i+1/2})(x_i - \alpha_j)}, & L'_{\alpha_j,i}(\alpha_j) &= \frac{1}{(\alpha_j - x_{i+1/2})} + \frac{1}{(\alpha_j - x_i)}, \\
L''_{i,\alpha_j}(x) &= \frac{2}{(x_i - x_{i+1/2})(x_i - \alpha_j)}, & L''_{\alpha_j,i}(x) &= \frac{2}{(\alpha_j - x_{i+1/2})(\alpha_j - x_i)}, \\
H''_{i+1,\alpha_j}(x) &= \frac{2}{(x_{i+1} - \alpha_j)^2}, & H''_{\alpha_j,0}(x) &= \frac{-2}{(\alpha_j - x_{i+1})^2}, & H''_{\alpha_j,1}(x) &= \frac{2}{(\alpha_j - x_{i+1})}.
\end{aligned} \tag{3.2}$$

In addition, by using the standard interpolation error analysis procedure, we derive the following estimates about these quadratic polynomials:

$$\begin{aligned}
&\|L_{\alpha_j,i}\|_{0,(x_i,\alpha_j)} + h\|L_{\alpha_j,i}\|_{1,(x_i,\alpha_j)} \leq h^{3/2}(\alpha_j - x_{i+1/2})^{-1}, \\
&\|H_{\alpha_j,1}\|_{0,(\alpha_j,x_{i+1})} + h\|H_{\alpha_j,1}\|_{1,(\alpha_j,x_{i+1})} \leq Ch^{3/2}, \\
&\|H_{\alpha_j,0}\|_{0,(\alpha_j,x_{i+1})} + h\|H_{\alpha_j,0}\|_{1,(\alpha_j,x_{i+1})} \leq Ch^{1/2}.
\end{aligned} \tag{3.3}$$

### 3.1 Local Quadratic IFE Space for the First Interface

Let  $T = [x_i, x_{i+1}]$  be an interface element containing the first interface point  $\alpha_0$ . Firstly, We propose three quadratic IFE shape functions on this interface element in the following formats:

$$\begin{aligned} \psi_i^0(x) &= \begin{cases} L_{i,\alpha_0}(x) + c_i^0 L_{\alpha_0,i}(x), & x \in [x_i, \alpha_0], \\ a_i^0 H_{\alpha_0,0}(x) + b_i^0 H_{\alpha_0,1}(x), & x \in [\alpha_0, x_{i+1}], \end{cases} \\ \psi_{i+1/2}^0(x) &= \begin{cases} L_{i+1/2,\alpha_0}(x) + c_{i+1/2}^0 L_{\alpha_0,i}(x), & x \in [x_i, \alpha_0], \\ a_{i+1/2}^0 H_{\alpha_0,0}(x) + b_{i+1/2}^0 H_{\alpha_0,1}(x), & x \in [\alpha_0, x_{i+1}], \end{cases} \\ \psi_{i+1}^0(x) &= \begin{cases} c_{i+1}^0 L_{\alpha_0,i}(x), & x \in [x_i, \alpha_0], \\ a_{i+1}^0 H_{\alpha_0,0}(x) + b_{i+1}^0 H_{\alpha_0,1}(x) + H_{i+1,\alpha_0}(x), & x \in [\alpha_0, x_{i+1}], \end{cases} \end{aligned} \quad (3.4)$$

whose coefficients  $a_k^0$ ,  $b_k^0$  and  $c_k^0$ ,  $k = i, i + 1/2, i + 1$  are to be chosen so that these piecewise quadratic functions satisfy the interface jump conditions (1.3) across  $\alpha_0$ . However, the two equations in the interface jump conditions (1.3)-(1.4) are obviously not enough to determine all three coefficients in each of the proposed quadratic IFE shape functions. Following the ideas in [3, 36], we therefore propose to impose one extra jump condition for the unique determination of the quadratic IFE shape functions:

$$D_0(\psi_k^0)''(\alpha_0^-) = D_1(\psi_k^0)''(\alpha_0^+) - 2\delta_1(\psi_k^0)'(\alpha_0^+), \quad k = i, i + 1/2, i + 1. \quad (3.5)$$

Other types of extra jump conditions can be considered, but the related error estimation confirms that the one given in (3.5) leads to an optimally convergent quadratic IFE space.

**Theorem 3.1.** *Functions  $\psi_i^0(x)$ ,  $\psi_{i+1/2}^0(x)$  and  $\psi_{i+1}^0(x)$  in (3.4) are uniquely determined by interface jump conditions in (1.3) and (3.5). In addition, the coefficients*

in these functions are as follows:

$$\begin{aligned}
c_k^0 &= \begin{cases} \frac{1}{\Delta}[\Theta' L'_{k,\alpha_0}(\alpha_0) + D_0 D_1 L''_{k,\alpha_0}], & k = i, i + 1/2, \\ \frac{-1}{\Delta} D_1^2 H''_{i+1,\alpha_0}, & k = i + 1, \end{cases} \\
a_k^0 &= \begin{cases} \lambda D_0 L'_{k,\alpha_0}(\alpha_0) + [1 + \lambda D_0 L'_{\alpha_0,k}(\alpha_0)] c_k^0, & k = i, i + 1/2, \\ [1 + \lambda D_0 L'_{\alpha_0,i}(\alpha_0)] c_{i+1}^0, & k = i + 1, \end{cases} \\
b_k^0 &= \begin{cases} \frac{1}{D_1} [D_0 L'_{k,\alpha_0}(\alpha_0) + D_0 L'_{\alpha_0,k}(\alpha_0) c_i^0 + 2\delta_1 a_k^0], & k = i, i + 1/2, \\ \frac{1}{D_1} [D_0 L'_{\alpha_0,i}(\alpha_0) c_{i+1}^0 + 2\delta_1 a_{i+1}^0], & k = i + 1, \end{cases}
\end{aligned} \tag{3.6}$$

with

$$\begin{aligned}
\Delta &= D_1^2 H''_{\alpha_0,0} - D_0 D_1 L''_{\alpha_0,i} + 2D_1 \delta_1 H''_{\alpha_0,1} - 4\delta_1^2 - \Theta' L'_{\alpha_0,i}(\alpha_0), \\
\Theta' &= -D_0 D_1 H''_{\alpha_0,1} + 2\delta_1 D_0 - 2D_0 D_1 \lambda \delta_1 H''_{\alpha_0,1} + 4D_0 \delta_1^2 \lambda - \lambda D_0 D_1^2 H''_{\alpha_0,0}.
\end{aligned} \tag{3.7}$$

*Proof.* Applying jump conditions in (1.3) and (3.5) to  $\psi_k^0(x)$ ,  $k = i, i + 1/2, i + 1$ , we have

$$\begin{cases} \psi_k^0(\alpha_0^+) - \psi_k^0(\alpha_0^-) = \lambda D_0 (\psi_k^0)'(\alpha_0^-), \\ D_0 (\psi_k^0)'(\alpha_0^-) = D_1 (\psi_k^0)'(\alpha_0^+) - 2\delta_1 \psi_k^0(\alpha_0^+), \\ D_0 (\psi_k^0)''(\alpha_0^-) = D_1 (\psi_k^0)''(\alpha_0^+) - 2\delta_1 (\psi_k^0)'(\alpha_0^+). \end{cases}$$

we know that this is a linear system for coefficients  $a_k^0, b_k^0$ , and  $c_k^0$ , and the determinant of its coefficient matrix is  $\Delta$ . It can be verified that  $\Delta < 0$  under the assumption  $x_i < x_{i+1/2} < \alpha_0 < x_{i+1}$ . Hence this linear system has a unique solution which yields the formulas in (3.6) for  $a_k^0, b_k^0$ , and  $c_k^0$ ,  $k = i, i + 1/2, i + 1$ .  $\square$

It is easy to verify that the quadratic IFE shape functions given in Theorem 3.1 have the following property:

$$\psi_j^{(0)}(x_k) = \delta_{j,k}, \quad j, k = i, i + 1/2, i + 1.$$

Hence, we can use these quadratic IFE shape functions to define a local quadratic IFE space on the interface element  $T = [x_i, x_{i+1}]$  containing  $\alpha_0$  as follows:

$$S_h(T) = \text{span}\{\psi_i, \psi_{i+1/2}, \psi_{i+1}\}.$$

We now consider the approximation capability of this local quadratic IFE space. For every  $u \in L^2(T)$  such that  $u|_{[x_i, \alpha_0]} \in C^0[x_i, \alpha_0]$  and  $u|_{[\alpha_0, x_{i+1}]} \in C^0[\alpha_0, x_{i+1}]$ , we define its quadratic IFE interpolation as

$$\tilde{I}_h^0 u(x) := u(x_i)\psi_i^0(x) + u(x_{i+1/2})\psi_{i+1/2}^0(x) + u(x_{i+1})\psi_{i+1}^0(x). \quad (3.8)$$

Using the formulas for the coefficients of  $\psi_k^0$ ,  $k = i, i + 1/2, i + 1$  given in Theorem 3.1, we show that

$$\tilde{I}_h^0 u(x) = \begin{cases} u(x_i)L_{i, \alpha_0}(x) + u(x_{i+1/2})L_{i+1/2, \alpha_0}(x) + \bar{u}_{\alpha_0}^- L_{\alpha_0, i}(x), & x \in [x_i, \alpha_0], \\ \bar{u}_{\alpha_0}^+ H_{\alpha_0, 0}(x) + \bar{u}'_{\alpha_0} H_{\alpha_0, 1}(x) + u(x_{i+1})H_{i+1, \alpha_0}(x), & x \in [\alpha_0, x_{i+1}], \end{cases} \quad (3.9)$$

where, constants  $\bar{u}_{\alpha_0}^-$ ,  $\bar{u}_{\alpha_0}^+$  and  $\bar{u}'_{\alpha_0}$  are defined by

$$\begin{aligned} \bar{u}_{\alpha_0}^- &= \frac{1}{\Delta} [\Theta' l'_0(\alpha_0) + D_0 D_1 l''_0(\alpha_0) - D_1^2 u(x_{i+1}) H''_{i+1, \alpha_0}], \\ \bar{u}_{\alpha_0}^+ &= \lambda D_0 l'_0(\alpha_0) + [1 + \lambda D_0 L'_{\alpha_0}(\alpha_0)] \bar{u}_{\alpha_0}^-, \\ \bar{u}'_{\alpha_0} &= \frac{1}{D_1} [D_0 l'_0(\alpha_0) + D_0 L'_{\alpha_0, i}(\alpha_0) \bar{u}_{\alpha_0}^- + 2\delta_1 \bar{u}_{\alpha_0}^+], \end{aligned} \quad (3.10)$$

with

$$l_0(x) = u(x_i)L_{i, \alpha_0}(x) + u(x_{i+1/2})L_{i+1/2, \alpha_0}(x). \quad (3.11)$$

$l'_0(\alpha_0)$  and  $l''_0(\alpha_0)$  denotes the value of the first and second order derivatives respect to  $x$  at  $\alpha_0$ , respectively. In addition, using (3.1) and the definition of  $\Delta$  given in (3.7), we derive the following estimate about  $\frac{1}{\Delta}$ :

$$\begin{aligned} \frac{1}{|\Delta|} &\leq C \min \{ (\alpha_0 - x_i), (\alpha_0 - x_i)(\alpha_0 - x_{i+1/2}), \\ &\quad (\alpha_0 - x_{i+1/2})(x_{i+1} - \alpha_0)^2, (\alpha_0 - x_i)(\alpha_0 - x_{i+1})^2 \}. \end{aligned} \quad (3.12)$$



On the other hand, we can also interpolation  $u$  by those quadratic polynomials in (3.1) as follows:

$$\tilde{I}_h^0 u(x) := \begin{cases} u(x_i)L_{i,\alpha_0}(x) + u(x_{i+1/2})L_{i+1/2,\alpha_0}(x) + u(\alpha_0^-)L_{\alpha_0,i}(x), & x \in [x_i, \alpha_0], \\ u(\alpha_0^+)H_{\alpha_0,0}(x) + u'(\alpha_0^+)H_{\alpha_0,1}(x) + u(x_{i+1})H_{i+1,\alpha_0}(x), & x \in [\alpha_0, x_{i+1}]. \end{cases} \quad (3.13)$$

The above Lagrange-Hermit interpolation have the following standard error estimates for  $\tilde{I}_h^0 u$  :

$$\begin{aligned} \|u - \tilde{I}_h^0 u\|_{0,(x_i,\alpha_0)} + h\|u - \tilde{I}_h^0 u\|_{1,(x_i,\alpha_0)} &\leq Ch^3\|u\|_{3,(x_i,\alpha_0)}, \\ \|u - \tilde{I}_h^0 u\|_{0,(\alpha_0,x_{i+1})} + h\|u - \tilde{I}_h^0 u\|_{1,(\alpha_0,x_{i+1})} &\leq Ch^3\|u\|_{3,(\alpha_0,x_{i+1})}, \end{aligned} \quad (3.14)$$

provided further that  $u|_{(x_i,\alpha_0)} \in H^3(x_i, \alpha_0)$  and  $u|_{(\alpha_0,x_{i+1})} \in H^3(\alpha_0, x_{i+1})$ . For the point-wise estimates, we have the following results:

$$\begin{aligned} |u''(\alpha_0^-) - (\tilde{I}_h^0 u)''(\alpha_0^-)| &\leq (\alpha_0 - x_i)^{1/2}\|u\|_{3,(x_i,\alpha_0)}, \\ |u''(\alpha_0^+) - (\tilde{I}_h^0 u)''(\alpha_0^+)| &\leq (x_{i+1} - \alpha_0)^{1/2}\|u\|_{3,(\alpha_0,x_{i+1})}, \\ |u'(\alpha_0^-) - (\tilde{I}_h^0 u)'(\alpha_0^-)| &\leq (\alpha_0 - x_{i+1/2})(\alpha_0 - x_i)^{1/2}\|u\|_{3,(x_i,\alpha_0)}, \\ |u'(\alpha_0^+) - (\tilde{I}_h^0 u)'(\alpha_0^+)| &\leq (x_{i+1} - \alpha_0)^{3/2}\|u\|_{3,(\alpha_0,x_{i+1})}. \end{aligned} \quad (3.15)$$

The next theorem shows that the local quadratic IFE space has the expected optimal convergence.

**Theorem 3.2.** *Let  $T = [x_i, x_{i+1}]$  be an interface element such that  $\alpha_0 \in [x_i, x_{i+1}]$ . Then, for every  $u \in L^2(T)$  such that  $u|_{(x_i,\alpha_0)} \in H^3(x_i, \alpha_0)$  and  $u|_{(\alpha_0,x_{i+1})} \in H^3(\alpha_0, x_{i+1})$ , we have the following estimate for the quadratic IFE interpolation:*

$$\|u - \tilde{I}_h^0 u\|_{0,(x_i,x_{i+1})} + h\|u - \tilde{I}_h^0 u\|_{1,(x_i,x_{i+1})} \leq Ch^3\|u\|_{3,(x_i,x_{i+1})}, \quad (3.16)$$

where  $C$  is a constant independent of  $\alpha_0 \in [x_i, x_{i+1}]$ .

*Proof.* Subtracting (3.9) from (3.13), we have

$$\tilde{I}_h^0 u - \check{I}_h^0 u = \begin{cases} (u(\alpha_0^-) - \bar{u}_{\alpha_0}^-) L_{\alpha_0, i}(x), & x \in [x_i, \alpha_0], \\ (u(\alpha_0^+) - \bar{u}_{\alpha_0}^+) H_{\alpha_0, 0}(x) + (u'(\alpha_0^+) - \bar{u}'_{\alpha_0}) H_{\alpha_0, 1}, & x \in [\alpha_0, x_{i+1}]. \end{cases} \quad (3.17)$$

Using (3.10) and the jump conditions in (1.3) and (3.5), we have

$$u(\alpha_0^-) - \bar{u}_{\alpha_0}^- = \tau_1 + \tau_2 + \tau_3 + \tau_4 + \tau_5, \quad (3.18)$$

where

$$\begin{aligned} \tau_1 &= -\frac{1}{\Delta} (D_0 D_1 + 2D_0 D_1 \delta_1 \lambda) H''_{\alpha_0, 1} e'(\alpha_0^-), \quad \tau_2 = \frac{1}{\Delta} (2D_0 \delta_1 + 4D_0 \lambda \delta_1^2) e'(\alpha_0^-), \\ \tau_3 &= \frac{1}{\Delta} D_0 D_1 e''(\alpha_0^-), \quad \tau_4 = -\frac{1}{\Delta} \lambda D_0 D_1^2 H''_{\alpha_0, 0} e'(\alpha_0^-), \quad \tau_5 = -\frac{1}{\Delta} D_1^2 e''(\alpha_0^+), \end{aligned} \quad (3.19)$$

with  $e(x) = u(x) - \tilde{I}_h^0 u(x)$ . (3.12) implies

$$\frac{1}{|\Delta|} \leq C(\alpha_0 - x_i)(x_{i+1} - \alpha_0),$$

Substituting the above inequality, the fact that  $H''_{\alpha_0, 1} = (\alpha_0 - x_{i+1})^{-1}$  derived from (3.2), and the estimate of  $|e'(\alpha_0^-)|$  given in (3.15) into (3.19), we obtain

$$|\tau_1| \leq Ch^{3/2}(\alpha_0 - x_{i+1/2}) \|u\|_{3, (x_i, x_{i+1})}.$$

Similarly, using (3.12), the bounds for  $|e'(\alpha_0^-)|$ ,  $|e''(\alpha_0^-)|$ ,  $|e''(\alpha_0^+)|$  given in (3.15) and the  $H''_{\alpha_0, 0}$  given in (3.2), we get

$$|\tau_k| \leq Ch^{3/2}(\alpha_0 - x_{i+1/2}) \|u\|_{3, (x_i, x_{i+1})}, \quad k = 2, 3, 4, 5.$$

Then, putting these estimates for  $\tau_k$ ,  $1 \leq k \leq 5$  in (3.18), we obtain

$$|u(\alpha_0^-) - \bar{u}_{\alpha_0}^-| \leq Ch^{3/2}(\alpha_0 - x_{i+1/2}) \|u\|_{3, (x_i, x_{i+1})}. \quad (3.20)$$

Substituting (3.20) and the estimate about  $L_{\alpha_0, i}$  given in (3.3) into (3.17), we obtain the following estimate on the left subelement  $(x_i, \alpha_0)$ :

$$\|\tilde{I}_h^0 u - \check{I}_h^0 u\|_{0, (x_i, \alpha_0)} + h \|\tilde{I}_h^0 u - \check{I}_h^0 u\|_{1, (x_i, \alpha_0)} \leq Ch^3 \|u\|_{3, (x_i, x_{i+1})}. \quad (3.21)$$

Now we aim to derive the estimate on the right subelement  $[\alpha_j, x_{i+1}]$ . Using (3.10), the jump conditions in (1.3), and (3.5), we have

$$\begin{aligned} u_{\alpha_0}^+ - u(\alpha_0^+) &= \frac{1}{\Delta} \left[ D_0 D_1 e''(\alpha_0^-) + 2D_0 \delta_1 e'(\alpha_0^-) - D_0 D_1 H''_{\alpha_0, 1} e'(\alpha_0^-) - D_1^2 e''(\alpha_0^+) \right. \\ &\quad \left. + \lambda D_0^2 D_1 (L'_{\alpha_0, i}(\alpha_0^-) e''(\alpha_0^-) - L''_{\alpha_0, i} e'(\alpha_0^-)) - D_0 D_1^2 L'_{\alpha_0, i}(\alpha_0^-) \lambda e''(\alpha_0^+) \right], \\ \bar{u}'_{\alpha_0} - u'(\alpha_0^+) &= \frac{D_0 L'_{\alpha_0, i}(\alpha_0^-)}{D_1} (\bar{u}_{\alpha_0}^- - u(\alpha_0^-)) + \frac{D_0}{D_1} e'(\alpha_0^-) + \frac{2\delta_1}{D_1} (\bar{u}_{\alpha_0}^+ - u(\alpha_0^+)). \end{aligned}$$

Using arguments similar to those we used in (3.20), we have

$$|\bar{u}_{\alpha_0}^+ - u(\alpha_0^+)| \leq Ch^{3/2} (\alpha_0 - x_{i+1/2}) \|u\|_{3, (x_i, x_{i+1})}, \quad (3.22)$$

and

$$\begin{aligned} |\bar{u}'_{\alpha_0} - u'(\alpha_0^+)| &\leq \left| \frac{D_0 L'_{\alpha_0, i}(\alpha_0^-)}{D_1} (\bar{u}_{\alpha_0}^- - u(\alpha_0^-)) \right| + \left| \frac{D_0}{D_1} e'(\alpha_0^-) \right| + \left| \frac{2\delta_1}{D_1} (\bar{u}_{\alpha_0}^+ - u(\alpha_0^+)) \right| \\ &\leq Ch^{3/2} \|u\|_{3, (x_i, x_{i+1})}. \end{aligned} \quad (3.23)$$

Then, applying (3.22), (3.23), and the estimates about  $H_{\alpha_0, k}$ ,  $k = 0, 1$  given in (3.3) to (3.17), we have the following estimate on the right subelement  $[\alpha_0, x_{i+1}]$ :

$$\|\tilde{I}_h^0 u - \check{I}_h^0 u\|_{0, (\alpha_0, x_{i+1})} + h \|\tilde{I}_h^0 u - \check{I}_h^0 u\|_{1, (\alpha_0, x_{i+1})} \leq Ch^3 \|u\|_{3, (x_i, x_{i+1})}. \quad (3.24)$$

Thus, the combination of (3.21) and (3.24) yields

$$\|\tilde{I}_h^0 u - \check{I}_h^0 u\|_{0, (x_i, x_{i+1})} + h \|\tilde{I}_h^0 u - \check{I}_h^0 u\|_{1, (x_i, x_{i+1})} \leq Ch^3 \|u\|_{3, (x_i, x_{i+1})}. \quad (3.25)$$

Finally, estimate given in (3.16) follows from

$$\begin{aligned}
& \|u - \check{I}_h^0 u\|_{0,(x_i,x_{i+1})} + h\|u - \check{I}_h^0 u\|_{1,(x_i,x_{i+1})} \\
& \leq \|u - \tilde{I}_h^0 u\|_{0,(x_i,x_{i+1})} + h\|u - \tilde{I}_h^0 u\|_{1,(x_i,x_{i+1})} \\
& \quad + \|\tilde{I}_h^0 u - \check{I}_h^0 u\|_{0,(x_i,x_{i+1})} + h\|\tilde{I}_h^0 u - \check{I}_h^0 u\|_{1,(x_i,x_{i+1})},
\end{aligned}$$

and then applying estimates in (3.14) and (3.25).  $\square$

## 3.2 Local Quadratic IFE Space for Other Interfaces

We now develop a local quadratic IFE space on the interface elements  $T = [x_i, x_{i+1}]$  that contains the interface point  $\alpha_j$ , for an integer  $j = 1, 2, \dots, n-1$ . We propose three shape functions  $\psi_i^j(x)$ ,  $\psi_{i+1/2}^j(x)$  and  $\psi_{i+1}^j(x)$  in the following piecewise quadratic polynomial formats:

$$\begin{aligned}
\psi_i^j(x) &= \begin{cases} L_{i,\alpha_j}(x) + a_i^j L_{\alpha_j,i}(x), & x \in [x_i, \alpha_j], \\ a_i^j H_{\alpha_j,0}(x) + b_i^j H_{\alpha_j,1}(x), & x \in [\alpha_j, x_{i+1}], \end{cases} \\
\psi_{i+1/2}^j(x) &= \begin{cases} L_{i+1/2,\alpha_j}(x) + a_{i+1/2}^j L_{\alpha_j,i}(x), & x \in [x_i, \alpha_j], \\ a_{i+1/2}^j H_{\alpha_j,0}(x) + b_{i+1/2}^j H_{\alpha_j,1}(x), & x \in [\alpha_j, x_{i+1}], \end{cases} \\
\psi_{i+1}^j(x) &= \begin{cases} a_{i+1}^j L_{\alpha_j,i}(x), & x \in [x_i, \alpha_j], \\ a_{i+1}^j H_{\alpha_j,0}(x) + b_{i+1}^j H_{\alpha_j,1}(x) + H_{i+1,\alpha_j}(x), & x \in [\alpha_j, x_{i+1}]. \end{cases}
\end{aligned} \tag{3.26}$$

For the unique determination of the above three quadratic IFE shape functions, we propose to use the following extra jump conditions because it leads to an optimally convergent quadratic IFE space:

$$D_j(\psi_k^j)''(\alpha_j^-) - 2\delta_j(\psi_k^j)'(\alpha_j^-) = D_{j+1}(\psi_k^j)''(\alpha_j^+) - 2\delta_{j+1}(\psi_k^j)'(\alpha_j^+), \quad k = i, i+1/2, i+1. \tag{3.27}$$

**Theorem 3.3.** Assume that  $\delta_{j+1} \geq \delta_j$  and  $D_j \delta_{j+1} \geq D_{j+1} \delta_j$ , then, the shape functions proposed in (3.26) are uniquely determined by the jump conditions (1.4) and (3.27). In addition, the coefficients in these functions have the following representations:

$$a_k^j = \begin{cases} -\frac{1}{\Delta} [\Theta L'_{k,\alpha_j}(\alpha_j) + D_j D_{j+1} L''_{k,\alpha_j}], & k = i, i + 1/2, \\ -\frac{1}{\Delta} D_{j+1}^2 H''_{i+1,\alpha_j}, & k = i + 1, \end{cases}$$

$$b_k^j = \begin{cases} \frac{1}{D_{j+1}} [\hat{\Theta} a_k^j + D_j L'_{k,\alpha_j}(\alpha_j)], & k = i, i + 1/2, \\ \frac{1}{D_{j+1}} \hat{\Theta} a_{i+1}^j, & k = i + 1, \end{cases}$$

with

$$\begin{aligned} \Theta &= -D_j D_{j+1} H''_{\alpha_j,1} + 2\delta_{j+1} D_j - 2\delta_j D_{j+1}, \quad \hat{\Theta} = D_j L'_{\alpha_j,i}(\alpha_j) - 2\delta_j + 2\delta_{j+1}, \\ \Delta &= -\Theta L'_{\alpha_j,i}(\alpha_j) - D_j D_{j+1} L''_{\alpha_j} + D_{j+1}^2 H''_{\alpha_j,0} + 2(\delta_{j+1} - \delta_j)(D_{j+1} H''_{\alpha_j,1} - 2\delta_{j+1}). \end{aligned} \tag{3.28}$$

*Proof.* The proof of the existence and uniqueness are similar to Theorem 3.1 by using jump conditions (1.4) and (3.5), and the coefficients are obtained by solving the related linear system.  $\square$

By direct verification, we can see that the quadratic shape functions given in (3.26) have the following property:

$$\psi_k^j(x_l) = \delta_{k,l}, \quad k, l = i, i + 1/2, i + 1.$$

Hence, they can be used to define the local quadratic IFE space on the interface element  $T = [x_i, x_{i+1}]$  containing the interface point  $\alpha_j$ ,  $j = 1, 2, \dots, n-1$  as follows:

$$S_h(T) = \text{span}\{\psi_i^j, \psi_{i+1/2}^j, \psi_{i+1}^j\}.$$

In order to get approximation capability of the local quadratic IFE space  $S_h(T)$ , we firstly consider the error in the quadratic IFE interpolation in  $S_h(T)$ . For every  $u \in C^0(T) = C^0([x_i, x_{i+1}])$ , we define its quadratic IFE interpolation as

$$\check{I}_h^j u(x) := u(x_i)\psi_i^j(x) + u(x_{i+1/2})\psi_{i+1/2}^j(x) + u(x_{i+1})\psi_{i+1}^j(x). \quad (3.29)$$

By using the formulas given in Theorem 3.3, the quadratic interpolation on  $T = [x_i, x_{i+1}]$  can be written as

$$\check{I}_h^j u(x) = \begin{cases} u(x_i)L_{i,\alpha_j}(x) + u(x_{i+1/2})L_{i+1/2,\alpha_j}(x) + \bar{u}_{\alpha_j}L_{\alpha_j,i}(x), & x \in [x_i, \alpha_j], \\ \bar{u}_{\alpha_j}H_{\alpha_j,0}(x) + \bar{u}'_{\alpha_j}H_{\alpha_j,1}(x) + u(x_{i+1})H_{i+1,\alpha_j}(x), & x \in [\alpha_j, x_{i+1}], \end{cases} \quad (3.30)$$

here,

$$\begin{aligned} \bar{u}_{\alpha_j} &= \frac{1}{\Delta} (\Theta l'_j(\alpha_j) + D_j D_{j+1} l''_j(\alpha_j) - D_{j+1}^2 u(x_{i+1}) H''_{i+1,\alpha_j}), \\ \bar{u}'_{\alpha_j} &= \frac{1}{D_{j+1}} (\hat{\Theta} \bar{u}_{\alpha_j} + D_j l'_j(\alpha_j)). \end{aligned} \quad (3.31)$$

In addition, by (3.1) and the definition of  $\Delta$  given in (3.28), we can derive the following estimation about  $\frac{1}{\Delta}$ :

$$\frac{1}{\Delta} \leq C \min\{(x_{i+1} - \alpha_j)(\alpha_j - x_i), (\alpha_j - x_i), (\alpha_j - x_i)(\alpha_j - x_{i+1/2}), (\alpha_j - x_i)^{3/2}(\alpha_j - x_{i+1/2})^{1/2}\}. \quad (3.32)$$

The Lagrange-Hermit interpolation of  $u$  using the quadratic polynomials in (3.1) has the following expression:

$$\tilde{I}_h^j u = \begin{cases} u(x_i)L_{i,\alpha_j}(x) + u(x_{i+1/2})L_{i+1/2,\alpha_j}(x) + u(\alpha_j)L_{\alpha_j,i}(x), & x \in [x_i, \alpha_j], \\ u(\alpha_j)H_{\alpha_j,0}(x) + u'(\alpha_j^+)H_{\alpha_j,1}(x) + u(x_{i+1})H_{i+1,\alpha_j}(x), & x \in [\alpha_j, x_{i+1}]. \end{cases} \quad (3.33)$$

If  $u|_{(x_i, \alpha_j)} \in H^3(x_i, \alpha_j)$  and  $u|_{(\alpha_j, x_{i+1})} \in H^3(\alpha_j, x_{i+1})$ , the standard finite element approximation theory provides the following estimates for  $\tilde{I}_h^j u$ :

$$\|u - \tilde{I}_h^j u\|_{0, (x_i, x_{i+1})} + h\|u - \tilde{I}_h^j u\|_{1, (x_i, x_{i+1})} \leq Ch^3 \|u\|_{3, (x_i, x_{i+1})}. \quad (3.34)$$

In addition, point-wise estimates in (3.15) can be readily extended to  $\alpha_j$  as follows:

$$\begin{aligned} |u''(\alpha_j^-) - (\tilde{I}_h^j u)''(\alpha_j^-)| &\leq (\alpha_j - x_i)^{1/2} \|u\|_{3, (x_i, \alpha_j)}, \\ |u''(\alpha_j^+) - (\tilde{I}_h^j u)''(\alpha_j^+)| &\leq (x_{i+1} - \alpha_j)^{1/2} \|u\|_{3, (\alpha_j, x_{i+1})}, \\ |u'(\alpha_j^-) - (\tilde{I}_h^j u)'(\alpha_j^-)| &\leq (\alpha_j - x_{i+1/2})(\alpha_j - x_i)^{1/2} \|u\|_{3, (x_i, \alpha_j)}. \end{aligned} \quad (3.35)$$

We now turn to the estimation for  $u - \check{I}_h^j u$ .

**Theorem 3.4.** *Let  $[x_i, x_{i+1}]$  be an interface element containing the interface point  $\alpha_j$ ,  $j = 1, 2, \dots, n-1$ , and assume that  $\delta_{j+1} \geq \delta_j$  and  $D_j \delta_{j+1} \geq D_{j+1} \delta_j$ , then for every  $u \in C^0(T)$  such that  $u|_{(x_i, \alpha_j)} \in H^3(x_i, \alpha_j)$  and  $u|_{(\alpha_j, x_{i+1})} \in H^3(\alpha_j, x_{i+1})$ , we have*

$$\|u - \check{I}_h^j u\|_{0, (x_i, x_{i+1})} + h\|u - \check{I}_h^j u\|_{1, (x_i, x_{i+1})} \leq Ch^3 \|u\|_{3, (x_i, x_{i+1})}, \quad (3.36)$$

where  $C$  is a constant independent of  $\alpha_j \in [x_i, x_{i+1}]$ .

*Proof.* Let us firstly consider the difference between  $\check{I}_h^j u$  and  $\tilde{I}_h^j u$ . Subtracting (3.30) from (3.33), we have

$$\check{I}_h^j u - \tilde{I}_h^j u = \begin{cases} (u(\alpha_j) - \bar{u}_{\alpha_j})L_{\alpha_j, i}(x), & x \in [x_i, \alpha_j], \\ (u(\alpha_j) - \bar{u}_{\alpha_j})H_{\alpha_j, 0}(x) + [u'(\alpha_j^+) - \bar{u}'_{\alpha_j}]H_{\alpha_j, 1}(x), & x \in [\alpha_j, x_{i+1}]. \end{cases} \quad (3.37)$$

By using jump conditions in (1.4) and (3.27), we have

$$\bar{u}_{\alpha_j} - u(\alpha_j) = \sigma_1 + \sigma_2 + \sigma_3 + \sigma_4,$$

here,

$$\begin{aligned}\sigma_1 &= -\frac{1}{\Delta}D_j D_{j+1} H''_{\alpha_j,1} e'(\alpha_j^-), \quad \sigma_2 = 2\frac{1}{\Delta}(D_j \delta_{j+1} e'(\alpha_j^-) - 2D_{j+1} \delta_j e'(\alpha_j^-)), \\ \sigma_3 &= \frac{1}{\Delta}D_j D_{j+1} e''(\alpha_j^-), \quad \sigma_4 = -\frac{1}{\Delta}D_{j+1}^2 e''(\alpha_j^+),\end{aligned}$$

with  $e(x) = \tilde{I}_h^j u(x) - u(x)$ . Using (3.32), we have

$$\left| \frac{1}{\Delta} \right| \leq C(x_{i+1} - \alpha_j)(\alpha_j - x_i).$$

The last equation in (3.2), together with the estimate for  $e'(\alpha_j^-)$  given in (3.35) imply that

$$|\sigma_1| \leq Ch^{3/2}(\alpha_j - x_{i+1/2}) \|u\|_{3,(x_i, x_{i+1})}.$$

Similarly, by using (3.32) and the bounds for  $|e'(\alpha_j^-)|$ ,  $|e''(\alpha_j^-)|$ ,  $|e''(\alpha_j^+)|$  given in (3.35), we obtain

$$|\sigma_k| \leq Ch^{3/2}(\alpha_j - x_{i+1/2}) \|u\|_{3,(x_i, x_{i+1})}, \quad k = 2, 3, 4.$$

Summing up  $\sigma_k$  from 1 to 4, we obtain

$$|u(\alpha_j) - \bar{u}_{\alpha_j}| \leq Ch^{3/2}(\alpha_j - x_{i+1/2}) \|u\|_{3,(x_i, x_{i+1})}. \quad (3.38)$$

Applying (3.38) and the estimate about  $L_{\alpha_j, i}$  given in (3.3) to (3.37) leads to the following estimate on the left subelement  $[x_i, \alpha_j]$ :

$$\|\tilde{I}_h^j u - \check{I}_h^j u\|_{0,(x_i, \alpha_j)} + h \|\tilde{I}_h^j u - \check{I}_h^j u\|_{1,(x_i, \alpha_j)} \leq Ch^3 \|u\|_{3,(x_i, x_{i+1})}. \quad (3.39)$$

Similar, using (3.31) and the jump conditions in (1.4) and (3.27), we have

$$|u'(\alpha_j^+) - \bar{u}'_{\alpha_j}| \leq Ch^{3/2} \|u\|_{3,(x_i, x_{i+1})}. \quad (3.40)$$

Then, using (3.38), (3.40), and the estimates of  $H_{\alpha_j, k}$ ,  $k = 0, 1$  given in (3.2), we have the following estimate on the right subelement  $[\alpha_j, x_{i+1}]$ :

$$\|\tilde{I}_h^j u - \check{I}_h^j u\|_{0,(\alpha_j, x_{i+1})} + h \|\tilde{I}_h^j u - \check{I}_h^j u\|_{1,(\alpha_j, x_{i+1})} \leq Ch^3 \|u\|_{3,(x_i, x_{i+1})}. \quad (3.41)$$



the above equation and (3.39) imply

$$\|\tilde{I}_h^j u - \hat{I}_h^j u\|_{0,(x_i,x_{i+1})} + h\|\tilde{I}_h^j u - \hat{I}_h^j u\|_{1,(x_i,x_{i+1})} \leq Ch^3\|u\|_{3,(x_i,x_{i+1})}. \quad (3.42)$$

Finally, (3.34) together with (3.42) imply (3.36) directly:

$$\|u - \check{I}_h^j u\|_{0,(x_i,x_{i+1})} + h\|u - \check{I}_h^j u\|_{1,(x_i,x_{i+1})} \leq Ch^3\|u\|_{3,(x_i,x_{i+1})}.$$

□

### 3.3 Convergence of quadratic IFE space

We can define a quadratic IFE space globally on the whole solution domain  $(\alpha_{-1}, \alpha_n)$  as follows:

$$S_h(\alpha_{-1}, \alpha_n) = \{v \in L^2(\alpha_{-1}, \alpha_n) \mid v|_{\Omega^\pm} \in C^0(\Omega^\pm), v|_T \in S_h(T), \forall T \in \mathcal{T}_h\},$$

where, we recall that the local quadratic IFE space  $S_h(T)$  is defined by

$$S_h^{(2)}(T) = \begin{cases} \text{span}\{L_i, L_{i+1/2}, L_{i+1}\}, & T = [x_i, x_{i+1}], T \cap \{\alpha_i\}_{i=0}^{n-1} = \emptyset, \\ \text{span}\{\psi_i^j, \psi_{i+1/2}^j, \psi_{i+1}^j\}, & T = [x_i, x_{i+1}], \alpha_j \in T, j \in \{0, 1, 2, \dots, n-1\}. \end{cases}$$

For a function  $u \in H_\alpha^1(\alpha_{-1}, \alpha_n)$ , we define its quadratic IFE interpolation  $\check{I}_h u \in S_h(\alpha_{-1}, \alpha_n)$  piecewise such that, for every element  $T = [x_i, x_{i+1}]$ ,

$$\check{I}_h u|_T = \begin{cases} u(x_i)L_i(x) + u(x_{i+1/2})L_{i+1/2}(x) + u(x_{i+1})L_{i+1}(x), & T \cap \{\alpha_i\}_{i=0}^{n-1} = \emptyset, \\ u(x_i)\psi_i^j(x) + u(x_{i+1/2})\psi_{i+1/2}^j(x) + u(x_{i+1})\psi_{i+1}^j(x), & \alpha_j \in T, j \in \{0, 1, 2, \dots, n-1\}. \end{cases}$$

Then, we get the error bound for the quadratic IFE interpolation which is given in the following theorem.

**Theorem 3.5.** *Assume that  $\delta_{j+1} \geq \delta_j$  and  $D_j\delta_{j+1} \geq D_{j+1}\delta_j$ , then there exists a positive constant  $C$  independent of  $h$  and the position of  $\alpha_j, j = 0, 1, \dots, n-1$  such that*

$$\|u - \check{I}_h u\|_{0,(\alpha_{-1}, \alpha_n)} + h\|u - \check{I}_h u\|_{1,(\alpha_{-1}, \alpha_n)} \leq Ch^3\|u\|_{3,(\alpha_{-1}, \alpha_n)}.$$

*Proof.* Since we already have the interpolation error estimate on each element, the proof follows from arguments similar to those used in Theorem 2.6.  $\square$

We now consider the quadratic IFE solution to the weak problem defined by (4.2).

Let

$$S_{h,0}(\alpha_{-1}, \alpha_n) = \{v | v \in S_h(\alpha_{-1}, \alpha_n), v|_{x=\alpha_n} = 0\}.$$

The quadratic IFE solution  $u_h \in S_{h,0}^{(2)}(\alpha_{-1}, \alpha_n)$  to the interface problem described by (1.3)-(1.7) is defined to be such that

$$a(u_h, v_h) = (f, v_h), \forall v_h \in S_{h,0}(\alpha_{-1}, \alpha_n). \quad (3.43)$$

Then the error bound for the quadratic IFE solution  $u_h$  is can be got directly which is stated in the following theorem.

**Theorem 3.6.** *Assume the condition required by Theorem 2.1 holds,  $\delta_{j+1} \geq \delta_j$  and  $D_j \delta_{j+1} \geq D_{j+1} \delta_j$ . Let  $u \in H_\alpha^3([\alpha_{-1}, \alpha_n])$  be the solution to the weak problem (4.2), then the quadratic IFE solution  $u_h$  defined by (3.43) satisfies the following estimate:*

$$\|u - u_h\|_{0,(\alpha_{-1}, \alpha_n)} + h\|u - u_h\|_{1,(\alpha_{-1}, \alpha_n)} \leq Ch^3 \|u\|_{3,(\alpha_{-1}, \alpha_n)}.$$

*Proof.* The proof follows form arguments similar to those used in Theorem 2.7.  $\square$

### 3.4 Numerical Experiments

In this section we present some numerical examples to demonstrate the convergence rate of the quadratic IFE method. We use the same examples as those we used in Section 2.5. Firstly, let us briefly review the exact solution for the problem. Recalling that the simulation interval is  $[0, 1]$ , and the three interface points are assumed to be  $\alpha_0 = 1/9$ ,  $\alpha_1 = 1/3$  and  $\alpha_2 = 2/3$ . These interface points separate the interval into four sub-intervals  $[0, 1/9]$ ,  $[1/9, 1/3]$ ,  $[1/3, 2/3]$  and  $[2/3, 1]$ . The exact solution  $u$  for

this problem is set to be

$$u(x) = \begin{cases} u_0(x), & x \in [0, 1/9], \\ u_1(x), & x \in [1/9, 1/3], \\ u_2(x), & x \in [1/3, 2/3], \\ u_3(x), & x \in [2/3, 1], \end{cases} \quad (3.44)$$

with

$$u_0(x) = \frac{1}{30}x^{n-1}, \quad u_1(x) = \frac{1}{3}x^n, \quad u_2(x) = x^{n+1}, \quad u_3(x) = 3(1-x)x^{n+1},$$

here,  $n$  is an integer. We also let

$$\begin{aligned} D_1 &= \frac{18(n-1)D_0}{10n}, & \delta_1 &= \frac{1}{2}(9nD_1 - 8.1(n-1)D_0), \\ D_2 &= \frac{6nD_1 - 2\delta_1}{3(n+1)}, & \delta_2 &= \frac{1}{2}(3(n+1)D_2 - 3nD_1 + 2\delta_1), \\ D_3 &= \frac{8\delta_2 - 3(n+1)D_2}{3(n+5)}, & \delta_3 &= \frac{1}{4}(3(n-1)D_3 - 3(n+1)D_2 + 4\delta_2), \\ \lambda &= \frac{1}{81(n-1)D_0}. \end{aligned}$$

It is clear that  $u(x)$  satisfies the jump conditions (1.3)-(1.4). In addition, the right hand side term  $f_i(x)$ ,  $i = 0, 1, 2, 3$ , is determined by (1.5). We now report numerical results generated by applying the IFE methods developed in Section 3 and Section 4 to the interface problem described by (1.3)-(1.7) whose exact solution is  $u(x)$  defined in (3.44).

**Example 3.1.** *In this group of numerical experiments, we observe that the proposed IFE methods work well for large values of  $\beta_i$ ,  $i = 1, 2, 3$  emphasizing a stronger reaction. We have tested these IFE methods with  $D_0$  arbitrarily chosen between  $10^{-2}$  and  $2 \times 10^{-2}$  and  $\beta_1 \in (1, 2)$ ,  $\beta_2 \in (10^2, 2 \times 10^2)$ ,  $\beta_3 \in (10^4, 2 \times 10^4)$ .*

Table 3.1 presents typical numerical results for errors and the convergence rates for the quadratic IFE method when  $n = 3$ , Table 3.2 contains correspondingly numerical results for the quadratic IFE method. In related computations for these data, we used the following parameters:

$$D_0 = 0.010616229584014, \beta_0 = 0, \beta_1 = 1.72333131659,$$

$$\beta_2 = 140.10036408113, \beta_3 = 16730.88858585343.$$

Data in these tables clearly show that the quadratic IFE methods converge optimally in both the  $L^2$  and  $H^1$  norm.

Table 3.1: Errors and convergence rates of the quadratic IFE method when  $n = 3$  with large values for  $\beta_j, j = 1, 2, 3$ .

N	$L^2$ norm	rate	$H^1$ norm	rate
10	2.6661e-04		1.8276e-02	
20	3.3866e-05	2.9768	4.5238e-03	2.0143
40	3.7201e-06	3.1865	9.6740e-04	2.2254
80	4.6298e-07	3.0063	2.4106e-04	2.0047
160	5.7719e-08	3.0038	5.9870e-05	2.0095
320	7.2261e-09	2.9977	1.4985e-05	1.9983
640	9.0293e-10	3.0005	3.7433e-06	2.0011
1280	1.1287e-10	2.9999	9.3613e-07	1.9995
2560	1.4107e-11	3.0002	2.3399e-07	2.0003

**Example 3.2.** *In this group of numerical experiments, we have tested the IFE methods for  $\beta_i, i = 1, 2, 3$  small enough such as, randomly chosen such that  $\beta_1 \in (0.01, 0.02)$ ,  $\beta_2 \in (0.001, 0.002)$ ,  $\beta_3 \in (0.0001, 0.0002)$ .*

Typical numerical results are presented in Tables 3.2-3.4 which, again, clearly demonstrate the optimal convergence of the proposed linear and quadratic IFE methods. In related computations for these data, we used the following parameters:

$$D_0 = 0.010616229584014, \beta_0 = 0, \beta_1 = 0.015482995717499,$$

$$\beta_2 = 0.001133907855848 \beta_3 = 0.000162651593614.$$

Table 3.2: Errors and convergence rates of the quadratic IFE method when  $n = 6$  with large values for  $\beta_j, j = 1, 2, 3$ .

N	$L^2$ norm	rate	$H^1$ norm	rate
10	5.3218e-04		3.7440e-02	
20	6.8757e-05	2.9523	9.2084e-03	2.0236
40	8.7238e-06	2.9785	2.2819e-03	2.0127
80	1.0967e-06	2.9918	5.6983e-04	2.0016
160	1.3729e-07	2.9978	1.4243e-04	2.0003
320	1.7170e-08	2.9993	3.5611e-05	1.9998
640	2.1465e-09	2.9999	8.9031e-06	1.9999
1280	2.6833e-10	2.9999	2.2259e-06	1.9999
2560	3.3541e-11	3.0000	5.5647e-07	2.0000

Table 3.3: Errors and convergence rates of the quadratic IFE method when  $n = 3$  with small values for  $\beta_j, j = 1, 2, 3$ .

N	$L^2$ norm	rate	$H^1$ norm	rate
10	2.3101e-04		1.5134e-02	
20	2.9875e-05	2.9510	3.8832e-03	1.9624
40	3.6881e-06	3.0180	9.5535e-04	2.0232
80	4.6321e-07	2.9932	2.4015e-04	1.9921
160	5.7849e-08	3.0013	5.9856e-05	2.0044
320	7.2484e-09	2.9966	1.4984e-05	1.9981
640	9.0585e-10	3.0003	3.7433e-06	2.0010
1280	1.1333e-10	2.9987	9.3613e-07	1.9995
2560	1.5537e-11	2.8669	2.3399e-07	2.0002

Table 3.4: Errors and convergence rates of the quadratic IFE method when  $n = 6$  (right) with small values for  $\beta_j, j = 1, 2, 3$ .

N	$L^2$ norm	rate	$H^1$ norm	rate
10	5.4047e-04		3.5801e-02	
20	6.9574e-05	2.9576	9.0744e-03	1.9801
40	8.7780e-06	2.9866	2.2754e-03	1.9957
80	1.0982e-06	2.9987	5.6951e-04	1.9983
160	1.3749e-07	2.9978	1.4242e-04	1.9996
320	1.7173e-08	3.0011	3.5611e-05	1.9997
640	2.1486e-09	2.9987	8.9031e-06	1.9999
1280	2.6835e-10	3.0012	2.2259e-06	1.9999
2560	3.4181e-11	2.9728	5.5647e-07	2.0000



# Chapter 4

## Long Time Stability and Asymptotic Analysis

In this chapter, we study the long time stability and asymptotic behavior for the multi-layer wall model using the IFE methods we constructed in Chapter 2 and Chapter 3. Taking advantage of IFE functions, we investigated the convergence of the discrete system as the time  $t \rightarrow +\infty$ , which can be used on Cartesian mesh regardless of the location of the interface, and get the similar error estimate as the continuous model. The numerical examples in the last section confirmed the theoretical analysis, which suggested that the discrete scheme is efficient. Firstly, we briefly review the notations and preliminaries for the problems which we will use at the rest of this chapter. The piecewise Sobolev spaces defined by

$$H_\alpha^k(\Omega) = \{v \in L^2(\Omega) \mid v|_{\Omega^\pm} \in H^k(\Omega^\pm), v(\alpha_n) = 0\},$$

where  $k \geq 1$  is an integer and  $\Omega = (\alpha_{-1}, \alpha_n)$ ,  $\Omega^- = (\alpha_{-1}, \alpha_0)$ ,  $\Omega^+ = (\alpha_0, \alpha_n)$ . The norm on the space  $H_\alpha^k(\Omega)$  is defined by:

$$\|u\|_{k,\Omega} = \sqrt{\|u\|_{k,\Omega^-}^2 + \|u\|_{k,\Omega^+}^2}.$$

We shall use  $\|\cdot\|_k$  denoting the above norm in the rest of this paper if there is no danger of causing confusion. In addition, the notation  $\|\cdot\|_0$  is used to denote the  $L^2$



norm. Under the norm defined above, we have the following Poincaré inequality on each subinterval  $\Omega^\pm$ :

$$\|v\|_{0,\Omega^\pm}^2 \leq (\lambda^\pm)^{-1} \|v\|_{1,\Omega^\pm}^2, \quad \forall v \in H^k(\Omega^\pm),$$

where  $\lambda^\pm$  is the minimal eigenvalue of the Laplace operator  $-\Delta$  on the space  $H^k(\Omega^\pm)$ , respectively. Let  $\lambda_1 = \max\{\lambda^+, \lambda^-\}$ , we have the following inequality

$$\|v\|_0^2 \leq \lambda_1^{-1} \|v\|_1^2, \quad \forall v \in H^k(\Omega^\pm). \quad (4.1)$$

By the standard procedure, the interface problem described by (1.3)-(1.5) leads to the following weak problem: find  $u \in H_\alpha^1(\Omega)$  such that

$$a(\bar{u}, v) = (\bar{f}, v), \quad \forall v \in H_\alpha^1(\Omega), \quad (4.2)$$

where the bilinear form  $a(u, v)$  is defined same as (2.4). Then, we get the weak formula for the parabolic system (1.1)-(1.4): find  $u \in H_\alpha^1(\Omega) \times (0, T]$ , such that,

$$\begin{aligned} (u_t, v) + a(u, v) &= (f, v), \quad \forall v \in H_\alpha^1(\Omega), \\ u(x, 0) &= u_0(x), \quad x \in \Omega. \end{aligned} \quad (4.3)$$

From (4.3), (4.2), and setting  $\bar{u}_t = 0$ , we have

$$\begin{aligned} (z_t, v) + a(z, v) &= (F, v), \quad \forall v \in H_\alpha^1(\Omega), \\ z(x, 0) &= u_0(x) - \bar{u}(x), \end{aligned} \quad (4.4)$$

here,  $z(x, t) = u(x, t) - \bar{u}(x)$ ,  $F(x, t) = f(x, t) - \bar{f}(x)$ . With the above notations, we get the semi-discrete scheme for the parabolic equation (4.3) as follows: find  $u_h \in S_h(\mathcal{T}_h)$  such that, for all  $t > 0$ ,

$$\begin{cases} (u_{h,t}, v_h) + a(u_h, v_h) = (f, v_h), \quad \forall v_h \in \mathcal{S}_h(\mathcal{T}_h), \\ u_h(x, 0) = u_{0h}(x), \quad x \in \Omega, \end{cases} \quad (4.5)$$

where  $u_{0h}$  is an approximation of  $u_0$  in the space  $\mathcal{S}_h(\mathcal{T}_h)$ . Throughout this chapter, we set  $u_{0h} = P_h u_0$ , here  $P_h : L^2(\Omega) \rightarrow \mathcal{S}_h(\mathcal{T}_h)$  is the  $L^2$  projection defined by

$$(u - P_h u, v_h) = 0, \quad \forall v_h \in \mathcal{S}_h(\mathcal{T}_h). \quad (4.6)$$

Let  $\Delta t$  satisfying  $0 < \Delta t < 1$  be the time step, and  $t^n = n\Delta t$  ( $n = 0, 1, 2, \dots$ ). Denoting  $\phi^n$  the value of  $\phi(t^n)$ , then, for a sequence  $\{\phi^n\}_{n=0}^\infty$ , we define

$$\partial_t \phi^n = \begin{cases} \frac{\phi^n - \phi^{n-1}}{\Delta t}, & n = 1, 2, \dots, \\ \phi_0, & n = 0. \end{cases}$$

Applying the backward Euler scheme, we have the fully discrete scheme for the problem (4.5): find a sequence  $\{u_h^n\}_{n=0}^\infty$  such that

$$\begin{cases} (\partial_t u_h^n, v_h) + a(u_h^n, v_h) = (f^n, v_h), \quad \forall v_h \in \mathcal{S}_h(\mathcal{T}_h), \\ u_h^0 = u_{0h}, \quad x \in \Omega. \end{cases} \quad (4.7)$$

Subtracting (4.2) from (4.7), and setting  $z_h^n = u_h^n - \bar{u}_h$ , we have

$$\begin{cases} (\partial_t z_h^n, v_h) + a(z_h^n, v_h) = (F^n, v_h), \quad \forall v_h \in \mathcal{S}_h(\mathcal{T}_h), \\ z_h(x, 0) = u_{0h}(x, 0) - \bar{u}_h(x), \end{cases} \quad (4.8)$$

here, we use the fact that  $\bar{u}_h(x)$  is independent of  $t$ , and  $F^n = f^n - \bar{f}$ . Before continuing the analysis below, we need to recall the following result [62]:

$$\|\bar{u} - \bar{u}_h\|_k \leq \mathcal{C} h^{p-k} \|\bar{u}\|_p, \quad k = 0, 1; \quad p = 2, 3. \quad (4.9)$$

## 4.1 Long Time Stability

In this section, we derive the long time stability for the problem (1.1)-(1.4). Firstly, we make the following assumptions.

(A1) Assume that the initial data  $u_0(x)$  and the body force  $f(x, t)$  satisfy that, for any given  $t > 0$ ,

$$u_0(x) \in L^2(\Omega), \text{ with } \|u_0\|_0 + e^{-\lambda_1 \mathcal{K}t} \int_0^t e^{\lambda_1 \mathcal{K}s} \|f\|_0 ds \leq \mathcal{C},$$

where  $\mathcal{C}$  is a positive constant. Hereafter, we will use the letter  $\mathcal{C}$  to denote a general positive constant which may take different values in different places but independent of the mesh size  $h$  and the time step  $\Delta t$ .

(A2) Assume that the initial data  $u_0(x)$  and the body force  $f(x, t)$  satisfy

$$u_0(x) \in H_\alpha^2(\Omega), \text{ with } \|u_0\|_2 + e^{-\lambda_1 \mathcal{K}t} \int_0^t e^{\lambda_1 \mathcal{K}s} \|f_s\|_0 ds \leq \mathcal{C}.$$

Obviously, from the first equation in (1.1) and (A2), it yields that  $\|u_{t0}\|_0 \leq \mathcal{C}$ , if  $\|f_t(0)\|_0$  is bounded.

**Theorem 4.1.** *Suppose that (A1) is valid. Then the solution  $u$  of the problem (1.1)-(1.4) satisfies the following regularities, for any given  $s > 0$ ,*

$$\|u\|_0 \leq e^{-\lambda_1 \mathcal{K}s} \|u_0\|_0 + e^{-\lambda_1 \mathcal{K}s} \int_0^s e^{\lambda_1 \mathcal{K}t} \|f\|_0 dt. \quad (4.10)$$

Furthermore, if (A2) holds, we have, for any given  $s > 0$ , that

$$\|u_s\|_0 \leq e^{-\lambda_1 \mathcal{K}s} \|u_{s0}\|_0 + e^{-\lambda_1 \mathcal{K}s} \int_0^s e^{\lambda_1 \mathcal{K}t} \|f_t\|_0 dt. \quad (4.11)$$

*Proof.* Setting  $v = u$  in (4.3), we have

$$(u_t, u) + a(u, u) = (f, u).$$

Using the fact that  $(u_t, u) = \frac{1}{2} \frac{d}{dt} \|u\|_0^2 = \|u\|_0 \frac{d}{dt} \|u\|_0$ , and Cauchy-Scharwz inequality, we have

$$\|u\|_0 \frac{d}{dt} \|u\|_0 + \mathcal{K} \|u\|_1^2 \leq \|f\|_0 \|u\|_0. \quad (4.12)$$

Using (4.1), eliminating the common factor  $\|u\|_0$ , and multiplying by  $e^{\lambda_1 \mathcal{K}t}$ , we have

$$\frac{d}{dt}(e^{\lambda_1 \mathcal{K}t} \|u\|_0) \leq e^{\lambda_1 \mathcal{K}t} \|f\|_0. \quad (4.13)$$

Integrating the above inequality respect to the time  $t$  from 0 to  $s$ , and multiplying by  $e^{-\lambda_1 \mathcal{K}s}$ , we get

$$\|u\|_0 \leq e^{-\lambda_1 \mathcal{K}s} \|u_0\|_0 + e^{-\lambda_1 \mathcal{K}s} \int_0^s e^{\lambda_1 \mathcal{K}t} \|f\|_0 dt. \quad (4.14)$$

Taking derivative in (4.3), we have

$$(u_{tt}, v) + a(u_t, v) = (f_t, v). \quad (4.15)$$

Letting  $v = u_t$ , and similar to (4.12)-(4.13), we have

$$\frac{d}{dt}(e^{\lambda_1 \mathcal{K}t} \|u_t\|_0) \leq e^{\lambda_1 \mathcal{K}t} \|f_t\|_0.$$

Integrating the above inequality respect to the time  $t$  from 0 to  $s$ , and multiplying by  $e^{-\lambda_1 \mathcal{K}s}$ , we get

$$\|u_s\|_0 \leq e^{-\lambda_1 \mathcal{K}s} \|u_{s0}\|_0 + e^{-\lambda_1 \mathcal{K}s} \int_0^s e^{\lambda_1 \mathcal{K}t} \|f_t\|_0 dt.$$

□

By the similar process, we can prove the following theorem for the semi-discrete approximation problem (4.5) using the IFE methods.

**Theorem 4.2.** *Suppose that (A1) is valid. Then the solution  $u$  of the problem (4.5) satisfies the following regularities, for any given  $s > 0$ ,*

$$\|u_h\|_0 \leq e^{-\lambda_1 \mathcal{K}s} \|u_0\|_0 + e^{-\lambda_1 \mathcal{K}s} \int_0^s e^{\lambda_1 \mathcal{K}t} \|f\|_0 dt,$$

*Furthermore, if (A2) holds, we have, for any given  $s > 0$ , that*

$$\|u_{h,s}\|_0 \leq e^{-\lambda_1 \mathcal{K}s} \|u_{s0}\|_0 + e^{-\lambda_1 \mathcal{K}s} \int_0^s e^{\lambda_1 \mathcal{K}t} \|f_t\|_0 dt.$$

Now, we consider the fully discrete approximation problem (4.7) of the problem (1.1)-(1.4).

**Theorem 4.3.** *Suppose assumption (A1) is valid. For any given integer  $n > 0$ , the solution sequence  $\{u_h^n\}$  generated by (4.7) satisfies*

$$\|u_h^n\|_0 \leq \frac{1}{(1 + \Delta t \mathcal{K} \lambda_1)^n} \|u_0\|_0 + \Delta t \sum_{m=1}^n \frac{\|f^m\|_0}{(1 + \Delta t \mathcal{K} \lambda_1)^{n-m+1}}. \quad (4.16)$$

Furthermore, if (A2) holds, we have, for any given  $s > 0$ , that

$$\|\partial_t u_h^n\|_0 \leq \frac{1}{(1 + \Delta t \mathcal{K} \lambda_1)^n} \|u_0\|_0 + \Delta t \sum_{m=1}^n \frac{\|\partial_t f^m\|_0}{(1 + \Delta t \mathcal{K} \lambda_1)^{n-m+1}}. \quad (4.17)$$

*Proof.* Taking  $v = \Delta t u_h^n$  in (4.7), we have

$$(u_h^n - u_h^{n-1}, u_h^n) + \Delta t a(u_h^n, u_h^n) = \Delta t (f^n, u_h^n).$$

Using Cauchy-Schwarz inequality, (4.1), and eliminatting the common factor  $\|u_h^n\|_0$ , we have

$$\|u_h^n\|_0 + \Delta t \mathcal{K} \lambda_1 \|u_h^n\|_0 \leq \|u_h^{n-1}\|_0 + \Delta t \|f^n\|_0, \quad (4.18)$$

which implies that

$$\begin{aligned} \|u_h^n\|_0 &\leq \frac{1}{1 + \Delta t \mathcal{K} \lambda_1} (\|u_h^{n-1}\|_0 + \Delta t \|f^n\|_0) \\ &\leq \frac{1}{(1 + \Delta t \mathcal{K} \lambda_1)^n} \|u_0\|_0 + \Delta t \sum_{m=1}^n \frac{\|f^m\|_0}{(1 + \Delta t \mathcal{K} \lambda_1)^{n-m+1}}. \end{aligned} \quad (4.19)$$

From (4.7), we have

$$(\partial_{tt} u_h^n, v_h) + a(\partial_t u_h^n, v_h) = (\partial_t f^n, v_h), \quad \forall v_h \in \mathcal{S}_h(\mathcal{T}_h).$$

Letting  $v_h = \partial_t u_h^n$ , we have

$$(\partial_t u_h^n - \partial_t u_h^{n-1}, \partial_t u_h^n) + \mathcal{K} \lambda_1 \Delta t \|\partial_t u_h^n\|_0^2 \leq \|\partial_t f^n\|_0 \|\partial_t u_h^n\|_0.$$

Using Cauchy-Schwarz inequality, and eliminatting the common factor  $\|\partial_t u_h^n\|_0$ , we have

$$\|\partial_t u_h^n\|_0 + \mathcal{K}\lambda_1 \Delta t \|\partial_t u_h^n\|_0 \leq \|\partial_t u_h^{n-1}\|_0 + \|\partial_t f^n\|_0.$$

Similar to (4.19), we have

$$\|\partial_t u_h^n\|_0 \leq \frac{1}{(1 + \Delta t \mathcal{K}\lambda_1)^n} \|u_0\|_0 + \Delta t \sum_{m=1}^n \frac{\|\partial_t f^m\|_0}{(1 + \Delta t \mathcal{K}\lambda_1)^{n-m+1}}.$$

The proof is completed. □

## 4.2 Asymptotic Analysis

In this section, we analyze the asymptotic behavior for the problem.

### 4.2.1 Asymptotic Analysis on the $L^2$ Norm

**Theorem 4.4.** *Suppose (A1) is valid, and there exists  $T > 0$ , such that*

$$\lim_{s \rightarrow +\infty} \int_T^s \|f - \bar{f}\|_0 dt = 0, \quad (4.20)$$

$\bar{u}$  and  $u$  are the solutions of the problems (4.2) and (4.3), respectively. Then, we have for any given  $s > 0$ ,

$$\|u - \bar{u}\|_0 \leq e^{-\lambda_1 \mathcal{K}s} \|u_0 - \bar{u}\|_0 + e^{-\lambda_1 \mathcal{K}s} \int_0^s e^{\lambda_1 \mathcal{K}t} \|f - \bar{f}\|_0 dt. \quad (4.21)$$

Furthermore, if (A2) holds, and there exists  $T > 0$ , such that

$$\lim_{s \rightarrow +\infty} \int_T^s \|f_t\|_0 dt = 0, \quad (4.22)$$

we have for any given  $s > 0$ , that

$$\begin{aligned}
e^{-\lambda_1 \mathcal{K} s} \int_0^s e^{\lambda_1 \mathcal{K} t} \|u - \bar{u}\|_1 dt &\leq \frac{1}{\mathcal{K} \lambda_1^{1/2}} e^{-\lambda_1 \mathcal{K} s} \int_0^s e^{\lambda_1 \mathcal{K} t} \|f - \bar{f}\|_0 dt \\
&+ \frac{1}{\mathcal{K} \lambda_1^{1/2}} e^{-\lambda_1 \mathcal{K} s} \int_0^s \|u_{t0}\|_0 dt + \frac{1}{\mathcal{K} \lambda_1^{1/2}} e^{-\lambda_1 \mathcal{K} s} \int_0^s \int_0^t e^{\lambda_1 \mathcal{K} \bar{s}} \|f_{\bar{s}}\|_0 d\bar{s} dt.
\end{aligned} \tag{4.23}$$

**Remark 4.1.** From Theorem 4.4, we can see that if  $f(x, t)$  is smooth enough with respect to the time  $t$ , (4.22) follows directly from (4.20) when the time  $t$  is large enough. Furthermore, the right hand side term in (4.21) and (4.33) will attend to zero when  $t \rightarrow +\infty$  which suggests that the solution of the problem (4.2) converges to that of the steady-state problem (4.3).

*Proof.* Letting  $v = z$  in (4.4), we have

$$(z_t, z) + a(z, z) = (F, z). \tag{4.24}$$

Using the similar technique as (4.12)-(4.14), we can get (4.21) easily.

From (4.24), we have

$$\mathcal{K} \|z\|_1^2 \leq (F, z) - (z_t, z).$$

Using Cauchy-Schwarz inequality, and (4.1), we have

$$\|z\|_1^2 \leq \frac{1}{\mathcal{K}} (\|F\|_0 \|z\|_0 + \|z_t\|_0 \|z\|_0) \leq \frac{1}{\mathcal{K} \lambda_1^{1/2}} (\|F\|_0 \|z\|_1 + \|z_t\|_0 \|z\|_1).$$

Eliminating the common factor, multiplying by  $e^{\lambda_1 \mathcal{K} t}$ , integrating from 0 to  $s$ , and multiplying by  $e^{-\lambda_1 \mathcal{K} s}$ , we have

$$e^{-\lambda_1 \mathcal{K} s} \int_0^s e^{\lambda_1 \mathcal{K} t} \|z\|_1 dt \leq \frac{1}{\mathcal{K} \lambda_1^{1/2}} e^{-\lambda_1 \mathcal{K} s} \int_0^s e^{\lambda_1 \mathcal{K} t} \|F\|_0 dt + \frac{1}{\mathcal{K} \lambda_1^{1/2}} e^{-\lambda_1 \mathcal{K} s} \int_0^s e^{\lambda_1 \mathcal{K} t} \|z_t\|_0 dt. \tag{4.25}$$

Similar to (4.11), we have

$$\|z_t\|_0 \leq e^{-\lambda_1 \mathcal{K}t} \|u_{t0}\|_0 + e^{-\lambda_1 \mathcal{K}t} \int_0^t e^{\lambda_1 \mathcal{K}\tilde{s}} \|F_{\tilde{s}}\|_0 d\tilde{s}.$$

Inserting the above inequality into (4.25), and recalling that  $F = f - \bar{f}$ , we obtain (4.33). The proof is completed.  $\square$

For the finite element semi-discrete approximation problem (4.5), we have the following theorem. The proof is similar to the continuous problem, which is omitted here.

**Theorem 4.5.** *Suppose assumption (A1) and (4.20) are valid.  $u_h$  and  $\bar{u}_h$  are the solutions of the problems (4.5) and (4.2), respectively. Then, we have, for any given  $s > 0$ ,*

$$\|u_h - \bar{u}_h\|_0 \leq e^{-\lambda_1 \mathcal{K}s} \|u_0 - \bar{u}\|_0 + e^{-\lambda_1 \mathcal{K}s} \int_0^s e^{\lambda_1 \mathcal{K}t} \|f - \bar{f}\|_0 dt. \quad (4.26)$$

*Futhermore, if (A2) and (4.22) hold, we have for any given  $s > 0$ , that*

$$\begin{aligned} e^{-\lambda_1 \mathcal{K}s} \int_0^s e^{\lambda_1 \mathcal{K}t} \|u_h - \bar{u}_h\|_1 dt &\leq \frac{1}{\mathcal{K}\lambda_1^{1/2}} e^{-\lambda_1 \mathcal{K}s} \int_0^s e^{\lambda_1 \mathcal{K}t} \|f - \bar{f}\|_0 dt \\ &+ \frac{1}{\mathcal{K}\lambda_1^{1/2}} e^{-\lambda_1 \mathcal{K}s} \int_0^s \|u_{t0}\|_0 dt + \frac{1}{\mathcal{K}\lambda_1^{1/2}} e^{-\lambda_1 \mathcal{K}s} \int_0^s \int_0^t e^{\lambda_1 \mathcal{K}\tilde{s}} \|f_{\tilde{s}}\|_0 d\tilde{s} dt. \end{aligned} \quad (4.27)$$

Finally, we have the following results for the fully discrete scheme.

**Theorem 4.6.** *Suppose assumption (A1) and (4.20) are valid.  $\bar{u}_h$  and  $u_h^n$  are the solutions of the problems (4.2) and (4.7), respectively. Then, we have for any given integer  $n > 0$ ,*

$$\|u_h^n - \bar{u}_h\|_0 \leq \frac{1}{(1 + \Delta t \mathcal{K} \lambda_1)^n} \|u_0\|_0 + \Delta t \sum_{m=1}^n \frac{\|f^m - \bar{f}\|_0}{(1 + \Delta t \mathcal{K} \lambda_1)^{n-m+1}}. \quad (4.28)$$



Futhermore, if (A2) and (4.22) hold, we have for any given  $n > 0$ , that

$$\begin{aligned} \mathcal{K}\Delta t \sum_{m=1}^n \|u_h^n - \bar{u}_h\|_1 &\leq \lambda_1^{-1/2} \Delta t \sum_{m=1}^n \|f^m - \bar{f}\|_0 + \lambda_1^{-1/2} \sum_{m=1}^n \frac{1}{(1 + \Delta t \mathcal{K} \lambda_1)^m} \|u_0\|_0 \\ &+ \lambda_1^{-1/2} \Delta t \sum_{m=1}^n \sum_{k=1}^m \frac{\|f^k - \bar{f}\|_0}{(1 + \Delta t \mathcal{K} \lambda_1)^{m-k+1}}. \end{aligned} \quad (4.29)$$

*Proof.* Letting  $n = m$ , and taking  $v_h = 2\Delta t z_h^m$  in (4.8), we have

$$(z_h^m - z_h^{m-1}, z_h^m) + \Delta t a(z_h^m, z_h^m) = \Delta t (F^m, z_h^m). \quad (4.30)$$

Then, similar to the proof of (4.16), we can get the estiamtes of  $u_h^n - \bar{u}_h$  in  $L^2$  norm easily.

From (4.30), using Cauchy-Schwarz inequality, the coerciveness of the bilinear form  $a(\cdot, \cdot)$ , and (4.1), we have

$$\begin{aligned} \|z_h^m\|_0^2 + \mathcal{K}\Delta t \|z_h^m\|_1^2 &\leq \Delta t \|F^m\|_0 \|z_h^m\|_0 + \|z_h^{m-1}\|_0 \|z_h^m\|_0 \\ &\leq \lambda_1^{-1/2} \Delta t \|f^m - \bar{f}\|_0 \|z_h^m\|_1 + \lambda_1^{-1/2} \|z_h^{m-1}\|_0 \|z_h^m\|_1. \end{aligned}$$

Eliminating the common factor, the above inequality implies that

$$\mathcal{K}\Delta t \|z_h^m\|_1 \leq \lambda_1^{-1/2} \Delta t \|f^m - \bar{f}\|_0 + \lambda_1^{-1/2} \|z_h^{m-1}\|_0.$$

Taking summation from 1 to  $n$ , we have

$$\mathcal{K}\Delta t \sum_{m=1}^n \|z_h^m\|_1 \leq \lambda_1^{-1/2} \Delta t \sum_{m=1}^n \|f^m - \bar{f}\|_0 + \lambda_1^{-1/2} \sum_{m=1}^n \|z_h^{m-1}\|_0,$$

Inserting the estimates of  $\|z_h^{n-1}\|_0$  into the above inequality, we can get the second inequalities in (4.28). The proof is completed.  $\square$

**Remark 4.2.** *Recalling the convergence results in (5.3) for the spatial discrete, we know immediately that the fully discrete solution converge to the exact solution of the steady-state solution when  $h \rightarrow 0$  and  $t \rightarrow +\infty$ .*

## 4.2.2 Asymptotic Analysis on the $H^1$ Norm

We discuss, further, the behavior of the solution as  $t \rightarrow +\infty$  assuming that the forcing term satisfying the following assumption:

$$(A3) \quad f_t, f \in L^\infty(\mathbb{R}^+, L^2(\Omega)), \text{ i.e. } \sup_{t \geq 0} (\|f\|_0 + \|f_t\|_0) \leq \mathcal{C},$$

$$\text{and } \lim_{t \rightarrow +\infty} \|f - \bar{f}\|_0 = 0.$$

**Theorem 4.7.** *Suppose assumption (A1) and (4.20) are valid.  $u_h$  and  $\bar{u}_h$  are the solutions of the problems (4.5) and (4.2), respectively. Then, we have, for any given  $s > 0$ ,*

$$\|u - \bar{u}\|_1^2 \leq \mathcal{C}e^{-2\delta_0 s} (\|u_0 - \bar{u}\|_0^2 + \|f_0\|_0^2) + \mathcal{C}e^{-2\delta_0 s} \int_0^s \|f - \bar{f}\|_0^2 + \|f_t\|_0^2 dt, \quad (4.31)$$

here,  $\mathcal{C}$  is a positive constant depended on the data  $(\Omega, \mathcal{K}, \delta_0, \lambda_1)$ , and  $0 < \delta_0 < \min\{1, \frac{1}{2}\mathcal{K}\lambda_1\}$ .

*Proof.* Letting  $v = e^{2\delta_0 t} z_t$  in (4.4), we have

$$(z_t, e^{2\delta_0 t} z_t) + a(z, e^{2\delta_0 t} z_t) = (F, e^{2\delta_0 t} z_t). \quad (4.32)$$

Since  $a(\cdot, \cdot)$  is nonsymmetric, we have

$$a(z, e^{2\delta_0 t} z_t) = \frac{1}{2} \frac{d}{dt} (e^{2\delta_0 t} a(z, z)) - \delta_0 e^{2\delta_0 t} a(z, z) + \frac{1}{2} e^{2\delta_0 t} a(z, z_t) - \frac{1}{2} e^{2\delta_0 t} a(z_t, z). \quad (4.33)$$

Substituting (4.33) into (4.32), integrating from 0 to  $s$ , using Cauchy-Schwarz inequality, Young's inequality, we get

$$\mathcal{K} \frac{1}{2} e^{2\delta_0 s} \|z\|_1^2 \leq \frac{1}{4} \int_0^s e^{2\delta_0 t} \|F\|_0^2 dt + \int_0^s (1 + \delta_0) e^{2\delta_0 t} \|z\|_1^2 dt + \int_0^s e^{2\delta_0 t} \|z_t\|_1^2 dt + \frac{1}{2} \|z(0)\|_1^2.$$

Multiplying by  $e^{-2\delta_0 s}$  in the above inequality, we have

$$\begin{aligned} \|z\|_1^2 &\leq \mathcal{C}(e^{-2\delta_0 s} \int_0^s e^{2\delta_0 t} \|F\|_0^2 dt + e^{-2\delta_0 s} \int_0^s e^{2\delta_0 t} \|z\|_1^2 dt \\ &\quad + e^{-2\delta_0 s} \int_0^s e^{2\delta_0 t} \|z_t\|_1^2 dt + e^{-2\delta_0 s} \|z(0)\|_1^2). \end{aligned} \quad (4.34)$$

Letting  $v = e^{2\delta_0 t} z$  in (4.4), we have

$$(z_t, e^{2\delta_0 t} z) + a(z, e^{2\delta_0 t} z) = (F, e^{2\delta_0 t} z),$$

which implies that

$$\frac{1}{2} \frac{d}{dt} (e^{2\delta_0 t} \|z\|_0^2) + \mathcal{K} \|z\|_1^2 \leq e^{2\delta_0 t} \|F\|_0 \|z\|_0 + \delta_0 e^{2\delta_0 t} \|z\|_0^2.$$

Since  $\delta_0 < \frac{\mathcal{K}\lambda_1}{2}$ , using Young's inequality, we have

$$\|F\|_0 \|z\|_0 \leq \frac{1}{4(\frac{\mathcal{K}\lambda_1}{2} - \delta_0)} \|F\|_0^2 + (\frac{\mathcal{K}\lambda_1}{2} - \delta_0) \|z\|_0^2.$$

Using the fact that  $\|z\|_0^2 \leq \lambda_1^{-1} \|z\|_1^2$ , and integration from time 0 to  $s$ , we have

$$e^{2\delta_0 s} \|z\|_0^2 + \int_0^s e^{2\delta_0 t} \|z\|_1^2 dt \leq \mathcal{C}(\int_0^s e^{2\delta_0 t} \|F\|_0^2 dx + \int_0^s e^{2\delta_0 t} \|z\|_0^2 dx).$$

Multiplying by  $e^{-2\delta_0 s}$ , we have

$$e^{-2\delta_0 s} \int_0^s e^{2\delta_0 t} \|z\|_1^2 dt \leq \mathcal{C}e^{-2\delta_0 s} \|z_0\|_0^2 + \mathcal{C}e^{-2\delta_0 s} \int_0^s \|F\|_0^2 dt. \quad (4.34)$$

Similarly, taking derivative in (4.4), we have

$$(z_{tt}, v)_a(z_t, v) = (F, v).$$

Letting  $v = e^{-2\delta_0 t} z_t$ , we have

$$(z_{tt}, e^{-2\delta_0 t} z_t) + a(z_t, e^{-2\delta_0 t} z_t) = (F, e^{-2\delta_0 t} z_t).$$

Similarly, we have

$$e^{-2\delta_0 s} \int_0^s e^{2\delta_0 t} \|z_t\|_1^2 dt \leq \mathcal{C} e^{-2\delta_0 s} \|u_{t0}\|^2 + \mathcal{C} e^{-2\delta_0 s} \int_0^s \|F_t\|_0^2 dt. \quad (4.32)$$

Inserting (4.2.2) and (4.2.2) into (4.34), it is easily to get (4.33).  $\square$

**Theorem 4.8.** *Suppose assumption (A1) and (4.20) are valid.  $u_h$  and  $\bar{u}_h$  are the solutions of the problems (4.5) and (4.2), respectively. Then, we have, for any given  $s > 0$ ,*

$$\|u_h - \bar{u}_h\|_1^2 \leq \mathcal{C} e^{-2\delta_0 s} (\|u_0 - \bar{u}\|_0^2 + \|f_0\|_0^2) + \mathcal{C} e^{-2\delta_0 s} \int_0^s \|f - \bar{f}\|_0^2 + \|f_t\|_0^2 dt, \quad (4.33)$$

here,  $\mathcal{C}$  is a positive constant depended on the data  $(\Omega, \mathcal{K}, \delta_0, \lambda_1)$ .

**Theorem 4.9.** *Suppose assumption (A1) and (4.20) are valid.  $\bar{u}_h$  and  $u_h^n$  are the solutions of the problems (4.2) and (4.7), respectively. Then, we have for any given integer  $n > 0$ ,*

$$\|u_h^n - \bar{u}_h\|_1^2 \leq \mathcal{C} e^{-2\delta_0 t^n} \|u_0 - \bar{u}_h\|_0^2 + \mathcal{C} e^{-2\delta_0 t^n} \sum_{m=1}^n (\|f^m - \bar{f}\|_0^2 + \|f_t^m\|_0^2), \quad (4.34)$$

here,  $\mathcal{C}$  is a positive constant depending on the data  $(\Omega, \mathcal{K}, \delta_0, \lambda_1)$ .

*Proof.* Let  $v_h = e^{2\delta_0 t^m} \partial_t z_h^m$  in (4.8), we have

$$(\partial_t z_h^m, e^{2\delta_0 t^m} \partial_t z_h^m) + a(z_h^m, e^{2\delta_0 t^m} \partial_t z_h^m) = (F^m, e^{2\delta_0 t^m} \partial_t z_h^m). \quad (4.35)$$

We know that

$$\begin{aligned} a(z_h^m, \partial_t z_h^m) &= \frac{1}{2\Delta t} (a(z_h^m, z_h^m) - a(z_h^{m-1}, z_h^{m-1})) + \frac{1}{2} a(z_h^m, \partial_t z_h^m) - \frac{1}{2} a(\partial_t z_h^m, z_h^{m-1}) \\ &\geq \frac{1}{2\Delta t} (a(z_h^m, z_h^m) - a(z_h^{m-1}, z_h^{m-1})) - \mathcal{C} (\|z_h^m\|_1^2 + \|z_h^{m-1}\|_1^2 + \|\partial_t z_h^m\|_1^2). \end{aligned}$$

Substituting above inequality into (4.35), and using Cauchy-Schwarz inequality, Young's inequality to the right hand side term, we have

$$\begin{aligned}
& e^{2\delta_0 t^m} \|\partial_t z_h^m\|_0^2 + \frac{1}{2\Delta t} e^{2\delta_0 t^m} (a(z_h^m, z_h^m) - a(z_h^{m-1}, z_h^{m-1})) \\
& \leq e^{2\delta_0 t^m} \|F^m\|_0^2 + \mathcal{C}(e^{2\delta_0 t^m} \|z_h^{m-1}\|_1^2 + e^{2\delta_0 t^m} \|z_h^m\|_1^2 + e^{2\delta_0 t^m} \|\partial_t z_h^m\|_1^2).
\end{aligned} \tag{4.36}$$

Multiplying by  $2\Delta t$ , using the fact that

$$e^{2\delta_0 t^n} \|z_h^{n-1}\|_0^2 \leq e^{2\delta_0 t^{n-1}} \|z_h^{n-1}\|_0^2 + 2\delta_0 \Delta t e^{2\delta_0 t^n} \|z_h^{n-1}\|_0^2, \tag{4.37}$$

and taking summing from 1 to  $n$ , then multiplying by  $e^{-2\delta_0 t^n}$ , we have

$$\begin{aligned}
& e^{-2\delta_0 t^n} 2\Delta t \sum_{m=1}^n e^{2\delta_0 t^m} \|\partial_t z_h^m\|_0^2 + \mathcal{K} \|z_h^n\|_1^2 \\
& \leq \mathcal{C} \Delta t e^{-2\delta_0 t^n} \sum_{m=1}^n e^{2\delta_0 t^m} \|z_h^m\|_1^2 + \mathcal{C} \Delta t e^{-2\delta_0 t^n} \sum_{m=1}^n e^{2\delta_0 t^m} \|\partial_t z_h^m\|_1^2 \\
& \quad + \mathcal{C} e^{-2\delta_0 t^n} \sum_{m=1}^n e^{2\delta_0 t^m} \|F^m\|_0^2 + \mathcal{C} \Delta t e^{-2\delta_0 t^n} e^{2\delta_0 \Delta t} \|z_h^0\|_1^2 + e^{-2\delta_0 t^n} \|z_h^0\|_1^2.
\end{aligned}$$

Then, we have

$$\begin{aligned}
& e^{-2\delta_0 t^n} 2\Delta t \sum_{m=1}^n e^{2\delta_0 t^m} \|\partial_t z_h^m\|_0^2 + \mathcal{K} \|z_h^n\|_1^2 \\
& \leq \mathcal{C} e^{-2\delta_0 t^n} \sum_{m=1}^n e^{2\delta_0 t^m} \|F^m\|_0^2 + \mathcal{C} \Delta t e^{-2\delta_0 t^n} \sum_{m=1}^n e^{2\delta_0 t^m} \|\partial_t z_h^m\|_1^2 + \mathcal{C} e^{-2\delta_0 t^n} \|z_h^0\|_1^2.
\end{aligned} \tag{4.38}$$

Now, we aim to estimate the second term on the right hand side  $\Delta t e^{-2\delta_0 t^n} \sum_{m=1}^n e^{2\delta_0 t^m} \|\partial_t z_h^m\|_1^2$ .

Taking derivative in (4.8), we have

$$(\partial_{tt} z_h^m, v_h) + a(\partial_t z_h^m, v_h) = (\partial_t F^m, v_h).$$

Let  $v_h = e^{2\delta_0 t^m} \partial_t z_h^m$ , we have

$$\begin{aligned} & \frac{1}{2\Delta t} (e^{2\delta_0 t^m} \|\partial_t z_h^m\|_0^2 - e^{2\delta_0 t^m} \|\partial_t z_h^{m-1}\|_0^2) + \mathcal{K} e^{2\delta_0 t^m} \|\partial_t z_h^m\|_1^2 \\ & \leq \frac{1}{4\epsilon} e^{2\delta_0 t^m} \|F_t^m\|_0^2 + \epsilon e^{2\delta_0 t^m} \|\partial_t z_h^m\|_0^2. \end{aligned}$$

Multiplying by  $2\Delta t$ , and using the fact that

$$e^{2\delta_0 t^m} \|\partial_t z_h^{m-1}\|_0^2 \leq e^{2\delta_0 t^{m-1}} \|\partial_t z_h^{m-1}\|_0^2 + 2\delta_0 \Delta t e^{2\delta_0 t^n} \|\partial_t z_h^{m-1}\|_0^2,$$

we have

$$\begin{aligned} & e^{2\delta_0 t^m} \|\partial_t z_h^m\|_0^2 - e^{2\delta_0 t^{m-1}} \|\partial_t z_h^{m-1}\|_0^2 + 2\Delta t \mathcal{K} e^{2\delta_0 t^m} \|\partial_t z_h^m\|_1^2 \\ & \leq \frac{1}{4\epsilon} 2\Delta t e^{2\delta_0 t^m} \|F_t^m\|_0^2 + 2\Delta t \epsilon e^{2\delta_0 t^m} \|\partial_t z_h^m\|_0^2 + 2\delta_0 \Delta t e^{2\delta_0 t^n} \|\partial_t z_h^{m-1}\|_0^2. \end{aligned}$$

Taking summation from 1 to  $n$ , and multiplying by  $e^{-2\delta_0 t^n}$ , we obtain

$$\begin{aligned} \|\partial_t z_h^n\|_0^2 + e^{-2\delta_0 t^n} \sum_{m=1}^n 2\Delta t \mathcal{K} e^{2\delta_0 t^m} \|\partial_t z_h^m\|_1^2 & \leq e^{-2\delta_0 t^n} \sum_{m=1}^n \frac{1}{2\epsilon} \Delta t e^{2\delta_0 t^m} \|F_t^m\|_0^2 \\ & + e^{-2\delta_0 t^n} \sum_{m=1}^n (\epsilon + \delta_0) 2\Delta t e^{2\delta_0 t^m} \|\partial_t z_h^m\|_0^2 + \mathcal{C} e^{-2\delta_0 t^n} \|z_h^0\|_0^2, \end{aligned}$$

where, we used the fact that  $\partial_t z_h^0 = z_h^0$ . Substituting above inequality into (4.38), choosing  $\epsilon = 1 - \delta_0$ , and noting (A1), we we have (4.34) immediately. The proof is completed.  $\square$

### 4.3 Numerical Experiments

In this section, we present some numerical results to verify the error estimates derived in the above section. Let  $x \in [0, 1]$ . Assume that there are two interface points:  $\alpha_0$  and  $\alpha_1$ , which separate the interval into there sub-intervals  $[0, \alpha_0]$ ,  $[\alpha_0, \alpha_1]$  and  $[\alpha_1, 1]$ .

The exact solution  $u$  for this problem is set to be

$$u(x, t) = \begin{cases} u_0(x)(1 + e^{-t}), & x \in [0, \alpha_0], t > 0, \\ u_1(x)(1 + e^{-t}), & x \in [\alpha_0, \alpha_1], t > 0, \\ u_2(x)(1 + e^{-t}), & x \in [\alpha_1, 1], t > 0, \end{cases}$$

with

$$u_0 = \frac{x^2 v_0(x)(\alpha_1 - 1)}{\alpha_0^2} - \frac{x^2 v_0(\alpha_0)(\alpha_1 - 1)}{\alpha_0^2} + \frac{1}{2} \frac{g x^2}{D_0 \alpha_0},$$

$$u_1 = v_1(x)(\alpha_1 - 1) + \frac{D_2}{D_1} v_2(x)(x - \alpha_1),$$

$$u_2 = v_2(x)(x - 1),$$

here,

$$v_0(x) = \frac{x^n}{D_0} - \frac{1}{D_0} \left( \frac{2\delta_1}{D_1} (\alpha_0^n - \alpha_1^n) + \alpha_1^n \right) (x - \alpha_0), \quad n \in \mathbb{Z}^+,$$

$$v_1(x) = \frac{x^n - \alpha_1^n}{D_1} + \frac{\alpha_1^n}{2\delta_1},$$

$$v_2(x) = (D_2 n)^{-1} \left( \frac{\delta_2}{\delta_1} - 1 \right) \alpha_1 (x^n - \alpha_1^n) + \frac{\alpha_1^n}{2\delta_1} + \frac{x^n - \alpha_1^n}{D_2},$$

$$g = D_2 v_2'(\alpha_0)(\alpha_0 - \alpha_1) + D_2 v_2(\alpha_0) - 2\delta_1 \frac{D_2}{D_1} v_2(\alpha_0)(\alpha_0 - \alpha_1).$$

The form of the exact solution  $u$  is designed to satisfy the parabolic equations, boundary condition and the jump conditions in (1.1)-(1.4). The right hand side term  $f(x, t)$  is determined by (1.1)-(1.4).

**Example 4.1.** *In the first example, we use the linear and quadratic IFE methods to solve the problem (1.1)-(1.4), respectively. In addition, we choose  $\alpha_0 = 1/3$ ,  $\alpha_1 = 2/3$ ,  $n = 6$ ,  $D_0 = 1.5$ ,  $D_1 = 0.3$ ,  $D_2 = 0.15$ ,  $\delta_0 = 0$ ,  $\delta_1 = 7.5$ ,  $\delta_2 = 10$ ,  $\beta_0 = 0$ ,  $\beta_1 = 30$ ,  $\beta_2 = 15$ , and set the mesh size  $h = 1/40$ , the time step  $\Delta t = 0.1$ .*

Based on linear and quadratic IFE methods, we plot the errors between the fully discrete solution  $u_h^n$  of the multi-layer porous wall model for the drug-eluting stents

and the IFE solution  $\bar{u}_h$  of the steady-state problem in Figures 4.1 and 4.3, respectively. We observe that the system (1.1)-(1.4) approaches to the steady problem (1.3)-(1.7) (about  $t > 5$ ) when  $\|f(t, x) - \bar{f}(x)\|_0 \rightarrow 0$  both in the  $L^2$  and  $H^1$  norms, which is consistent with the theoretical predictions. Then, we compare the values of the fully discrete IFE scheme of the unsteady problem (1.1)-(1.4), and the exact solution of the steady problem (1.3)-(1.7) by using the linear and quadratic IFE methods in Figures 4.2 and 4.4, respectively. The values of the two solutions are almost same, which suggests that the multi-layer porous wall model converges to a steady problem. In addition, we can see that there is no difference between the two graphs when  $n = 50$  and  $n = 100$ , the theoretical analysis stated in the above section is verified again. We also plot the procedure how the numerical solution of the unsteady problem converge to the exact solution of the steady problem in Figure 4.5. The graphs of the numerical solution coincide with the exact solution of the steady problem when iteration times  $n > 50$ , which illustrates that the numerical solutions based on the IFE method have a well performance in solving the interface problem. In Figure 4.6, we plot the logarithm of  $\|u_h^n - \bar{u}_h\|_0$  and  $\|u_h^n - \bar{u}_h\|_1$  by using linear and quadratic IFE methods respectively. All of them are straight lines with negative slope, which illustrates that the fully discrete solution of the unsteady problem converges to the exact solution of the steady-state problem exponentially.

**Example 4.2.** *In this example, we choose the coefficients have a large jump, for example, letting  $D_0 = 1000$ ,  $D_1 = 10$ ,  $D_2 = 0.1$ . Of course, we can change the interface points, for example let  $\alpha_0 = 1/7$ ,  $\alpha_1 = 6/7$ . The other parameters are same to the first example.*

In Figure 4.7, we compare the numerical solutions of the unsteady problem generated by the linear and quadratic IFE methods and the exact solution of the steady-



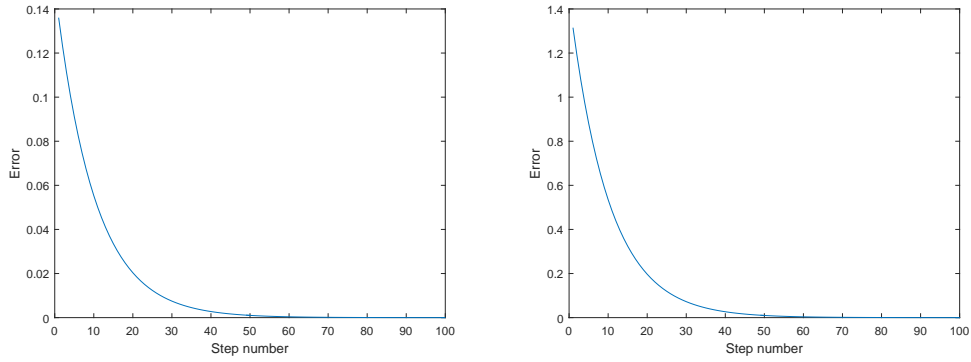


Figure 4.1: Errors  $\|u_h^n - \bar{u}_h\|_0^2$  (left), and  $\|u_h^n - \bar{u}_h\|_1^2$  (right) using the linear IFE method ( $h = 1/40$ ).

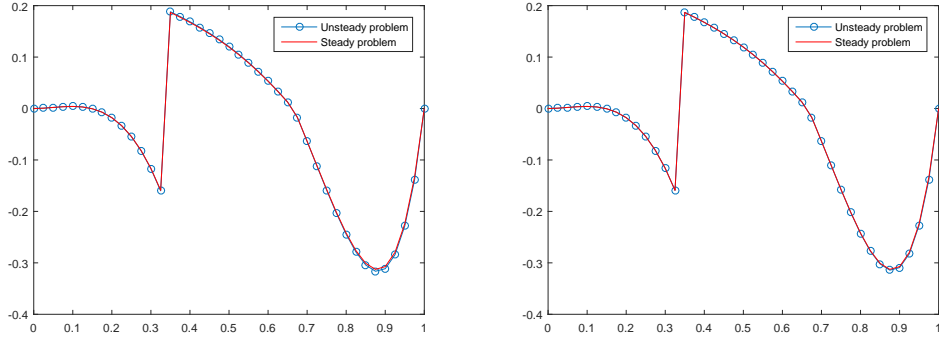


Figure 4.2: The values of  $u_h^n(x)$  when iterate 50 times (left), and 100 times (right) using the linear IFE method by comparison with the exact solution of the steady problem ( $h = 1/40$ ).

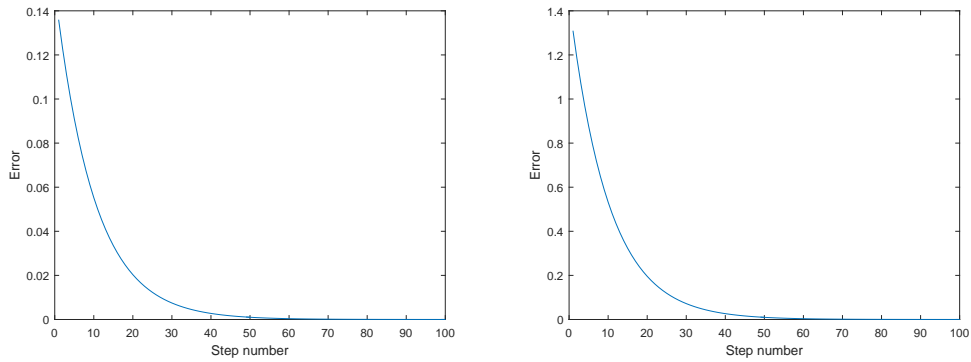


Figure 4.3: Errors  $\|u_h^n - \bar{u}_h\|_0$  (left), and  $\|u_h^n - \bar{u}_h\|_1$  (right) using the quadratic IFE method ( $h = 1/40$ ).

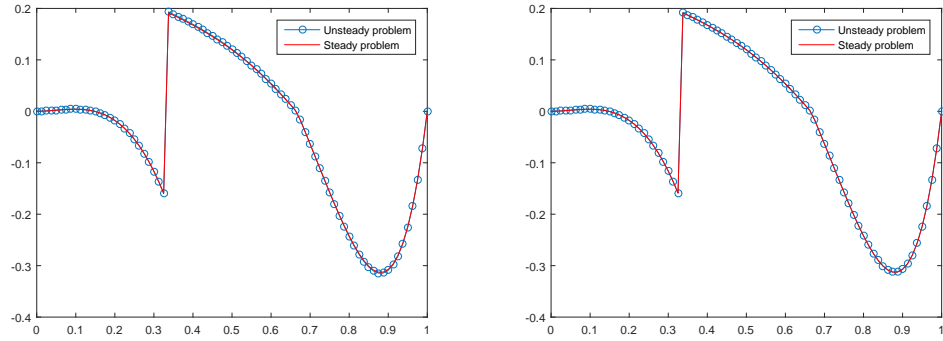


Figure 4.4: The values of  $u_h^n(x)$  when iterate 50 times (left), and 100 times (right) using the quadratic IFE method by comparison with the exact solution of the steady problem ( $h = 1/40$ ).

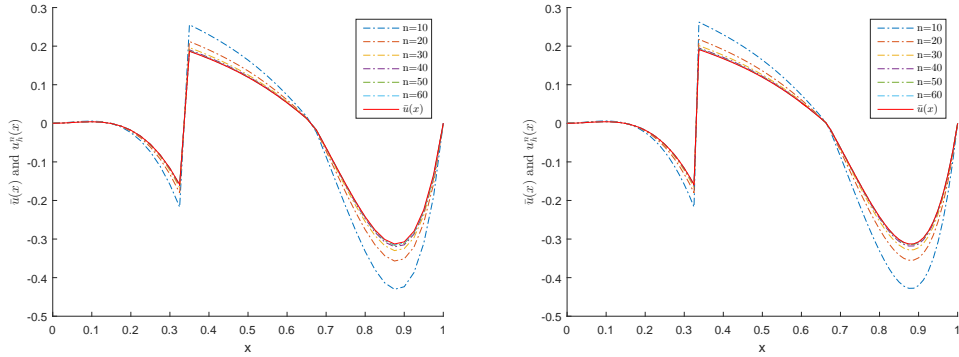


Figure 4.5: Linear IFE method (left) and Quadratic IFE method (right) ( $h = 1/40$ ).

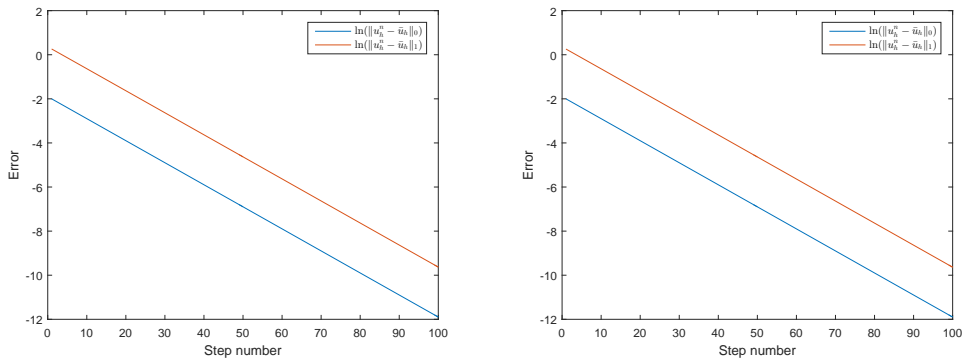


Figure 4.6: The errors of  $\ln(\|u_h^n - \bar{u}_h\|_0)$  and  $\ln(\|u_h^n - \bar{u}_h\|_1)$  using linear (left) and Quadratic (right) IFE method ( $h = 1/40$ ).

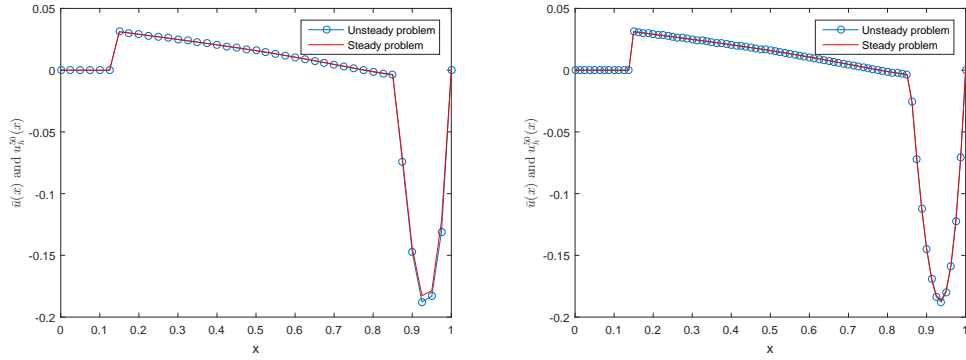


Figure 4.7: Linear IFE method (left) and Quadratic IFE method (right) ( $h = 1/40$ ).

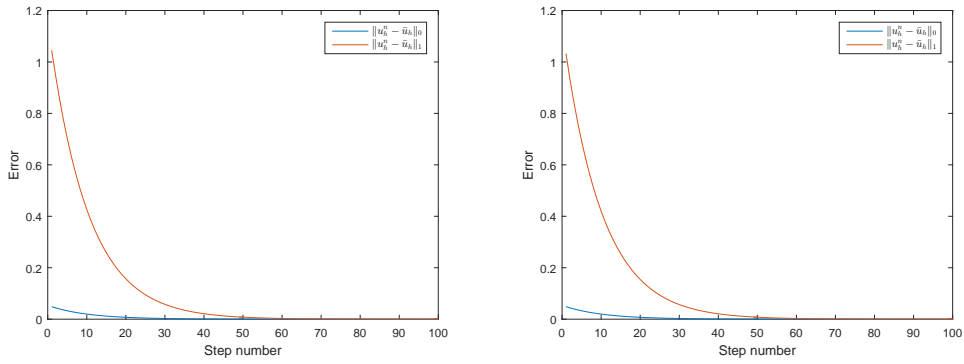


Figure 4.8: Linear IFE method (left) and Quadratic IFE method (right) ( $h = 1/40$ ).

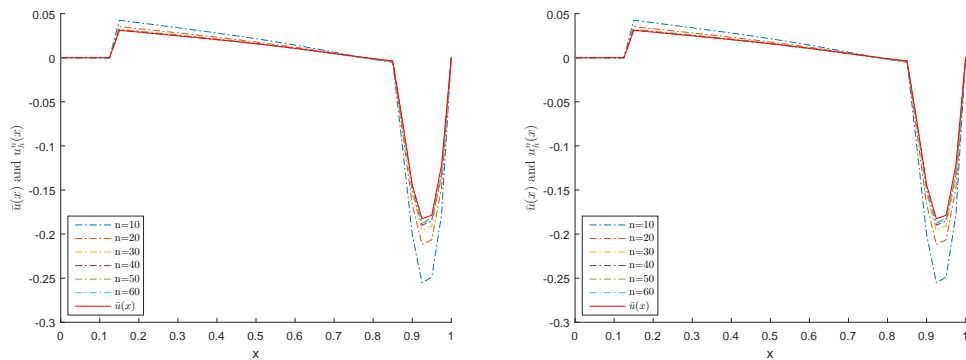


Figure 4.9: Linear IFE method (left) and Quadratic IFE method (right) ( $h = 1/40$ ).

state problem. When the iteration times  $n > 50$ , they have already coincide with each other, which shows that the IFE method can produce accurate solutions to the interface problems, even if the jump of the coefficient is very large. Errors at the each time level in  $L^2$  and  $H^1$  norms are plotted in Figure 4.8, from which we can see that the IFE method has a well control on the error. To observe the convergence performance of the IFE method, we plot the numerical solution on several time level in Figure 4.9. We can see that the IFE method can handle the interface problem very well. Since we change the location of the interface points in this example, it in addition demonstrates that the convergence is independent of the location of the interface points. Figure 4.10 plots the logarithm of the error  $\|u_h^n - \bar{u}_h\|_0$  and  $\|u_h^n - \bar{u}_h\|_1$  using linear and quadratic IFE methods, respectively. We can see that they are all straight lines, which indicates the errors between the fully discrete solution of the unsteady problem and the exact solution of the steady problem exponential decay. The phenomenon is consistent with our theoretical results.

**Remark 4.3.** *In Figure 4.9, we can see that the IFE solutions of (1.1)-(1.4) is not exactly same to the exact solution of the steady-state problem when  $x \in (0.9, 1)$ . The reason causing this phenomenon is that we used a rough mesh ( $h=1/40$ ). This phenomenon will disappear as the mesh size becomes smaller, such as  $h = 1/160$ . Meanwhile the figures show that the numerical solutions and the exact solution are almost same near the two interface points even for the rough mesh size. Therefore, these experiments strongly suggest that our method can handle the interface very well.*

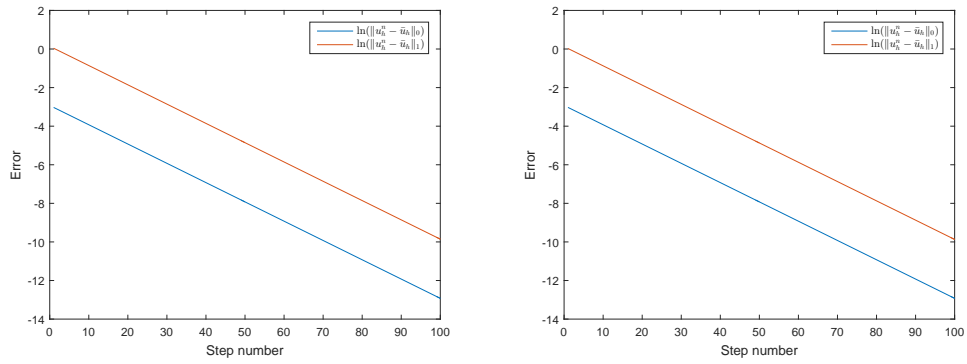


Figure 4.10: The errors of  $\ln(\|u_h^n - \bar{u}_h\|_0)$  and  $\ln(\|u_h^n - \bar{u}_h\|_1)$  using linear (left) and Quadratic (right) IFE method ( $h = 1/40$ ).

# Chapter 5

## IFE Methods for the Time Dependent Multi-layer Porous Wall Model

In this chapter, IFE method are employed to solve the time dependent multi-layer porous wall model. Typical semi-discrete and fully discrete schemes are presented and analyzed. Optimal convergence rate for both semi-discrete and fully discrete schemes is proved. Some numerical experiments are provided to validate our theoretical results. In this chapter, we use the same notation introduced in Section 2.1. Recalling that the weak formula for the parabolic system (1.1)-(1.4) is that: find  $u \in H_\alpha^1(\Omega)$ , such that for all  $t > 0$ ,

$$(u_t, v) + a(u, v) = (f, v), \quad \forall v \in H_\alpha^1(\Omega), \quad (5.1)$$

$$u(x, 0) = u_0(x), \quad x \in \Omega. \quad (5.2)$$

where the bilinear form  $a(u, v)$  is defined as

$$a(u, v) = \frac{[v]_{\alpha_0}[u]_{\alpha_0}}{\lambda} + \int_{\alpha_{-1}}^{\alpha_n} (v'(x)(Du'(x) - 2\delta u(x)) + \beta v(x)u(x)) dx, \quad \forall u, v \in H_\alpha^1(\Omega).$$

As usual, we also denote  $\mathcal{T}_h$  the partition for the domain  $\Omega$ .  $\mathcal{T}^{int}$  and  $T^{non}$  are used to denote the collection of the interface elements and non-interface elements,

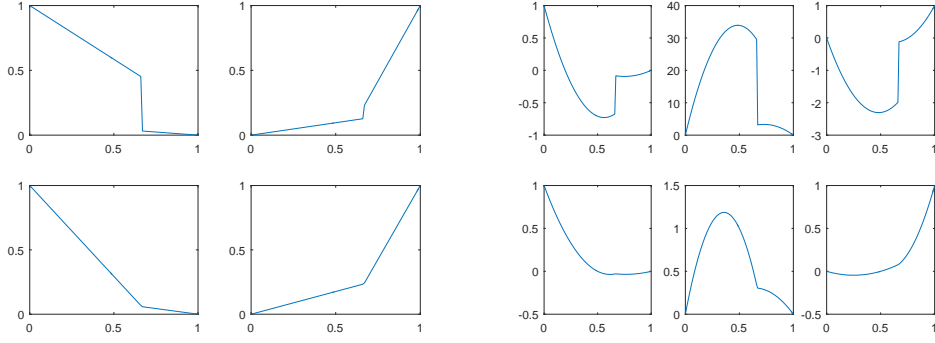


Figure 5.1: 1D linear (left) and quadratic (right) IFE local basis function.

respectively. In addition, we also assume that each interface element contains only one interface point. Following the general framework of IFE, on each non-interface element  $T \in \mathcal{T}_h^{non}$ , the local IFE space is the standard linear or quadratic finite element space. Otherwise, on each interface element  $T \in \mathcal{T}_h^{int}$ , we use the linear or quadratic IFE space constructed in Chapter 2 and Chapter 3. We plot the local linear and quadratic basis in Figure 5.1. We recall that the local IFE space  $\mathcal{S}_h(T)$  is defined by

$$\mathcal{S}_h(T) = \text{span}\{\phi_i, i = 1, \dots, p\},$$

where,  $p = 2$  or  $p = 3$  depends on the IFE space (linear or quadratic). So, for each element  $T \in \mathcal{T}_h$ , we can define the the linear and quadratic IFE space on the whole solution domain  $\Omega$  as follows:

$$\mathcal{S}_h(\mathcal{T}_h) = \{v | v \in L^2(\Omega), v|_{\Omega^\pm} \in C^0(\Omega^\pm), v|_T \in \mathcal{S}_h(T), v(\alpha_n) = 0, \forall T \in \mathcal{T}_h\}.$$

The following convergence results are carried out in Chapter 2 and Chapter 3:

$$\|u - u_h\|_k \leq \mathcal{C}h^{p-k} \|u\|_p, \quad k = 0, 1; \quad p = 2, 3. \quad (5.3)$$

With the above notations, we recall that the semi-discrete scheme in (4.5) for the parabolic equation as follows: find  $u_h \in \mathcal{S}_h(\mathcal{T}_h)$  such that, for all  $t > 0$ ,

$$\begin{cases} (u_{h,t}, v_h) + a(u_h, v_h) = (f, v_h), \quad \forall v_h \in \mathcal{S}_h(\mathcal{T}_h), \\ u_h(x, 0) = u_{0h}(x), \quad x \in \Omega, \end{cases} \quad (5.4)$$

where  $u_{0h}$  is an approximation of  $u_0$  in the space  $\mathcal{S}_h(\mathcal{T}_h)$ . Let  $\Delta t = \frac{T}{N_t}$  satisfying  $0 < \Delta t < 1$  be the time step, and  $t^n = n\Delta t$  ( $n = 0, 1, 2, \dots, N_t$ ). Denoting  $\phi^n$  the value of  $\phi(t^n)$ , then, for a sequence  $\{\phi^n\}_{n=0}^{N_t}$ , we define

$$\partial_t \phi^n = \begin{cases} \frac{\phi^n - \phi^{n-1}}{\Delta t}, \quad n = 2, \dots, N_t, \\ \frac{\phi_1}{\Delta t}, \quad n = 1, \end{cases}$$

Applying the backward Euler scheme, we have the fully discrete scheme for the problem (4.5): find a sequence  $\{u_h^n\}_{n=0}^{N_t}$  such that

$$\begin{cases} (\partial_t u_h^n, v_h) + a(u_h^n, v_h) = (f^n, v_h), \quad \forall v_h \in \mathcal{S}_h(\mathcal{T}_h), \\ u_h^0 = u_{0h}, \quad x \in \Omega. \end{cases} \quad (5.5)$$

## 5.1 Error Estimation for Semi-discrete Scheme

In this section, we derive a priori error estimates for semi-discrete scheme (5.4). The error bound based on the norm defined in (2.2). Firstly, Let  $R_h : H_1^\alpha(\Omega) \rightarrow \mathcal{S}_h(\mathcal{T}_h)$  be the elliptic projection defined by

$$a(u - R_h u, v_h) = 0, \quad \forall v_h \in \mathcal{S}_h(\mathcal{T}_h). \quad (5.6)$$

Note that  $R_h u$  is well defined by the coercivity of  $a(\cdot, \cdot)$  on the space  $\mathcal{S}_h(\mathcal{T}_h)$  if the coefficients of problem (1.1) satisfy the same assumption in Theorem 2.1. In addition, we present the following lemma, the proof is similar to the Lemma 3.3 in [53], so we omit it here.



**Lemma 5.1.** *Assume that  $u \in H^2(0, T; H_\alpha^p(\Omega))$ ,  $t \in [0, T]$ ,  $R_h$  is the elliptic projection defined above. Then, for  $p = 2, 3$ , the following error estimates hold,*

$$\begin{aligned} \|u - R_h u\|_0 + h \|u - R_h u\|_1 &\leq \mathcal{C}h^p \|u\|_p, \\ \|(u - R_h u)_t\|_0 + h \|(u - R_h u)_t\|_1 &\leq \mathcal{C}h^p \|u_t\|_p, \\ \|(u - R_h u)_{tt}\|_0 + h \|(u - R_h u)_{tt}\|_1 &\leq \mathcal{C}h^p \|u_{tt}\|_p. \end{aligned} \quad (5.7)$$

**Remark 5.1.** *The value of  $p$  in the error estimates for the elliptic projection depends on which IFE method were used, such as, if we use the linear IFE space, then  $p = 2$ . Analogously, if the quadratic IFE space is used, then  $p$  should be 3.*

It is clearly that, the results when we use quadratic IFE space are similarly to the results linear IFE space is used. Therefore, we used the linear IFE method in the following. The same properties can be get for the quadratic IFE methods.

**Theorem 5.1.** *Assume that the exact solution  $u$  of the problem (1.3)-(1.7) satisfies  $u \in H^1(0, T; H_\alpha^2(\Omega))$ , and  $u_0 \in H_\alpha^2(\Omega)$ . Let  $u_h$  be the IFE solution of (5.4) and let  $u_{0h} = R_h u_0$  be the elliptic projection of  $u_0$ . Then, there exist a constant  $\mathcal{C}$  such that for all  $t \in (0, T]$ ,*

$$\|u_h - u\|_0 \leq \mathcal{C}h^2 (\|u_0\|_2 + \|u\|_2 + \int_0^t \|u_t\|_2 ds).$$

*Proof.* Subtracting (5.1) from (5.4), and denoting  $\gamma = u_h - u$ , we have

$$(\gamma_t, v_h) + a(\gamma, v_h) = 0. \quad (5.8)$$

Now, letting the total error  $\gamma = \theta + \rho$ , where  $\theta = u_h - R_h u$ ,  $\rho = R_h u - u$ . From (5.8), we obtain

$$(\gamma_t, v_h) + a(\theta, v_h) + a(\rho, v_h) = 0, \quad \forall v_h \in \mathcal{S}_h(\mathcal{T}_h),$$

which implies

$$(\theta_t, v_h) + (\rho_t, v_h) + a(\theta, v_h) = 0, \quad \forall v_h \in \mathcal{S}_h(\mathcal{T}_h). \quad (5.9)$$

Letting  $v_h = \theta$ , and using (5.6), it is easy to get

$$(\theta_t, \theta) + (\rho_t, \theta) + a(\theta, \theta) = 0,$$

which together with  $a(\theta, \theta) \geq 0$  implies that

$$\|\theta\|_0 \frac{d}{dt} \|\theta\|_0 \leq \|\rho_t\|_0 \|\theta\|_0.$$

Eliminating the common factor  $\|\theta\|_0$ , and integrating from 0 to  $t$ , the following estimate holds:

$$\|\theta\|_0 \leq \mathcal{C}(\|\theta(0)\|_0 + \int_0^t \|\rho_t\|_0 ds). \quad (5.10)$$

Letting  $u_h(0) = \check{I}_h u_0$ , we have

$$\begin{aligned} \|\theta(0)\|_0 &\leq \|u_h(0) - u_0\|_0 + \|u_0 - R_h u(0)\|_0 \\ &\leq \mathcal{C}h^2 \|u_0\|_2 + \mathcal{C}h^2 \|u_0\|_2, \\ &\leq \mathcal{C}h^2 \|u_0\|_2, \end{aligned} \quad (5.11)$$

here,  $\check{I}_h$  is the IFE interpolation we defined in Chapter 2. Substituting (5.11) and (5.7) into (5.10), we get

$$\begin{aligned} \|\theta\|_0 &\leq \mathcal{C}h^2 (\|u_0\|_2 + \int_0^t \|u_t\|_2 dt) \\ &\leq \mathcal{C}h^2 (\|u_0\|_2 + \int_0^t \|u_t\|_2 ds). \end{aligned}$$

Then, by using the triangle inequality, we have

$$\|u - u_h\|_0 \leq \|\theta\|_0 + \|\rho\|_0 \leq \mathcal{C}h^2 (\|u_0\|_2 + \|u\|_2 + \int_0^t \|u_t\|_2 ds). \quad (5.12)$$

□

**Theorem 5.2.** *Assume that the exact solution  $u$  of the problem (1.3)-(1.7) satisfies  $u \in H^2(0, T; H_\alpha^2(\Omega))$ , and  $u_0 \in H_\alpha^2(\Omega)$ . Let  $u_h$  be the IFE solution of (5.5) and let  $u_{0h} = R_h u_0$  be the elliptic projection of  $u_0$ . Then, there exists a constant  $\mathcal{C}$  such that, for all  $t \in (0, T]$ ,*

$$\|u_h - u\|_1 \leq \mathcal{C}h(\|u_0\|_2 + \|u_t(0)\|_2 + \int_0^t \|u_t\|_2 ds + \int_0^t \|u_{tt}\|_2 ds).$$

*Proof.* Recalling that  $\gamma = u_h - u = u_h - R_h u + R_h u - u = \theta + \rho$ , and

$$\|\rho\|_1 \leq \mathcal{C}h \|u\|_2 \leq \mathcal{C}h(\|u_0\|_2 + \int_0^t \|u_t\|_2 ds), \quad (5.13)$$

it suffices to bound the error  $\|\theta\|_1$ . Letting  $v_h = \theta_t$  in (5.9), we have

$$\|\theta_t\|_0^2 + a(\theta, \theta_t) = -(\rho_t, \theta_t). \quad (5.14)$$

Since  $a(\cdot, \cdot)$  is nonsymmetric,

$$\begin{aligned} a(\theta, \theta_t) &= \frac{1}{2} \frac{d}{dt} a(\theta, \theta) + \frac{1}{2} a(\theta, \theta_t) - \frac{1}{2} a(\theta_t, \theta) \\ &\geq \frac{1}{2} \frac{d}{dt} a(\theta, \theta) - \frac{1}{2} \|\theta_t\|_1^2 - \frac{1}{2} \|\theta\|_1^2. \end{aligned} \quad (5.15)$$

Inserting (5.15) into (5.14), and integrating from 0 to  $t$ , we can obtain

$$\int_0^t \|\theta_t\|_0^2 ds + \|\theta\|_1^2 \leq \mathcal{C} \int_0^t (\|\rho_t\|_0^2 + \|\theta_t\|_1^2 + \|\theta\|_1^2) ds. \quad (5.16)$$

Taking derivative in (5.9), we have

$$(\theta_{tt}, v_h) + (\rho_{tt}, v_h) + a(\theta_t, v_h) = 0, \quad \forall v_h \in \mathcal{S}_h(\mathcal{T}_h).$$

Letting  $v_h = \theta_t$  in above equation, and using the coercivity of the bilinear form  $a(\cdot, \cdot)$ ,

it is easy to obtain

$$\frac{1}{2} \frac{d}{dt} \|\theta_t\|_0^2 + \mathcal{K} \|\theta_t\|_1^2 \leq \mathcal{C}(\|\rho_{tt}\|_0^2 + \|\theta_t\|_0^2).$$

Integrating the above inequality from 0 to  $t$ , we get easily

$$\|\theta_t\|_0^2 + \int_0^t \|\theta_t\|_1^2 ds \leq \mathcal{C} \left( \int_0^t \|\rho_{tt}\|_0^2 ds + \int_0^t \|\theta_t\|_0^2 ds \right) + \mathcal{C} \|\theta_t(\cdot, 0)\|_0^2.$$

Using Gronwall inequality and the nonnegativity of the term  $\|\theta_t\|_0^2$ , it is natural to get

$$\int_0^t \|\theta_t\|_1^2 ds \leq \mathcal{C} \left( \int_0^t \|\rho_{tt}\|_0^2 ds + \|\theta_t(\cdot, 0)\|_0^2 \right). \quad (5.17)$$

Letting  $t = 0$ , and  $v_h = \theta_t(\cdot, 0)$ , (5.9) becomes

$$\|\theta_t(\cdot, 0)\|_0^2 + \mathcal{K} \|\theta_t(\cdot, 0)\|_1^2 \leq \|\rho_t(\cdot, 0)\|_0 \|\theta_t(\cdot, 0)\|_0,$$

which implies that

$$\|\theta_t(\cdot, 0)\|_0 \leq \|\rho_t(\cdot, 0)\|_0. \quad (5.18)$$

Inserting (5.18) and (5.17) into (5.16), we have

$$\int_0^t \|\theta_t\|_0^2 ds + \|\theta\|_1^2 \leq \mathcal{C} \left( \int_0^t (\|\rho_t\|_0^2 ds + \int_0^t \|\rho_{tt}\|_0^2 ds + \|\rho_t(\cdot, 0)\|_0 + \int_0^t \|\theta\|_1^2 ds) \right).$$

Using Gronwall inequality, and the estimation of  $\|\rho_t\|_0$ ,  $\|\rho_{tt}\|_0$  in Lemma 5.1, we have

$$\int_0^t \|\theta_t\|_0^2 ds + \|\theta\|_1^2 \leq \mathcal{C}h(\|u_t(\cdot, 0)\|_2 + \int_0^t \|u_t\|_2 + \|u_{tt}\|_2 ds).$$

The above inequality together with (5.13) complete the proof.  $\square$

## 5.2 Error Estimation for Fully Discrete Scheme

In this section, we study the error estimates in  $L^2$  and  $H^1$  norms using the backward Euler scheme.

**Theorem 5.3.** *Let  $u$  and  $\{u_h^n\}_{n=1}^{N_t}$  be the solutions of problem (1.3)-(1.7) and the fully discrete problem (4.7), respectively. In addition, we assume  $u \in H^2(0, T; H_\alpha^2(\Omega))$ , and  $u_0 \in H_\alpha^2(\Omega)$ . Then, we have for  $n = 1, 2, \dots, N_t$ ,*

$$\|u_h^n - u^n\|_0 \leq Ch^2(\|u_0\|_2 + \|u\|_2) + \Delta t \int_0^{t^n} \|u_{tt}\|_0 ds. \quad (5.19)$$

*Proof.* From (4.3) and (4.7), we have

$$(u_t^n - \partial_t u_h^n, v_h) + a(u^n - u_h^n, v_h) = 0, \quad \forall v_h \in \mathcal{S}_h(\mathcal{T}_h). \quad (5.20)$$

As the previous theorem, we write  $u^n - u_h^n = u^n - (R_h u)^n + (R_h u)^n - u_h^n = \rho^n + \theta^n$ . Since the estimates for  $\rho^n$  are known, we now aim to bound the term  $\theta^n$ . From the definition of the elliptic projection  $R_h$  defined in (5.6), we have

$$a(u_h^j - (R_h u)^j, v_h) = a(u_h^j - u^j + u^j - (R_h u)^j, v_h) = a(u_h^j - u^j, v_h).$$

In addition, (5.20) implies

$$\begin{aligned} (\partial_t \theta^j, v_h) + a(\theta^j, v_h) &= (\partial_t(u_h^j - (R_h u)^j), v_h) + a(u_h^j - (R_h u)^j, v_h) \\ &= (\partial_t(u_h^j - u^j + u^j - (R_h u)^j), v_h) + a(u_h^j - u^j, v_h) \\ &= (\partial_t \rho^j, v_h) + (\partial_t(u_h^j - u^j), v_h) + (u_t^j - \partial_t u_h^j, v_h) \\ &= (\partial_t \rho^j, v_h) + (u_t^j - \partial_t u^j, v_h). \end{aligned} \quad (5.21)$$

Letting  $v_h = \theta^j$ , multiplying by  $\Delta t$ , using Cauchy-Schwarz inequality and the non-negativity of  $a(\theta^j, \theta^j)$ , we obtain

$$\|\theta^j\|_0^2 \leq \|\theta^j\|_0 \|\theta^{j-1}\|_0 + \Delta t \|\partial_t \rho^j\|_0 \|\theta^j\|_0 + \Delta t \|u_t^j - \partial_t u^j\|_0 \|\theta^j\|_0.$$

Eliminate the common factor  $\|\theta^j\|_0$  in the above inequality, we can get easily

$$\|\theta^j\|_0 \leq \|\theta^{j-1}\|_0 + \Delta t \|\partial_t \rho^j\|_0 + \Delta t \|u_t^j - \partial_t u^j\|_0.$$

Taking summation from 1 to  $n$ , the above inequality becomes

$$\|\theta^n\|_0 \leq \|\theta(0)\|_0 + \Delta t \sum_{j=1}^n \|\partial_t \rho^j\|_0 + \Delta t \sum_{j=1}^n \|u_t^j - \partial u^j\|. \quad (5.22)$$

Now, we bound the second term on the right hand side.

$$\begin{aligned} \Delta t \sum_{j=1}^n \|\partial_t \rho^j\|_0 &= \sum_{j=1}^n \left\| \int_{t^{j-1}}^{t^j} \rho_t ds \right\|_0 \\ &\leq \sum_{j=1}^n \mathcal{C} h^2 \int_{t^{j-1}}^{t^j} \|u_t\|_2 ds \\ &\leq \mathcal{C} h^2 \int_0^{t^n} \|u_t\|_2 ds. \end{aligned} \quad (5.23)$$

By using the fact that

$$\int_{t^{j-1}}^{t^j} (s - t^{j-1}) u_{tt} ds = \int_{t^{j-1}}^{t^j} (s - t^{j-1}) du_t = \Delta t u_t^j - u^j + u^{j-1},$$

we have

$$\Delta t \sum_{j=1}^n \|u_t^j - \partial u^j\| = \sum_{j=1}^n \Delta t u_t^j - u^j + u^{j-1} = \sum_{j=1}^n \int_{t^{j-1}}^{t^j} (s - t^{j-1}) u_{tt} ds \leq \Delta t \int_0^{t^n} u_{tt} ds. \quad (5.24)$$

Inserting (5.11), (5.23), and (5.24) into (5.22), we can get (5.19) easily.  $\square$

**Theorem 5.4.** *Assume that  $u$  is the exact solution (1.3)-(1.7). Letting  $\{u_h^n\}_{n=1}^{N_t}$  be the solution of the backward Euler scheme (4.7). If  $u \in H^3(0, T; H_\alpha^2(\Omega))$ , and  $u_0 \in H_\alpha^2(\Omega)$ , we have the following estimates satisfies for all  $0 < n \leq N_t$ ,*

$$\begin{aligned} \|u_h^n - u^n\|_1^2 &\leq \mathcal{C} h^2 (\|u_0\|_2 + \int_0^{t^n} \|u_t\|_2^2 dt + \int_0^{t^n} \|u_{tt}\|_0^2 ds + \frac{1}{\Delta t} \int_0^{\Delta t} \|u_t\|_2 dt) \\ &\quad + \mathcal{C} (\Delta t)^2 (\int_0^{t^n} \|u_{tt}\|_0^2 dt + \int_0^{t^n} \|u_{ttt}\|_0^2 dt + \frac{1}{\Delta} \int_0^{\Delta t} \|u_{tt}\|_0^2 dt). \end{aligned}$$

*Proof.* Letting  $v_h = \partial_t \theta^j$  in (5.21), and using Cauchy-Schwarz inequality, it is easy to get

$$\begin{aligned} \|\partial_t \theta^j\|_0^2 + a(\theta^j, \partial_t \theta^j) &= (\partial_t \rho^j, \partial_t \theta^j) + (u_t^j - \partial_t u^j, \partial_t \theta^j) \\ &\leq \|\partial_t \rho^j\|_0^2 + \|u_t^j - \partial_t u^j\|_0^2 + \frac{1}{2} \|\partial_t \theta^j\|_0^2. \end{aligned} \quad (5.25)$$

Since the bilinear form  $a(\cdot, \cdot)$  is nonsymmetric,

$$\begin{aligned} a(\theta^j, \partial_t \theta^j) &= \frac{1}{2\Delta t} (a(\theta^j, \theta^j) - a(\theta^{j-1}, \theta^{j-1})) + \frac{1}{2\Delta t} a(\theta^j, \theta^j - \theta^{j-1}) \\ &\quad - \frac{1}{2\Delta t} a(\theta^j - \theta^{j-1}, \theta^{j-1}) \\ &= \frac{1}{2\Delta t} (a(\theta^j, \theta^j) - a(\theta^{j-1}, \theta^{j-1})) + \frac{1}{2} a(\theta^j, \partial_t \theta^j) - \frac{1}{2} a(\partial_t \theta^j, \theta^{j-1}) \\ &\geq \frac{1}{2\Delta t} (a(\theta^j, \theta^j) - a(\theta^{j-1}, \theta^{j-1})) - \mathcal{C}(\|\theta^j\|_1^2 + \|\theta^{j-1}\|_1^2 + \|\partial_t \theta^j\|_1^2). \end{aligned}$$

Substituting the above inequality into (5.25), we obtain

$$\begin{aligned} \frac{1}{2} \|\partial_t \theta^j\|_0^2 + \frac{1}{2\Delta t} (a(\theta^j, \theta^j) - a(\theta^{j-1}, \theta^{j-1})) &\leq \|\partial_t \rho^j\|_0^2 + \|u_t^j - \partial_t u^j\|_0^2 \\ &\quad + \mathcal{C}(\|\theta^j\|_1^2 + \|\theta^{j-1}\|_1^2 + \|\partial_t \theta^j\|_1^2). \end{aligned}$$

Multiply by  $2\Delta t$ , take summation from 1 to  $n$ , and use the coercivity of the bilinear form of  $a(\cdot, \cdot)$  to get

$$\begin{aligned} \Delta t \sum_{j=1}^n \|\partial_t \theta^j\|_0^2 + \mathcal{K} \|\theta^j\|_1^2 &\leq 2\Delta t \sum_{j=1}^n (\|\partial_t \rho^j\|_0^2 + \|u_t^j - \partial_t u^j\|_0^2) \\ &\quad + \mathcal{C}\Delta t \sum_{j=1}^n \|\partial_t \theta^j\|_1^2 + \mathcal{C}\Delta t \sum_{j=0}^n \|\theta^j\|_1^2. \end{aligned} \quad (5.26)$$

(5.21) implies

$$(\partial_{tt} \theta^j, v_h) + a(\partial_t \theta^j, v_h) = (\partial_{tt} \rho^j, v_h) + (\partial_t u_t^j - \partial_{tt} u^j, v_h).$$

Letting  $v_h = \partial_t \theta^j$ , we have

$$\frac{1}{\Delta t}(\partial_t \theta^j - \partial_t \theta^{j-1}, \partial_t \theta^j) + a(\partial_t \theta^j, \partial_t \theta^j) = (\partial_{tt} \rho^j, \partial_t \theta^j) + (\partial_t u_t^j - \partial_{tt} u^j, \partial_t \theta^j).$$

Then, by using the fact that

$$(\partial_t \theta^{j-1}, \partial_t \theta^j) \geq -|(\partial_t \theta^{j-1}, \partial_t \theta^j)| \geq -\frac{1}{2} \|\partial_t \theta^j\|_0^2 - \frac{1}{2} \|\partial_t \theta^{j-1}\|_0^2,$$

it is easy to get

$$\frac{1}{2\Delta t}(\|\partial_t \theta^j\|_0^2 - \|\partial_t \theta^{j-1}\|_0^2) + \mathcal{K} \|\partial_t \theta^j\|_1^2 \leq \mathcal{C}(\|\partial_{tt} \rho^j\|_0 + \|\partial_t u_t^j - \partial_{tt} u^j\|_0) \|\partial_t \theta^j\|_0.$$

Multiplying the above inequality by  $2\Delta t$ , and taking summation from 2 to  $n$ , we can obtain

$$\|\partial_t \theta^n\|_0^2 + \Delta t \sum_{j=2}^n \|\partial_t \theta^j\|_1^2 \leq \Delta t \sum_{j=2}^n (\|\partial_{tt} \rho^j\|_0^2 + \|\partial_t u_t^j - \partial_{tt} u^j\|_0^2) + \mathcal{C} \|\partial_t \theta^1\|_0^2. \quad (5.27)$$

Letting  $t = 1$  and  $v_h = \partial_t \theta^1 = \frac{\theta^1}{\Delta t}$  in (5.21), we have

$$\|\partial_t \theta^1\|_0^2 + \frac{1}{2\Delta t} a(\theta^1, \theta^1) \leq (\|\partial_t \rho^1\|_0 + \|u_t^1 - \partial_t u^1\|_0) \|\partial_t \theta^1\|_0.$$

The coercivity of the bilinear form  $a(\cdot, \cdot)$  implies

$$\|\partial_t \theta^1\|_0^2 + \frac{1}{\Delta t} \|\theta^1\|_1^2 \leq \mathcal{C}(\|\partial_t \rho^1\|_0^2 + \|u_t^1 - \partial_t u^1\|_0^2).$$

Substituting the above inequality into (5.27), and using the fact that  $\Delta t \|\partial_t \theta^1\|_1^2 = \|\theta^1\|_1^2 / \Delta t$ , we can get easily

$$\|\partial_t \theta^n\|_0^2 + \Delta t \sum_{j=1}^n \|\partial_t \theta^j\|_1^2 \leq \sum_{j=2}^n \Delta t (\|\partial_{tt} \rho^j\|_0^2 + \|\partial_t u_t^j - \partial_{tt} u^j\|_0^2) + \mathcal{C}(\|\partial_t \rho^1\|_0^2 + \|u_t^1 - \partial_t u^1\|_0^2).$$



Combining the above inequality together with (5.26), and using Gronwall inequality, we have

$$\begin{aligned} \|\theta^j\|_1^2 &\leq \Delta t \sum_{j=1}^n (\|\partial_t \rho^j\|_0^2 + \|u_t^j - \partial_t u^j\|_0^2) + \sum_{j=2}^n \Delta t (\|\partial_{tt} \rho^j\|_0^2 + \|\partial_t u_t^j - \partial_{tt} u^j\|_0^2) \\ &\quad + \mathcal{C} (\|\partial_t \rho^1\|_0^2 + \|u_t^1 - \partial_t u^1\|_0^2). \end{aligned} \tag{5.28}$$

By using Hölder's inequality, we have

$$\begin{aligned} \|\partial_t \rho^j\|_0^2 &= \int_{\Omega} \left( \frac{1}{\Delta t} \int_{t^{j-1}}^{t^j} \rho_t dt \right)^2 dx \leq \frac{1}{\Delta t} \int_{t^{j-1}}^{t^j} \|\rho_t\|_0^2 dt \leq \mathcal{C} \frac{h^2}{\Delta t} \int_{t^{j-1}}^{t^j} \|u_t\|_2^2 dt, \\ \|u_t^j - \partial_t u^j\|_0^2 &= \int_{\Omega} \left( \frac{1}{\Delta t} \int_{t^{j-1}}^{t^j} (t - t^{j-1}) u_{tt} dt \right)^2 dx \leq \mathcal{C} \Delta t \int_{t^{j-1}}^{t^j} \|u_{tt}\|_0^2 dt. \end{aligned} \tag{5.29}$$

Hence,

$$\Delta t \sum_{j=1}^n (\|\partial_t \rho^j\|_0^2 + \|u_t^j - \partial_t u^j\|_0^2) \leq \mathcal{C} h^2 \int_0^{t^n} \|u_t\|_2^2 dt + \mathcal{C} (\Delta t)^2 \int_0^{t^n} \|u_{tt}\|_0^2 dt. \tag{5.30}$$

By using integrating by parts, we have

$$\begin{aligned} \int_{t^{j-1}}^{t^j} \rho_{tt} (t^j - t) dt &= \rho_t (t^j - t) \Big|_{t^{j-1}}^{t^j} + \int_{t^{j-1}}^{t^j} \rho_t dt \\ &= -\Delta t \rho_t^{j-1} + \rho^j - \rho^{j-1}. \end{aligned}$$

Similarly,

$$\int_{t^{j-2}}^{t^{j-1}} \rho_{tt} (t - t^{j-2}) dt = \Delta t \rho^{j-1} - \rho^{j-1} + \rho^{j-2}.$$

Then, it is easy to get

$$\begin{aligned}
\|\partial_{tt}\rho^j\|_0^2 &= \int_{\Omega} \left( \frac{\rho^j - 2\rho^{j-1} + \rho^{j-2}}{(\Delta t)^2} \right)^2 dx \\
&= \frac{1}{(\Delta t)^2} \int_{\Omega} \left( \int_{t^{j-1}}^{t^j} \rho_{tt}(t^j - t) dt + \int_{t^{j-2}}^{t^{j-1}} \rho_{tt}(t - t^{j-2}) dt \right) dx \\
&\leq \frac{1}{(\Delta t)} \int_{t^{j-2}}^{t^j} \|\rho_{tt}\|_0^2 ds.
\end{aligned}$$

Use the estimation of  $\|\rho_{tt}\|_0$ , to get

$$\sum_{j=2}^n \Delta t \|\partial_{tt}\rho^j\|_0^2 \leq Ch^2 \int_0^{t^n} \|u_{tt}\|_0^2 ds. \quad (5.31)$$

Using integrating by parts, we have

$$\begin{aligned}
\int_{t^{j-1}}^{t^j} u_{ttt}(t^{j-1} - t)^2 dt &= (\Delta t)^2 u_{tt}^j - 2\Delta t u_t^j + 2(u_t^j - u_t^{j-1}), \\
\int_{t^{j-2}}^{t^{j-1}} u_{ttt}(t - t^{j-2})^2 dt &= (\Delta t)^2 u_{tt}^{j-1} - 2\Delta t u_t^{j-1} + 2(u_t^{j-1} - u_t^{j-2}).
\end{aligned}$$

The definition of the  $\partial_t$  implies

$$\begin{aligned}
\partial_t u_t^j - \partial_{tt} u^j &= \frac{u_t^j - u_t^{j-1}}{\Delta t} - \frac{u^j - 2u^{j-1} + u^{j-2}}{(\Delta t)^2} \\
&= \frac{1}{2} \left( \int_{t^{j-1}}^{t^j} u_{ttt} dt - \frac{1}{(\Delta t)^2} \int_{t^{j-1}}^{t^j} u_{ttt}(t^{j-1} - t)^2 dt \right. \\
&\quad \left. + \frac{1}{(\Delta t)^2} \int_{t^{j-2}}^{t^{j-1}} u_{ttt}(t - t^{j-2})^2 dt \right)
\end{aligned}$$

By using the Hölder's inequality, we have

$$\begin{aligned}
\sum_{j=2}^n \Delta t \|\partial_t u_t^j - \partial_{tt} u^j\|_0^2 &\leq \mathcal{C}(\Delta t)^2 \sum_{j=2}^n \left( \int_{t^{j-1}}^{t^j} \|u_{ttt}\|_0^2 dt + \int_{t^{j-1}}^{t^j} \|u_{ttt}\|_0^2 dt + \int_{t^{j-2}}^{t^{j-1}} \|u_{ttt}\|_0^2 dt \right) \\
&\leq \mathcal{C}(\Delta t)^2 \int_0^{t^n} \|u_{ttt}\|_0^2 dt.
\end{aligned} \tag{5.32}$$

On the other hand, the following estimate holds

$$\|\partial_t \rho^1\|_0^2 = \frac{1}{\Delta t} \int_0^{\Delta t} \|\partial_t \rho\| dt \leq h^2 \left( \frac{1}{\Delta t} \int_0^{\Delta t} \|u_t\|_2 dt \right). \tag{5.33}$$

The second inequality in (5.29) implies

$$\|u_t^1 - \partial_t u^1\|_0^2 = \int_{\Omega} |u_t^1 - \partial_t u^1|^2 dx \leq \mathcal{C} \Delta t \int_0^{\Delta t} \|u_{tt}\|_0^2 dt. \tag{5.34}$$

Inserting (5.30)-(5.34) into (5.28), we have

$$\begin{aligned}
\|\theta^j\|_1^2 &\leq \mathcal{C} h^2 \left( \int_0^{t^n} \|u_t\|_3^2 dt + \int_0^{t^n} \|u_{tt}\|_0^2 dt + \left( \frac{1}{\Delta t} \int_0^{\Delta t} \|u_t\|_3 dt \right) \right) \\
&\quad + \mathcal{C}(\Delta t)^2 \left( \int_0^{t^n} \|u_{tt}\|_0^2 dt + \int_0^{t^n} \|u_{ttt}\|_0^2 dt + \frac{1}{\Delta t} \int_0^{\Delta t} \|u_{tt}\|_0^2 dt \right).
\end{aligned}$$

The above inequality together with the estimation of  $\|\rho\|_1$  implies that

$$\begin{aligned}
\|u_h^n - u^n\|_1 &\leq \mathcal{C} h^2 \left( \|u_0\|_2 + \int_0^{t^n} \|u_t\|_3^2 dt + \int_0^{t^n} \|u_{tt}\|_0^2 ds + \left( \frac{1}{\Delta t} \int_0^{\Delta t} \|u_t\|_3 dt \right) \right) \\
&\quad + \mathcal{C}(\Delta t)^2 \left( \int_0^{t^n} \|u_{tt}\|_0^2 dt + \int_0^{t^n} \|u_{ttt}\|_0^2 dt + \frac{1}{\Delta t} \int_0^{\Delta t} \|u_{tt}\|_0^2 dt \right).
\end{aligned}$$

The proof is completed. □

### 5.3 Numerical Experiments

In this section we present numerical examples for IFE methods for the time dependent multi-layer wall model. We let the simulation interval be  $[0, 1]$ , and there are three interface points:  $1/9$ ,  $1/3$ , and  $2/3$ . The exact solution  $u$  is set to be

$$u(x) = \begin{cases} (1 - e^{-t})u_0(x), & x \in [0, 1/9], \\ (1 - e^{-t})u_1(x), & x \in [1/9, 1/3], \\ (1 - e^{-t})u_2(x), & x \in [1/3, 2/3], \\ (1 - e^{-t})u_3(x), & x \in [2/3, 1], \end{cases} \quad (5.35)$$

with

$$u_0(x) = \frac{1}{30}x^{n-1}, \quad u_1(x) = \frac{1}{3}x^n, \quad u_2(x) = x^{n+1}, \quad u_3(x) = 3(1-x)x^{n+1},$$

here,  $n$  is an integer. We also let

$$\begin{aligned} D_1 &= \frac{18(n-1)D_0}{10n}, & \delta_1 &= \frac{1}{2}(9nD_1 - 8.1(n-1)D_0), \\ D_2 &= \frac{6nD_1 - 2\delta_1}{3(n+1)}, & \delta_2 &= \frac{1}{2}(3(n+1)D_2 - 3nD_1 + 2\delta_1), \\ D_3 &= \frac{8\delta_2 - 3(n+1)D_2}{3(n+5)}, & \delta_3 &= \frac{1}{4}(3(n-1)D_3 - 3(n+1)D_2 + 4\delta_2), \\ \lambda &= \frac{1}{81(n-1)D_0}. \end{aligned}$$

We use the uniform partition  $\mathcal{T}_h$  with the mesh size  $h = 1/N$ . For the fully discretization, we divided the time interval  $[0, T]$  uniformly into  $N_t$  subintervals with  $t^n = n\Delta t$ ,  $n = 1, 2, \dots, N_t$ , here,  $\Delta t = T/N_t$ .

**Example 5.1.** *In this example, we set the parameters  $\beta_i$  is small, for example,  $\beta_1 = 10$ ,  $\beta_2 = 1$ ,  $\beta_3 = 0.1$ . Both linear and quadratic IFE methods are used to solve the problem (1.1)-(1.4).*

Table 5.1: Errors and convergence rates of the linear IFE methods when  $n = 6$  with small values for  $\beta_j$  ( $j = 1, 2, 3$ ).

N	$L^2$ norm	rate	$H^1$ norm	rate
10	4.4506e-03		1.6272e-01	
20	3.1104e-04	1.8870	4.2506e-02	0.9487
40	3.0870e-04	1.9518	5.3986e-02	0.9879
80	7.8347e-05	1.9891	2.1323e-02	0.9953
160	1.9182e-05	2.0302	1.0666e-02	0.9994
320	4.6431e-06	2.0466	5.3353e-03	0.9994

Table 5.2: Errors and convergence rates of the quadratic IFE methods when  $n = 6$  with small values for  $\beta_j$  ( $j = 1, 2, 3$ ).

N	$L^2$ norm	rate	$H^1$ norm	rate
10	3.4162e-04		2.2631e-02	
20	4.3977e-05	2.9576	5.7361e-03	1.9801
40	5.5477e-06	2.9868	1.4383e-03	1.9957
80	6.9407e-07	2.9987	3.6000e-04	1.9983
160	8.6812e-08	2.9991	9.0025e-05	1.9996
320	1.0967e-08	2.9848	2.2511e-05	1.9997

Firstly, we use the linear IFE method to solve the problem (1.1)-(1.4). In Table 5.1, the errors in  $L^2$  and  $H^1$  norms at the final time level  $T = 1$  are presented with the time step  $\Delta t = 0.01h$ . We can see that both the  $L^2$  and  $H^1$  norms have the optimal convergence rate. Then, we test by using quadratic IFE method, and present the numerical results in Table 5.2. These results confirm our theoretical error analysis in Theorems 5.1-5.4.

**Example 5.2.** *In this example, we set the parameter  $\beta_i$ ,  $i = 1, 2, 3$ , are large.*

In this example, we test both the linear and quadratic algorithm by flipping the coefficients  $\beta_i$ ,  $i = 1, 2, 3$ , such as  $\beta_1 = 1$ ,  $\beta_2 = 150$ ,  $\beta_3 = 15000$ . The numerical result were reported in Tables 5.3 and 5.4. We can see that the pattern of error decay is similar to the first example. Then the results of these numerical experiments confirm our theory again.

Table 5.3: Errors and convergence rates of the linear IFE methods when  $n = 6$  with large values for  $\beta_j$  ( $j = 1, 2, 3$ ).

N	$L^2$ norm	rate	$H^1$ norm	rate
10	3.6947e-03		1.7144e-01	
20	8.2675e-04	2.1599	8.6976e-02	0.9790
40	1.9069e-04	2.1163	4.2979e-02	1.0170
80	4.7059e-05	2.0187	2.1382e-02	1.0072
160	1.2286e-05	1.9374	1.0672e-02	1.0026
320	3.1576e-06	1.9610	5.3356e-03	1.0001

Table 5.4: Errors and convergence rates of the quadratic IFE methods when  $n = 6$  with large values for  $\beta_j$  ( $j = 1, 2, 3$ ).

N	$L^2$ norm	rate	$H^1$ norm	rate
10	3.2857e-04		2.2720e-02	
20	4.3487e-05	2.9176	5.7409e-03	1.9846
40	5.5230e-06	2.9770	1.4384e-03	1.9968
80	6.9359e-07	2.9933	3.6000e-04	1.9984
160	8.6794e-08	2.9984	9.0025e-05	1.9996
320	1.0855e-08	2.9993	2.2511e-05	1.9997



# Chapter 6

## Conclusions and Future Work

In this chapter, we give some conclusions and list a few research topics beyond this dissertation.

### 6.1 Conclusions

In this dissertation, we carried out the linear and quadratic IFE methods for the multi-layer porous wall model. We have discussed all the three fundamental aspects for a new finite element method, including the development of the IFE spaces, the implementation of numerical methods with these spaces, and the corresponding convergence analysis.

Firstly, we construct the IFE spaces whose functions satisfy nonhomogeneous jump conditions. Then we investigate basic properties for this space and carry out the error estimation for the linear and quadratic IFE interpolation of a Sobolev function. The interpolation error estimates indicate that these spaces have the usual approximation capability expected, which is  $O(h^2)$  in  $L^2$  norm and  $O(h)$  in  $H^1$  norm for the linear IFE method, and  $O(h^3)$  in  $L^2$  norm and  $O(h^2)$  in  $H^1$  norm for the quadratic IFE method.

Secondly, we analyze the long time stability and asymptotic behavior for the multi-layer wall model. With the IFE method for the spatial discretization, and



the implicit Euler scheme for the temporal discretization, respectively, we deduce the global stability of fully discrete scheme. In addition, based on the uniform stability of the numerical solution, we investigate the discrete asymptotic behavior and claim that the multi-layer porous wall model converges to the corresponding elliptic equation if  $f(x, t)$  approaches to a steady-state  $\bar{f}(x)$  in  $L^2$  norm as  $t \rightarrow \infty$ . Those theoretical results were also verified by the numerical examples.

Finally, we develop semi-discrete and fully discrete scheme for the multi-layer wall model. Taking advantages of the immersed finite functions, the proposed methods can be used on the Cartesian mesh regardless of the location of interface. A priori error estimates shows that these IFE methods converge to exact solution with an optimal order in both  $L^2$  norm and  $H^1$  norm.

## 6.2 Future Work

In this dissertation, we consider a one dimensional interface model with piecewise constant coefficients. The design of the DES is a very complex task because their performance in widening the arterial lumen and preventing further restenosis is influenced by many factors, such as those discussed in [29], the geometrical design of the stents, the mechanical properties of the materials, the chemical properties of the drug that is release, and so on. Considering the complex geometries of the stents, this model can be improved by the variable coefficients to address directly the problems.

Several computational approaches to drug release from stents have been employed, such as the two dimensional model was computed in [16, 22, 65] and we can find the three dimensional computation in [21, 26, 27, 66], etc. But, there are no work related to the IFE methods. Therefore, we want to extended the theoretical and numerical results to the two dimensional or three dimensional case.

Furthermore, this dissertation is examined when the drug is distributed in the

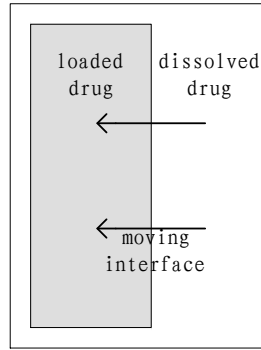


Figure 6.1: Controlled release polymeric device

polymeric coating uniformly. The drug inside the polymeric coating is gradually dissolved and then release outward. Therefore, the drug may be delivered at a constant solubility whether the body need it or not. For some drug, a pattern of input could be more appropriate. An even better approach for an optimal delivery system is to design a polymeric coating device so that the drug is released under the control of some physiological restraints. Under this circumstance, the concentration at the boundary is no longer a constant, but is time dependent. In addition, the boundary between the dissolved and loaded drug in the polymeric coating is an moving interface, see Figure. 6.1. If the drug concentration at the boundary is time independent, then it is a one dimensional moving interface problem. This motivates the study of the IFE approximation of the solution of the moving interface problem.



# Bibliography

- [1] S. Adjerid, N. Chaabane, and T. Lin. An immersed discontinuous finite element method for stokes interface problems. *Comput. Methods Appl. Mech. Engrg.*, 293:170–190, 2015.
- [2] S. Adjerid and T. Lin. Higher-order immersed discontinuous Galerkin methods. *Int. J. Inform. Syst. Sci.*, 3(4):555–568, 2007.
- [3] S. Adjerid and T. Lin. A p-th degree immersed finite element for boundary value problems with discontinuous coefficients. *Appl. Numer Math*, 59(6):1303–1321, 2009.
- [4] C. Attanayake and S.H. Chou. An immersed interface method for pennes bioheat transfer equation. *Disc. Cont. Dyn. Syst.Ser. B*, 20(2):323–337, 2015.
- [5] C. Attanayake and D. Senaratne. Convergence of an immersed finite element method for semilinear parabolic interface problems. *Appl. Math. Sci*, 5(3):135–147, 2011.
- [6] I. Babuška and J. Osborn. Can a finite element method perform arbitrarily badly? *Math. Comput.*, 69(230):443–462, 2000.
- [7] I. Babuška and J.E. Osborn. *Finite element methods for the solution of problems with rough input data*. Springer, 1985.
- [8] B. Camp, T. Lin, Y.P. Lin, and W.W. Sun. Quadratic immersed finite element spaces and their approximation capabilities. *Adv. Comput. Math.*, 24(1-4):81–112, 2006.
- [9] Y. Cao, Y.C. Chu, X.s. Zhang, and X. Zhang. Immersed finite element methods for unbounded interface problems with periodic structures. *J. of Comput. and Appl. Math.*, 307:72–81, 2016.
- [10] S Chou. An immersed linear finite element method with interface flux capturing recovery. *Disc. Cont. Dyn. Syst. Ser. B*, 17(7):2343–2357, 2012.
- [11] S.H. Chou, D.Y Kwak, and K.T Wee. Optimal convergence analysis of an immersed interface finite element method. *Adv. Comput. Math.*, 33(2):149–168, 2010.

- [12] X.M. Feng, W.Q. and He, Y.P. Lin, and X. Zhang. Immersed finite element method for interface problems with algebraic multigrid solver. *Commun. Comput. Phys.*, 15(04):1045–1067, 2014.
- [13] Y. Gong. *Immersed-interface finite-element methods for elliptic and elasticity interface problems*. PhD thesis, north carolina state university, 2007.
- [14] Y. Gong, B. Li, and Z.L. Li. Immersed-interface finite-element methods for elliptic interface problems with nonhomogeneous jump conditions. *SIAM J. Numer. Anal.*, 46(1):472–495, 2008.
- [15] Y. Gong and Z.L. Li. Immersed interface finite element methods for elasticity interface problems with non-homogeneous jump conditions. *Numer. Math. Theory Methods Appl.*, 3(1), 2010.
- [16] M. Grassi, G. Pontrelli, L. Teresi, G. Grassi, L. Comel, A. Ferluga, and L. Galasso. Novel design of drug delivery in stented arteries: a numerical comparative study. *Math. Biosci. Eng.*, 6(3):493–508, 2009.
- [17] X.M. He. *Bilinear immersed finite elements for interface problems*. PhD thesis, Virginia Polytechnic Institute and State University, 2009.
- [18] X.M. He, T. Lin, and Y.P. Lin. Approximation capability of a bilinear immersed finite element space. *Numer. Methods Partial Differential Equations*, 24(5):1265–1300, 2008.
- [19] X.M. He, T. Lin, and Y.P. Lin. Immersed finite element methods for elliptic interface problems with non-homogeneous jump conditions. *Int. J. Numer. Anal. Model.*, 8(2):284–301, 2011.
- [20] X.M. He, T. Lin, Y.P. Lin, and X. Zhang. Immersed finite element methods for parabolic equations with moving interface. *Numer. Methods Partial Differential Equations*, 29(2):619–646, 2013.
- [21] D.R. Hose, A.J. Narracott, B. Griffiths, S. Mahmood, J. Gunn, D. Sweeney, and P.V. Lawford. A thermal analogy for modelling drug elution from cardiovascular stents. *Comput. methods biomech. biomed. eng.*, 7(5):257–264, 2004.
- [22] C.W. Hwang, D. Wu, and E.R. Edelman. Physiological transport forces govern drug distribution for stent-based delivery. *Circulation*, 104(5):600–605, 2001.
- [23] R. Kafafy, T. Lin, Y.P. Lin, and J. Wang. Three-dimensional immersed finite element methods for electric field simulation in composite materials. *Int. J. Numer. Methods Engrg.*, 64(7):940–972, 2005.

- [24] M. Khakpour and K. Vafai. A comprehensive analytical solution of macromolecular transport within an artery. *Int. J. Heat. Mass Tran.*, 51(11):2905–2913, 2008.
- [25] M. Khakpour and K. Vafai. Critical assessment of arterial transport models. *Int. J. Heat. Mass Tran.*, 51(3):807–822, 2008.
- [26] V. B. Kolachalama, E. G. Levine, and E. R. Edelman. Luminal flow amplifies stent-based drug deposition in arterial bifurcations. *PloS one*, 4(12):e8105, 2009.
- [27] V.B. Kolachalama, A. R. Tzafiriri, D. Y. Arifin, and E. R. Edelman. Luminal flow patterns dictate arterial drug deposition in stent-based delivery. *J. Controlled Release*, 133(1):24–30, 2009.
- [28] D.Y. Kwak, K.T. Wee, and K.S. Chang. An analysis of a broken p<sub>1</sub>-nonconforming finite element method for interface problems. *SIAM J. Numer. Anal.*, 48(6):2117–2134, 2010.
- [29] Mark L. and Elazer E. Computational simulations of local vascular heparin deposition and distribution. *American Journal of Physiology-Heart and Circulatory Physiology*, 271(5):H2014–H2024, 1996.
- [30] Z.L. Li. The immersed interface method using a finite element formulation. *Appl. Numer. Math.*, 27(3):253–267, 1998.
- [31] Z.L. Li, T. Lin, Y.P. Lin, and R.C. Rogers. An immersed finite element space and its approximation capability. *Numer. Methods Partial Differential Equations*, 20(3):338–367, 2004.
- [32] Z.L. Li, T. Lin, and X.H. Wu. New cartesian grid methods for interface problems using the finite element formulation. *Numer. Math.*, 96(1):61–98, 2003.
- [33] Z.L. Li and X.Z. Yang. An immersed finite element method for elasticity equations with interfaces. *Contemp. Math.*, 383:285–298, 2005.
- [34] P. Libby. Atherosclerosis: the new view. *Sci. Amer.*, 286(5):46–55, 2002.
- [35] T. Lin, Y.P. Lin, R. Rogers, and M.L. Ryan. A rectangular immersed finite element space for interface problems. *Adv. Comput. Theory Pract.*, 7:107–114, 2001.
- [36] T. Lin, Y.P. Lin, and W.W. Sun. Error estimation of a class of quadratic immersed finite element methods for elliptic interface problems. *Disc. Cont. Dyn. Syst. Ser. B*, 7(4):807–823, 2007.
- [37] T. Lin, Y.P. Lin, W.W. Sun, and Z. W. Immersed finite element methods for 4th order differential equations. *J. Comput. Appl. Math.*, 235(13):3953–3964, 2011.

- [38] T. Lin, Y.P. Lin, and X. Zhang. Immersed finite element method of lines for moving interface problems with nonhomogeneous flux jump. *Contemp. Math.*, 586:257–265, 2013.
- [39] T. Lin, Y.P. Lin, and X. Zhang. A method of lines based on immersed finite elements for parabolic moving interface problems. *Adv. Appl. Math. and Mech.*, 5(04):548–568, 2013.
- [40] T. Lin, Y.P. Lin, and X. Zhang. Partially penalized immersed finite element methods for elliptic interface problems. *SIAM J. Numer. Anal.*, 53(2):1121–1144, 2015.
- [41] T. Lin and D. Sheen. The immersed finite element method for parabolic problems using the laplace transformation in time discretization. *Int. J. Numer. Anal. Model.*, 10(2):298–313, 2013.
- [42] T. Lin, D. Sheen, and X. Zhang. A locking-free immersed finite element method for planar elasticity interface problems. *J. Comput. Phys.*, 247:228–247, 2013.
- [43] T. Lin, Q. Yang, and X. Zhang. A priori error estimates for some discontinuous Galerkin immersed finite element methods. *J. Sci. Comput.*, 65(3):875–894, 2015.
- [44] T. Lin and X. Zhang. Linear and bilinear immersed finite elements for planar elasticity interface problems. *J. Comput. Appl. Math.*, 236(18):4681–4699, 2012.
- [45] A. J. Lusis. Atherosclerosis. *Nature*, 407(6801):233–241, 2000.
- [46] S. McGinty, S. McKee, R. Wadsworth, and C. McCormick. Modelling drug-eluting stents. *Math. Med. Biol.*, 28(1):1–29, 2011.
- [47] S. McGinty, S. McKee, R. M. Wadsworth, and C. McCormick. Modeling arterial wall drug concentrations following the insertion of a drug-eluting stent. *SIAM J. Appl. Math.*, 73(6):2004–2028, 2013.
- [48] R. Mongrain, I. Faik, R.L. Leask, J. R., O.F. Bertrand, et al. Effects of diffusion coefficients and struts apposition using numerical simulations for drug eluting coronary stents. *J. Biomech. Engrg.*, 129(5):733–742, 2007.
- [49] C.J. Murray and A.D. Lopez. Alternative projections of mortality and disability by cause 1990–2020: Global burden of disease study. *The Lancet*, 349(9064):1498–1504, 1997.
- [50] G. Pontrelli and F. de Monte. Mass diffusion through two-layer porous media: an application to the drug-eluting stent. *Int. J. Heat. Mass Tran.*, 50(17):3658–3669, 2007.

- [51] G. Pontrelli and F. De Monte. A multi-layer porous wall model for coronary drug-eluting stents. *Int. J. Heat. Mass Tran.*, 53(19):3629–3637, 2010.
- [52] S. Prabhu and S. Hossainy. Modeling of degradation and drug release from a biodegradable stent coating. *J. Biomed. Mater. Res. Part A*, 80(3):732–741, 2007.
- [53] X. Zhang Q. Yang. Discontinuous Galerkin immersed finite element methods for parabolic interface problems. *J. Comput. Appl. Math.*, 299:127 – 139, 2016.
- [54] R. Rannacher and S. Turek. Simple nonconforming quadrilateral stokes element. *Numer. Methods Partial Differential Equations*, 8(2):97–111, 1992.
- [55] S.A. Sauter and R. Warnke. Composite finite elements for elliptic boundary value problems with discontinuous coefficients. *Computing*, 77(1):29–55, 2006.
- [56] R. S. Schwartz, E. Edelman, R. Virmani, A. Carter, J.F. Granada, G.L. Kaluza, N. A. Chronos, K. A. Robinson, R. Waksman, J. Weinberger, et al. Drug-eluting stents in preclinical studies updated consensus recommendations for preclinical evaluation. *Circulation. Cardiovascular Interventions*, 1(2):143, 2008.
- [57] G. Vairo, M. Cioffi, R. Cottone, G. Dubini, and F. Migliavacca. Drug release from coronary eluting stents: a multidomain approach. *J. Biomech.*, 43(8):1580–1589, 2010.
- [58] G. M. WRITING, J. D. Lloyd, R.J. Adams, T.M. Brown, M. Carnethon, S. Dai, G. De Simone, T.B. Ferguson, E. Ford, K. Furie, et al. Heart disease and stroke statistics–2010 update: a report from the american heart association. *Circulation*, 121(7):e46, 2010.
- [59] C.T. Wu, Z.L. Li, and M.C. Lai. Adaptive mesh refinement for elliptic interface problems using the non-conforming immersed finite element method. *Int. J. Numer. Anal. Model*, 8(3):466–483, 2011.
- [60] C.M. Yang and H. M. Burt. Drug-eluting stents: factors governing local pharmacokinetics. *Adv. drug delivery rev.s*, 58(3):402–411, 2006.
- [61] N. Yang and K. Vafai. Modeling of low-density lipoprotein (ldl) transport in the artery effects of hypertension. *Int. J. Heat and Mass Transf.*, 49(5):850–867, 2006.
- [62] H.L. Zhang, T. Lin, and Y.P. Lin. Linear and quadratic immersed finite element methods for the multi-layer porous wall model. *Int. J. Numer. Anal. Model.*, to be appear.
- [63] X. Zhang. *Nonconforming immersed finite element methods for interface problems*. PhD thesis, Virginia Polytechnic Institute and State University, 2013.



- [64] H. Q. Zhao, D. Jayasinghe, S. Hossainy, and L. B. Schwartz. A theoretical model to characterize the drug release behavior of drug-eluting stents with durable polymer matrix coating. *J. of Biome. Mater. Res. Part A*, 100(1):120–124, 2012.
- [65] P. Zunino. Multidimensional pharmacokinetic models applied to the design of drug-eluting stents. *Cardiov. Engrg. Int. J.*, 4(2):181–191, 2004.
- [66] P. Zunino, C. D'Angelo, L. Petrini, C. Vergara, C. Capelli, and F. Migliavacca. Numerical simulation of drug eluting coronary stents: mechanics, fluid dynamics and drug release. *Comput. Methods Appl. Mech. and Engrg.*, 198(45):3633–3644, 2009.